No induction of apoptosis by IFN-β in human antigen-specific T cells

Article abstract—Interferon (IFN)-β, the most effective immunomodulatory treatment for MS, inhibits the proliferation of myelin-specific T cells. We report that IFN-β moderately enhances the expression of the death receptor, CD95, at the surface of human antigen-specific T cells. However, T-cell apoptosis was not induced by IFNβ-1a or IFNβ-1b as assessed by caspase activity or DNA fragmentation. Immunomodulation mediated by IFN-β does not directly involve apoptotic pathways in human T cells. **Key words:** MS—Interferon-β—Apoptosis—CD95—Caspase.

NEUROLOGY 2000;54:485–487

F. Zipp, MD; M. Beyer, MD; H. Gelderblom, MD; D. Wernet, MD; R. Zschenderlein, MD; and M. Weller, MD

The pathogenesis of MS involves myelin-specific T cells that invade the CNS and promote demyelination. Induction of T-cell death, especially through CD95 (Fas/APO-1)–mediated apoptosis, would decrease T-cell numbers and reduce autoimmune-mediated tissue damage. This regulatory process is effective during recovery and experimental treatment of the MS model of disease, experimental autoimmune encephalomyelitis.[1] Interferon (IFN)-β probably is the most effective current treatment for MS.[2-5] The mechanism of action for IFNβ-1a and IFNβ-1b, two different recombinant preparations of IFN-β in MS, remains unclear but may involve inhibition of antigen presentation and proliferation of myelin-specific T-cell lines.[6] Here, we ask whether these inhibitory effects of INF-β involve induction of T-cell apoptosis. IFN-β enhances the expression of the death receptor CD95 at the cell surface, but no evidence was found for direct induction of apoptosis by INFβ-1a or IFNβ-1b in human antigen-specific T cells from MS patients or healthy individuals.

Methods. *Polyclonal and antigen-specific T cells.* Peripheral blood mononuclear cells were obtained from MS patients and healthy volunteers. The cells were nonspecifically stimulated with phytohemagglutinin (1 μg/ml) leading to polyclonal T cells. Myelin basic protein–specific or tetanus toxoid–specific $CD4^+$ T-cell lines were established using a modified "split-well" protocol.[7] All antigen-specific T-cell lines had at least three restimulations before assay use and a stimulation index above 3.

Asparagine-Glutamine-Valine-Asparagine-7-amido-4-methylcumarine (DEVD-amc)–cleaving caspase activity. The cells were exposed to APO-1 antibody (1 μg/ml) (provided by P.H. Krammer, DKFZ, Heidelberg, Germany), performed with protein A (10 ng/ml), and to IFNβ-1a (Serono, Unterschleissheim, Germany) or IFNβ-1b (Schering, Berlin, Germany) (both IFN-β: 10 U/ml to 10,000 U/ml). To measure caspase activity, 10^5 cells were plated in 96 flat-bottom well plates, incubated with various stimuli for 1 to 48 hours in serum-free medium, and subsequently lysed in lysis buffer (60 mM NaCl, 5 mM Tris-HCl, 2.5 mM ethylenediamine tetra-acetic acid, 0.25% NP40) for 10 minutes. The fluorogenic caspase substrate DEVD-amc (20 μM) (BIOMOL, Hamburg, Germany) was added to the lysates, and fluorescence was measured after 30 and 60 minutes at 360 nm excitation and 480 nm emission wavelengths, respectively, using a CytoFluor 2400 cytofluorometer (Millipore Corp., Eschborn, Germany).

DNA fragmentation. Quantitative analysis of DNA fragmentation was performed using a hypotonic fluorochrome solution (propidium iodide 50 μl/ml in 0.1% sodium citrate and 0.1% Triton X-100) added to 10^5 cells treated as indicated, followed by overnight incubation at 4 °C. The magnitude of the hypodiploid DNA peak was determined as the percentage of total events by flow cytometry.

Flow cytometry. The APO-1 antibody, mouse IgG_3 isotype antibody (Becton-Dickinson, Heidelberg, Germany), and dichlorotriazinyl amino fluorescein–conjugated anti-mouse antibody (DIANOVA, Hamburg, Germany) were used. Flow cytometric analysis followed a standard protocol.

Reverse transcriptase–PCR. The PCR conditions were as follows: CD95 40 cycles, 45 seconds/94 °C, 60 seconds/58 °C, 60 seconds/72 °C, primer sequences GACCCAGAATACCAAGTGCAGATGTA (nucleotides 557-582) and CTGTTTCAGGATTTAAGGTTGGAGATT (nucleotides 852-826); β-actin 35 cycles, 45 seconds/95 °C, 45 seconds/55 °C, 45 seconds/72 °C, primer sequences TGTTTGAGACCTTCAACACCC (nucleotides 409-429) and AGCACTGTGTTGGCGTACAG (nucleotides 937-918). For all genes, PCR protocols were standardized so that the cycle number ensured PCR amplification was in its exponential phase. To quantify the expression level, optical density (OD) was determined using BioDocII (Biometra, Göttingen, Germany) documentation system, and the ratio of the integrated OD

From the Department of Neurology, Division of Neuroimmunology (Drs. Zipp, Beyer, Gelderblom, and Zschenderlein), University Hospital Charité, Berlin; and the Departments of Transfusion Medicine (Dr. Wernet) and Neurology, Division of Neurooncology (Dr. Weller), University of Tübingen, Germany.

Supported by grants from the Gemeinnützige Hertie, Stiftung, the Deutsche Multiple Sklerose, Gesellschaft, and from the Forschungskommission Charité.

Received June 3, 1999. Accepted in final form August 31, 1999.

Address correspondence and reprint requests to Dr. F. Zipp, Department of Neurology, Division of Neuroimmunology, University Hospital Charité, Campus Virchow, Forschungshaus, 2.OG, R. 535, Augustenburger Platz 1, 13353 Berlin, Germany.

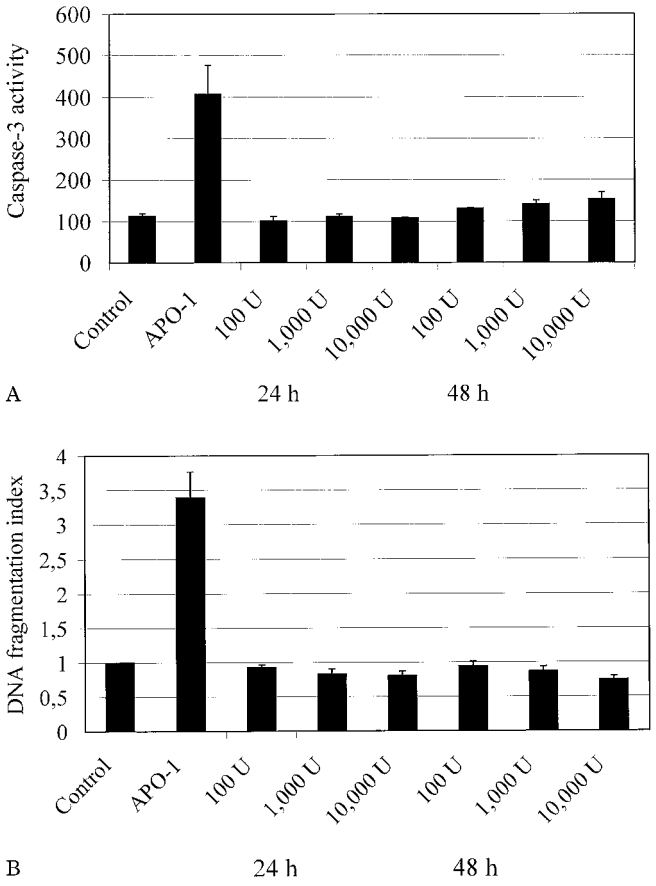

Figure 1. No activation of caspase-3 or induction of apoptosis by interferon (IFN)-β in antigen-specific T-cell lines is seen. (A) Antigen-specific T-cell lines (three myelin basic protein [MBP]–specific from patients; three MBP-specific and three tetanus toxoid [TT]–specific from controls) were untreated or exposed to IFN-β at 10 to 10,000 U/ml for 24 hours and 48 hours, respectively, or to APO-1 antibody (1 μg/ml) for 3 hours, which was a positive control. Caspase-3–like enzyme activity was assessed by DEVD-amc cleavage (see Methods). Data are expressed as mean fluorescence units and SEM. (B) In the same assays, DNA fragmentation was detected by flow cytometry (see Methods) and is given as DNA fragmentation index (with stimulus/control, control = 1) ± SEM. Here, incubation with APO-1 antibody also was performed for up to 48 hours.

of CD95 to the OD of β-actin was calculated using Scanalytics ONE-Dscan software (Scanalytics Inc., Fairfax, VA).

Results. The induction of caspase activity and DNA fragmentation were measured in response to incubation with IFNβ-1a or IFNβ-1b (10 to 10,000 U/ml) for 24 or 48 hours at 0, 2, 6, and 8 days after stimulation, respectively, to assess whether IFN-β promotes apoptosis of human antigen-specific and polyclonal T cells. Caspase activity also was measured 1, 3, and 6 hours after incubation with IFN-β to avoid missing earlier, potentially reversible activity. This is because activity peaks at 3 hours after incubation with the proapoptotic APO-1 antibody. Neither relevant DEVD-amc–cleaving caspase activity nor DNA fragmentation were detected at any of the IFN-β concentrations, at any time point, in any T-cell line (figure 1).

In the three myelin basic protein–specific and three tetanus toxoid–specific T-cell lines from healthy individuals, there was an increased surface CD95 expression at 24 hours after incubation with IFN-β (specific fluorescence index ± SEM = 1.0 for 0 U/ml IFN-β as control, 1.1 ± 0.03 for 10 U/ml, 0.8 ± 0.06 for 100 U/ml), and most clearly at 1,000 U/ml IFN-β (1.4 ± 0.20) ($p = 0.05$, Mann-Whitney U test). The overall difference was not statistically significant ($p > 0.05$, Kruskal-Wallis test). We found no evidence for altered CD95 mRNA expression assessed by reverse transcriptase–PCR at 6, 16, 24, and 48 hours of incubation of nonspecifically stimulated peripheral blood mononuclear cells with IFN-β. At the protein level, there was no difference in CD95 surface expression on polyclonal T cells between MS patients and controls (figure 2). Interestingly, IFN-β at 10 U/ml enhanced CD95 expression in MS patients ($p = 0.01$, Mann-Whitney U test) but not in controls. This difference was not apparent at higher concentrations of IFN-β in either MS patients or in controls (patients, $p = 0.04$; controls, $p > 0.05$, Kruskal-Wallis test) (see figure 2).

Apoptosis inhibitory properties were recently attributed to IFN-β.[8] We examined whether preincubation with IFN-β modulates CD95-mediated apoptosis in antigen-specific T-cell lines. Exposure to APO-1 (CD95) antibody (1 μg/ml) induced DNA fragmentation, which was not modulated by pre-exposure to IFN-β (10 to 1,000 U/ml) for 24 hours ($p > 0.05$, Kruskal-Wallis test). Figure 3 indicates that T-cell vulnerability was not altered by IFN-β in our system.

Discussion. The mechanism of action of IFN-β in MS is unclear. The goal of increasing efficacy and decreasing adverse reactions in future treatment

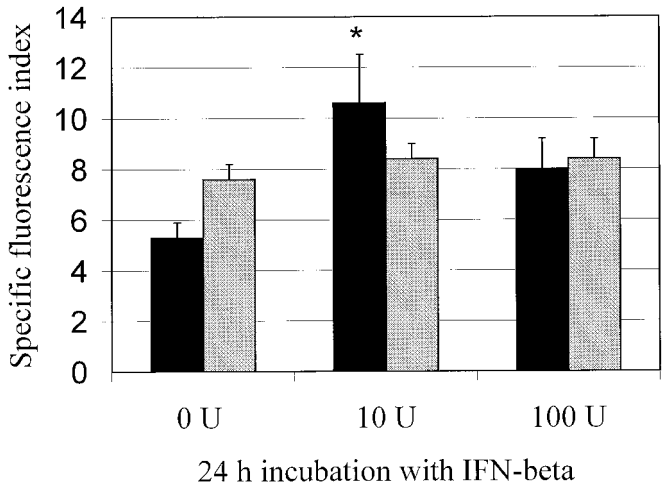

*Figure 2. Modulation of CD95 expression in polyclonal T cells by interferon (IFN)-β is shown. CD95 protein expression was assessed by flow cytometry and expressed as mean specific fluorescence index (mean fluorescence intensity with APO-1 antibody/mean fluorescence intensity with isotype antibody) values and SEM. The figure compares polyclonal T cells at 7 days after stimulation with phytohemagglutinin of 9 MS patients (black bars) and 11 healthy individuals (gray bars) untreated or at 24 hours after exposure to IFN-β at 10 U/ml or 100 U/ml (*p = 0.01, Mann-Whitney U-test).*

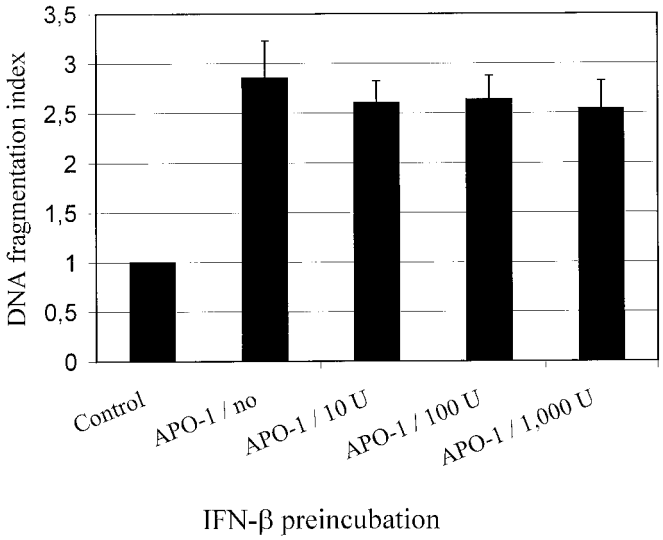

Figure 3. No evidence is seen for protection or enhancement of APO-1 antibody-induced apoptosis in human antigen-specific T-cell lines by interferon (IFN)-β preincubation. Antigen-specific T-cell lines (six myelin basic protein [MBP]–specific and three tetanus toxoid [TT]–specific from healthy individuals) were preincubated with 10, 100, and 1,000 U/ml of IFNβ-1a for 24 hours and thereafter exposed to APO-1 antibody (1 μg/ml) for another 24 hours. DNA fragmentation was detected by flow cytometry and is demonstrated as index and SEM (see Methods).

makes it necessary to clarify how established therapeutic agents interfere with the pathomechanisms of the disease. In melanoma cells, it has been shown that IFN-β inhibits growth, partially through induction of apoptosis.[9] Several recent observations indicate that IFN-α/β modulates the CD95/CD95 ligand system, a death receptor/ligand system crucial for the peripheral deletion of activated T cells by apoptosis.[1] We found that IFNβ-1a and IFNβ-1b do not induce caspase activity or DNA fragmentation in antigen-specific T-cell lines from MS patients and healthy individuals in vitro. This is true for the IFN-β levels likely to be achieved in the serum after therapeutic application (10 to 100 U/ml), as well as IFN-β concentrations that greatly exceed the therapeutic range (up to 10,000 U/ml).

Both IFN-α and IFN-β can rescue nonspecifically stimulated T cells from activation-induced cell death, known to be CD95-mediated, in vitro.[8] We did not observe significant IFN-β–mediated T-cell protection from CD95-mediated apoptosis. Moreover, no enhancement of CD95-mediated apoptosis was induced by IFN-β pretreatment of the T cells. We confirm a moderate upregulation of CD95 cell surface expression after exposure to IFN-β, which has been reported in some cell types.[10]

These findings do not exclude the possibility that IFN-β might promote T-cell apoptosis through unknown pathways in vivo. This would explain a reduction of clinical exacerbations in MS.[2-5] Interestingly, in longitudinally studied MS patients, the serum levels of apoptosis-inhibiting soluble CD95 increase during the formation of neutralizing IFN-β antibodies, which parallels clinical deterioration.[1] Because our data neither suggest a direct modulation of CD95-mediated apoptosis in antigen-specific T-cell lines by IFN-β nor direct proapoptotic effects of IFN-β on human T cells, other mechanisms are likely to account for these effects of IFN-β in MS patients.

References

1. Zipp F, Krammer PH, Weller M. Immune (dys)regulation in multiple sclerosis: role of the CD95/CD95 ligand system. Immunol Today 1999;20:550–554.
2. The IFNB Multiple Sclerosis Study Group, The University of British Columbia MS/MRI Analysis Group. Interferon beta-1b in the treatment of multiple sclerosis: final outcome of the randomized controlled trial. Neurology 1995;45:1277–1285.
3. Jacobs LD, Cookfair DL, Rudick RA, et al. The Multiple Sclerosis Collaborative Research Group (MSCRG): intramuscular interferon beta-1a for disease progression in relapsing multiple sclerosis. Ann Neurol 1996;39:285–294.
4. PRISMS study group. Randomised double-blind placebo-controlled study of interferon beta-1a in relapsing/remitting multiple sclerosis. Lancet 1998;352:1498–1504.
5. European Study Group on Interferon Beta-1b in Secondary Progressive MS. Interferon beta-1b delays progression of disability in secondary progressive multiple sclerosis. Lancet 1998;352:1491–1497.
6. Pette M, Pette DF, Muraro PA, Farnon E, Martin R, McFarland HF. Interferon-β interferes with the proliferation but not with the cytokine secretion of myelin basic protein-specific, T-helper type 1 lymphocytes. Neurology 1997;49:385–392.
7. Zipp F, Martin R, Lichtenfels R, et al. Human autoreactive and foreign antigen-specific T cells resist apoptosis induced by soluble recombinant CD95 ligand. J Immunol 1997;159:2108–2115.
8. Pilling D, Akbar AN, Girdlestone J, et al. Interferon-β mediates stromal cell rescue of T cells from apoptosis. Eur J Immunol 1999;29:1041–1050.
9. Nagatani T, Okazawa H, Kambara T, et al. Effect of natural interferon-beta on the growth of melanoma cell lines. Melanoma Res 1998;8:295–299.
10. Rep MHG, Schrijver HM, van Lopik T, et al. Interferon (IFN)-β treatment enhances CD95 and interleukin 10 expression but reduces interferon-γ producing T cells in MS patients. J Neuroimmunol 1999;96:92–100.

Identification of new and common mutations in the *EPM2A* gene in Lafora disease

Article abstract—Lafora disease is a teenage onset progressive myoclonus epilepsy caused by mutations in the *EPM2A* gene. In this report, we describe new mutations within *EPM2A*, review the known mutations to date to identify the most common, and describe three simple tests for prenatal and carrier screening. **Key words:** Lafora disease—*EPM2A*—Laforin—Epilepsy—Mutation—*EPM2B*.

NEUROLOGY 2000;54:488–490

Berge A. Minassian, MD; Leonarda Ianzano, PhD; Antonio V. Delgado-Escueta, MD; and Stephen W. Scherer, PhD

Lafora disease (LD) is an autosomal recessive progressive myoclonus epilepsy (PME) that presents in teenage years with myoclonias, photoconvulsive seizures, generalized convulsions, and mental decline. This is followed by rapidly progressive neurodegeneration manifested by increasing severity of the above symptoms until dementia and death within 10 years.[1] Pathognomonic periodic acid-Schiff–positive Lafora bodies can be demonstrated in almost any organ,[2] but falsely negative biopsies do occur.[3]

We recently identified the LD gene *EPM2A* and detected seven distinct mutations in it in patients from nine families.[4] Serratosa et al. described additional mutations,[5] and in the current communication, we report new deletion mutations. Altogether, 14 different mutations in 24 families are now known.

The discovery of *EPM2A* makes prenatal diagnosis, carrier screening, and genetic confirmation of clinical diagnosis feasible. However, the extent of mutation heterogeneity makes this difficult. In this article, we describe simple genetic methods to screen for the more common mutations.

Patients and methods. Patients reported here had biopsy-proven LD. PCR primer sequences and conditions were: JRGXBF: 5′-TCCATTGTGCTAATGCTATCTC-3′; JRGXBR: 5′-TCAGCTTGCTTTGAGGATATTT-3′; H1F: 5′-GAATGCTCTTTCCACTTTGC-3′; PTPR: 5′-GGCTCCTTAGGGAAATCAG-3′; annealing: 62 °C; $MgCl_2$ = 1.25 mM. Stock DNA was used; PCR products were purified on Qiagen columns (Germany). Restriction digests were performed at 37 °C, and products were run on 3% agarose gels.

Results. *New mutations.* *EPM2A* is composed of four exons located within a 130,000–base pair (bp) span of chromosome 6q24[4] (figure 1). As a first step toward screening exon 2 for mutations, it was amplified by PCR with primers JRGXBF and JRGXBR. In the affected members from three families, LD-L4, LD9, and LD1, no PCR product was observed, indicating a possible homozygous deletion in these patients. To confirm and characterize the extent of this deletion, PCR was performed with primers covering the rest of the gene (see figure 1). The extent of the deletion in families LD-L4 and LD9 was determined to be ~75,000 bp encompassing both exons 1 and 2. A smaller deletion of ~25,000 bp was found in family LD1.

Screening tests for the more common mutations. The most common *EPM2A* mutation to date is a C→T nonsense change of the second bp of exon 4 observed in nine families[4,5] (table). Primers H1F and PTPR amplify a 520-bp DNA fragment encompassing exon 4 including several recognition sites for the restriction enzyme *Hae*III, one of which is destroyed by the C→T mutation. Digestion of this PCR product with *Hae*III in normal noncarrier individuals results in nine small bands, the largest of which is 102 bp. Digestion with *Hae*III in carriers or patients results in the appearance of an abnormal 199-bp band (figure 2, A and B). Using this test, carriers cannot be distinguished from patients who harbor this mutation on both chromosomes (see figure 2B).

The second most common mutation is another point mutation (G→A, bp 115) in exon 4 observed in four families[4,5] (see the table). This mutation creates a unique *Pst*I restriction site in the sequence of the HIF/PTPR PCR product. *Pst*I does not digest this 520-bp PCR product in normal noncarrier individuals. Carriers will therefore have one normal 520 bp band and two variant bands 195 bp and 315 bp in size (see figure 2). Patients homozygous for this mutation will only have the abnormal bands.

Finally, four families with deletions of EPM2A have been described, including the three families in this report and one family from reference 5 (see the table). Two of these families (LD-L4 and LD9) appear to have identical 75 Kb deletions (see figure 1), which are different from the other two (see the table). Nonetheless, these three different deletion mutations all encompass exon 2 (see figure 1, table). Patients homozygous for any of these deletions can be identified by absence of PCR amplification using primers JRGXBF/JRGXBR and appropriate controls (see figure 1).

Discussion. LD is most frequently diagnosed in societies with high rates of consanguinity. There also seems to be an excess reporting from countries surrounding the Mediterranean basin, and many of

From the Division of Neurology, Departments of Paediatrics (Dr. Minassian) and Genetics (Drs. Minassian, Ianzano, and Scherer), The Hospital for Sick Children and The University of Toronto, Canada; and the Comprehensive Epilepsy Program (Dr. Delgado-Escueta), Department of Neurology and Brain Research Institute, University of California, Los Angeles School of Medicine and West Los Angeles DVA Medical Center.

Supported by The Medical Research Council of Canada (MRC) and NIH grant 5P01-NS21908 (A.V.D.-E.). S.W.S. is a Scholar of the MRC.

Received June 21, 1999. Accepted in final form August 18, 1999.

Address correspondence and reprint requests to Dr. Stephen W. Scherer, Department of Genetics, The Hospital for Sick Children and The University of Toronto, 555 University Ave., Toronto, Ontario, M5G 1X8, Canada.

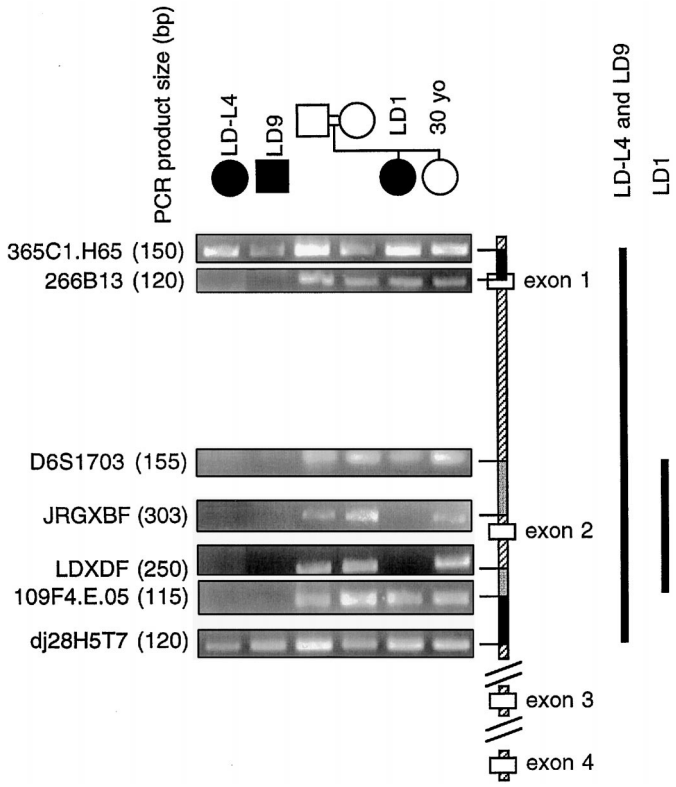

Figure 1. Refined map of the deletion breakpoints in families LD-L4, LD9, and LD1. Filled symbols indicate patients with Lafora disease (LD). Open rectangles on the map are the exons of EPM2A*. Genomic structure around exons 1 and 2 is shown to scale. Polymerase chain reaction markers 365C1.H65, 266B13, D6S1703A, JRGBF/R, LDXDF/R, 109F4.E.05, and dj28H5T7 were tested. Primer sequences can be obtained by looking up PAC 466P17 at http:/ /www.sanger.ac.uk. The positions of the forward primers of these markers on the PAC are at 58336, 59869, 98214, 108805, 123524, 124039, and 132487 base pairs, respectively. The maximum extent of the deletions are shown on the right. The deletion breakpoint regions for LD-L4 and LD9 are colored black on the map and are distinct from the deletion breakpoint regions for LD1, which are colored gray. Each of the four deletion breakpoints contains a mammalian-wide interspersed repeat.*

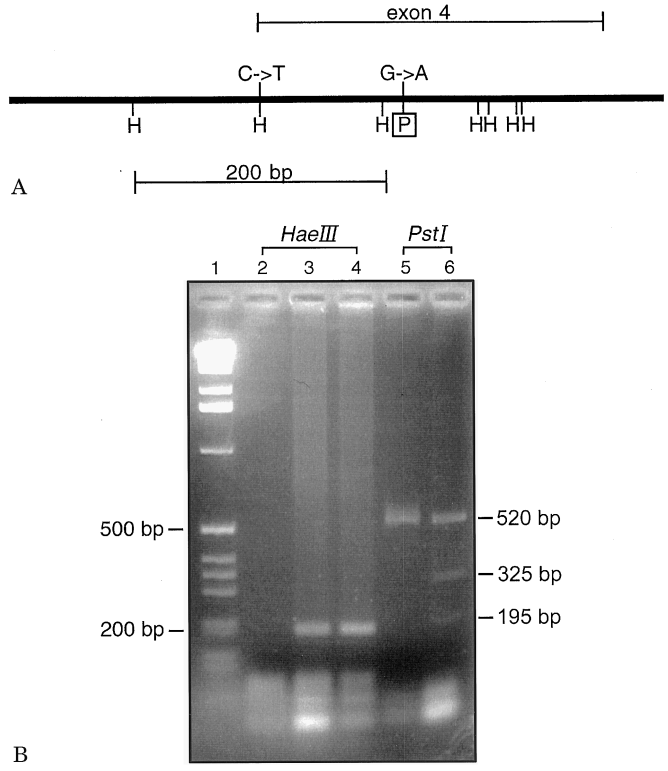

Figure 2. Restriction endonuclease screening for the two common mutations in exon 4. (A) Restriction map (to scale) of PCR product with primers H1F/PTPR. H, Hae*III restriction enzyme sites, one of which is destroyed by the C→T mutation; boxed P,* Pst*I site created by the G→A mutation. (B)* Hae*III and* Pst*I digestion of the H1F/PTPR PCR product. Lane 1: 1 Kb ladder; lane 2: normal noncarrier individual with* Hae*III digestion; lanes 3 and 4: appearance of an abnormal 199 base pair (bp) band in a carrier with the C→T mutation (lane 3) and a patient with a homozygous mutation (lane 4); lane 5:* Pst*I digestion does not affect normal noncarriers; lane 6:* Pst*I digests the PCR product into two smaller fragments in a carrier of the G→A mutation. In patients with a homozygous G→A mutation,* Pst*I digestion should result in the disappearance of the 520-bp original band. However, we do not have such a patient in our collection.*

those families appear not to be consanguineous. This initially suggested that, like other PME such as Unverricht-Lundborg disease[6] or the neuronal ceroid lipofuscinoses,[7] LD might be caused by a common mutation in most cases. This was shown not to be the case.[4,5] The large number of different mutations renders their detection for clinical purposes difficult.

The simple DNA-based tests described above can be used to screen for the three more common mutations in the following way. Digestion of the HIF/PTPR PCR product with *Hae*III and *Pst*I detects the two more common mutations and will confirm that an individual is a carrier of one or the other mutation. The *Pst*I test can further establish whether a patient or fetus is homozygous for the G→A mutation. To establish if a patient is homozygous for the mutation detected by the *Hae*III test, further analyses will be required such as allele-specific oligonucleotide hybridization or DNA sequencing.[4]

PCR using JRGXBF/JRGXBR will detect the deletion mutations described in this report, but only in homozygous state. This simple test can therefore serve for prenatal or symptomatic diagnosis, but cannot detect carriers. For carrier testing in these families further work will be required. For example, in three of the deletions (LD-L4, LD9, and the example in reference 5), the polymorphic microsatellite marker *D6S1703* is encompassed in the deletion and can be used to detect carriers by testing for loss of heterozygosity.[4,5]

The C→T mutation appears to be common in patients of Spanish (or Iberian) origin[4] (see the table). Three of the four G→A mutations were described in reference 5 and their ethnic origin was not specified.[5]

Table *Common EPM2A mutations*

Mutation	Reference	No. of patients	Ethnic origin
C → T nonsense mutation of bp 2, exon 4	4	5	Spanish
	Unpublished	2	1 Spanish, 1 Italian
	5	2	Unspecified
G → A missense mutation of bp 115, exon 4	4	1	Spanish
	5	3	Unspecified
~75 Kb deletion	This report and 4	2	Arabic
~25 Kb deletion	This report and 4	1	Iranian
~65 Kb deletion	5	1	Unspecified

bp = base pairs.

The 75 Kb deletion was observed in two of two Arabic families in our set (LD-L4 and LD9). Parenthetically, LD9 is the same Arabic family described in reference 3, in which two affected siblings had discordant biopsy results. Whereas false negative biopsies are usually due to insufficient sampling or biopsies done early in the course of the disease, genetic testing should not have these limitations.

Additional EPM2A mutations remain to be found as currently we have identified mutations in only 65% of families. Furthermore, we have recently shown that an altogether different gene (or genes) other than EPM2A can cause LD in up to 20% of patients, including the families from the French Canadian province of Quebec.[4,8] These patients are clinically and pathologically indistinguishable from those with EPM2A mutations.[2,8]

Two deletions with different deletion breakpoints are described in this report. Interestingly, analysis of the sequences of the breakpoint regions revealed the presence of the mammalian-wide interspersed repeat (MIR)[9] in all four breakpoint regions (see figure 1). Duplicated or repetitive sequences flanking deleted genes or exons of a gene have been implicated in the generation of such deletions via the mechanism of unequal recombination. A well-studied example of this from the neurologic literature is hereditary neuropathy with liability to pressure palsies (HNPP). The putative mechanism in the HNPP deletion is complex, involving a large DNA repeat that codes for a transposase (named a mariner repeat) that apparently facilitates the recombination.[10]

References

1. Van Heycop Ten Ham MW. Lafora disease, a form of progressive myoclonus epilepsy. Handbook Clin Neurol 1974;15:382–422.
2. Carpenter S, Karpati G. Sweat gland duct cells in Lafora disease: diagnosis by skin biopsy. Neurology 1981;31:1564–1568.
3. Drury I, Blaivas M, Abou-Khalil BW, Beydoun A. Biopsy results in a kindred with Lafora disease. Arch Neurol 1993;50: 102–105.
4. Minassian BA, Lee JR, Herbrick JA, et al. Mutations in a gene encoding a novel protein tyrosine phosphatase cause progressive myoclonus epilepsy. Nat Genet 1998;20:171–174.
5. Serratosa JM, Gomez-Garre P, Gallardo ME, et al. A novel protein tyrosine phosphatase gene is mutated in progressive myoclonus epilepsy of the Lafora type (EPM2). Hum Mol Genet 1999;8:345–352.
6. Lafreniere RG, Rochefort DL, Chretien N, et al. Unstable insertion in the 5′ flanking region of the cystatin B gene is the most common mutation in progressive myoclonus epilepsy type 1, EPM1. Nat Genet 1997;15:298–302.
7. Goebel HH. Seventh International Congress on Neuronal Ceroid-Lipofuscinoses (NCL-98), June 13–16, 1998; Dallas, TX. Brain Pathol 1998;8:809–810.
8. Minassian BA, Sainz J, Serratosa JM, et al. Genetic locus heterogeneity in Lafora's progressive myoclonus epilepsy. Ann Neurol 1999;45:262–265.
9. Smit AF, Riggs AD. MIRs are classic tRNA-derived SINEs that amplified before the mammalian radiation. Nucleic Acids Res 1995;23:98–102.
10. Reiter LT, Murakami T, Koeuth T, et al. A recombination hotspot responsible for two inherited peripheral neuropathies is located near a mariner transposon-like element. Nat Genet 1996;12:288–297.

An interrupted 34-CAG repeat SCA-2 allele in patients with sporadic spinocerebellar ataxia

Article abstract—In spinocerebellar ataxia type 2 (SCA-2), a difference of three CAG repeats distinguishes normal alleles (14 to 31 repeats) from pathogenic alleles (34 to 57 repeats). All sequenced pathogenic alleles have a pure CAG repeat structure, whereas interrupted repeats have been seen exclusively in normal alleles. The authors present two patients with sporadic SCA with an interrupted 34-CAG repeat allele, $(CAG)_{24}(CAA)(CAG)_9$, who showed a phenotype compatible with SCA-2. The interrupted allele coding for a 34 pure polyglutamine tract may cause the SCA phenotype. **Key words:** SCA-2—CAG—Interrupted repeats—Penetrance.

NEUROLOGY 2000;54:491–493

S. Costanzi-Porrini, PhD; D. Tessarolo, MD; C. Abbruzzese, PhD; M. Liguori, MD; T. Ashizawa, MD; and M. Giacanelli, MD

Spinocerebellar ataxia type 2 (SCA-2) manifests itself with progressive gait and limb ataxia, dysarthria, slow saccadic eye movements with ophthalmoparesis, extrapyramidal signs, areflexia, and cognitive dysfunctions, which largely overlap with clinical manifestations of other types of the autosomal dominant cerebellar ataxias.[1-3] The SCA-2 mutation is an expansion of an unstable CAG repeat located in the 5′ coding region of the ataxin-2 gene on chromosome 12q24.1.[1-3] The normal alleles are polymorphic with 14 to 31 CAG repeats and stably transmitted from generation to generation, whereas affected individuals' SCA-2 alleles with 34 to 59 CAG repeats are unstably transmitted.[1-7] Within SCA-2 families, 34-CAG repeat alleles initially were observed only in asymptomatic members who were considered to be at-risk carriers.[4] However, subsequent reports[6,7] documented that 34-CAG repeat alleles can be found in affected members of SCA-2 families. All normal alleles tested, except one with 14 CAG repeats, showed interruptions by 1 to 3 CAA repeats, whereas expanded alleles, including the at-risk allele with 34 CAG repeats, had a stretch of pure CAG tandem repeats.[4] We report two patients (Patients 1 and 2), both with apparently sporadic cases of SCA, who exhibited clinical signs compatible with an SCA-2 phenotype and had interrupted 34-CAG repeats in the ataxin-2 gene.

Methods. Genomic DNA was obtained from blood leukocytes of 32 patients with sporadic spinocerebellar degeneration (11 from Italy and 21 from the United States). The DNA samples were tested for SCA-1, SCA-2, SCA-3, SCA-6, SCA-7, and dentatorubral-pallidoluysian atrophy mutations. SCA-2 allele sizes were determined by comparing migration of the PCR products[2] relative to an M13 sequencing ladder using polyacrylamide gel electrophoresis. We also studied SCA-2 alleles in hair follicles and buccal cells in Patient 1.

The amplified fragment containing 34 CAG repeats of the ataxin-2 gene was purified on a low-melting agarose gel and directly subcloned into pCR2.1-TOPO vector (Invitrogen; Carlsbad, CA) according to the manufacturer's instructions. Positive colonies were directly sequenced (AmpliCycle Sequencing kit, Perkin-Elmer, Foster City, CA). To verify the sequencing results, PCRs and clonings were repeated from different blood samples in two different laboratories, and both strands were sequenced.

Results. The analysis of CAG repeats at the SCA-2 locus showed a 34/22 genotype in two Italian patients. The sequence of the 34-CAG repeat allele showed a $(CAG)_{24}(CAA)(CAG)_9$ configuration in both patients (figure 1). Two other Italian patients showed an SCA-2 allele in the larger pathologic range. The remaining patients showed no expansions at any loci studied. The finding of 4 SCA-2 patients of 11 with sporadic late-onset cerebellar ataxia in the Italian series is unexpected. Although this probably resulted from the small sample size, further studies on SCA-2 prevalence in the region may be of interest. DNA samples obtained from hair follicles and buccal cells of Patient 1 showed no variability of the 34- and 22-CAG repeat alleles.

Clinical features. Patient 1. A 65-year-old man had noted mild ataxia in his gait since age 25 years. At age 50, he developed an extrapyramidal syndrome (postural instability, diffuse cogwheel rigidity, and hypomimia) partially responsive to L-DOPA. In the following years, his gait ataxia slightly worsened. He had been hospitalized recently for a subacute onset of medial rectus muscle weakness, ptosis, and exophthalmus in the right eye. However, saccadic and pursuit ocular movements were otherwise normal with no ocular dysmetria or nystagmus. A moderate degree of finger-nose-finger and heel-to-shin dysmetria with dysdiadochokinesia was detected. Other findings included mild dementia, "mumbling" dysarthria, dysphagia, and decreased vibration sense in the feet with normal reflexes.

The patient had four asymptomatic siblings, ages 46, 59, 68, and 70 years. His parents, both dead at age 68, had no neurologic disorders. His family members declined our evaluation.

From the Department of Neurosciences (Drs. Costanzi-Porrini, Tessarolo, Abbruzzese, Liguori, and Giacanelli), San Camillo Hospital, Rome, Italy; and Department of Neurology, Baylor College of Medicine, and VAMC (Dr. Ashizawa), Houston, TX.

Supported by grants from Department of Neurosciences, San Camillo Hospital (PCN/97) and Oxnard Foundation/National Ataxia Foundation (T.A.).

Received November 24, 1998. Accepted in final form September 6, 1999.

Address correspondence and reprint requests to Dr. Tetsuo Ashizawa, Department of Neurology, Baylor College of Medicine, One Baylor Plaza, SM1801, Houston, TX 77030.

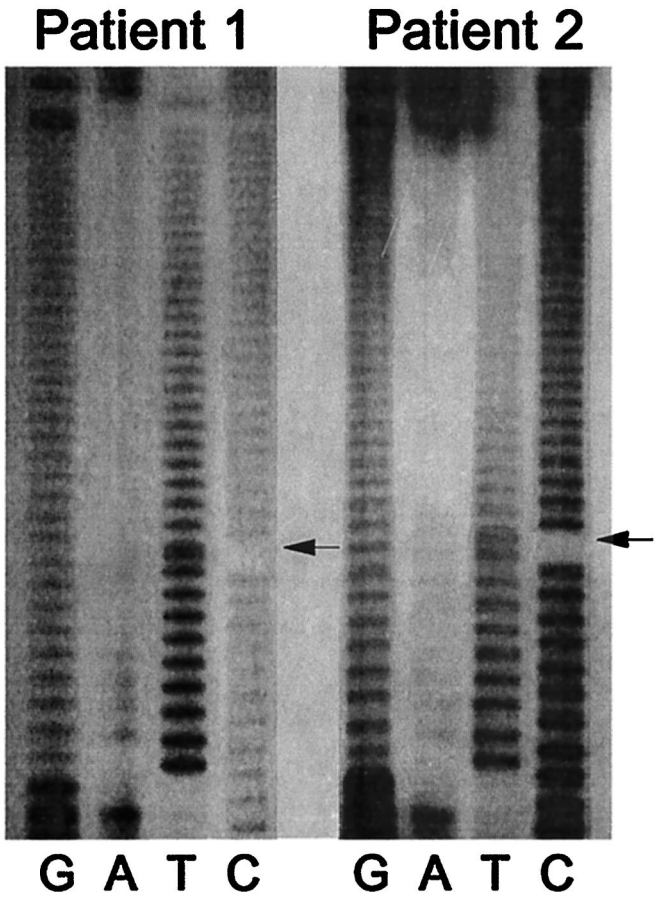

Figure 1. Autoradiograph of the SCA-2 CAG repeat sequence from Patients 1 and 2. The 34-CAG repeat tract is interrupted by CAA in position 25 (arrows) of the stretch in both patients. The sequence was obtained from the opposite strand; therefore, the sequence shown reads $(CTG)_9TTG(CTG)_{24}$ *from the bottom to the top of gels.*

Patient 2. A 66-year-old man developed gait ataxia over the last 5 years. Neurologic examinations showed a wide-base gait and truncal ataxia with marked heel-to-shin dysmetria, mild scanning and tremulous speech, postural tremor, cogwheel rigidity, and mild dementia. No abnormal ocular motility, dysphagia, dysautonomia, or hyporeflexia was detected.

The patient had three asymptomatic siblings, ages 51, 54, and 63 years, and two asymptomatic sons. His parents died at ages 46 and 97, without neurologic disorders. His family declined our evaluation.

Neuroradiologic, electrophysiologic, and other laboratory examinations. The brain MRI showed, in both patients, mild atrophy of cerebellar cortex and milder atrophy in the bilateral parieto-occipital regions and brainstem (figure 2). In both patients, SPECT showed reductions of perfusion in the frontal cortex, subcortical white matter, and cerebellum. The patients also showed a pathologic increase of the P1 latency in sensory evoked potentials (evoked by lower limbs) and a mildly increased P2-N2 latency in visual evoked potentials. Our patients showed no clinical or laboratory findings suggestive of alcoholism, thyroid dysfunction, or gluten sensitivity.

Discussion. We describe an interrupted 34-CAG repeat allele in the ataxin-2 gene in two patients with a progressive cerebellar ataxia and extrapyramidal signs. The clinical findings of our patients were consistent with SCA-2. Although the most characteristic SCA-2 features—such as slow saccade, hyporeflexia, action and postural tremor, and myoclonus—were missing, these findings may not always be present in SCA-2 patients, especially those with less than 37 CAG repeats.[4] Parkinsonism, which has been reported rarely in SCA-2, clearly was present in Patient 1 and possibly in Patient 2. Whether their parkinsonism was a coincidental phenomenon or a phenotype produced by the interrupted 34-repeat allele

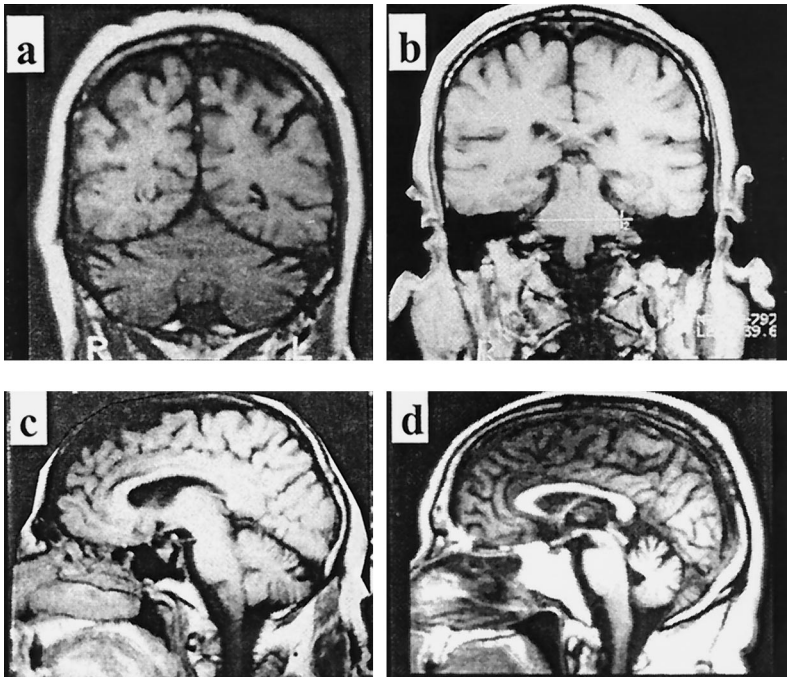

Figure 2. Brain MRI of Patient 1 shows mild atrophy of the cerebellar cortex and mild reduction of the transverse diameter of the basis pontis in coronal views (a and b), and mild atrophy of the cerebellar vermis in a sagittal view (c). Brain MRI of Patient 2 shows mild atrophy of the cerebellar vermis (d). All are T1-weighted images (SE = 460).

remains unknown. The slow progression of our patients' illness may be seen in the SCA-2 phenotype associated with relatively small expansions of the CAG repeat.[4,8] The age at onset was variable in our patients (25 and 61 years of age, respectively). Although the onset at age 25 seems earlier than expected from 34 repeats, the age at onset has been highly variable at a given repeat size.[1-3] Therefore, it is difficult to determine whether the onset at age 25 is compatible with 34 CAG repeats in SCA-2.

SCA-2 is an autosomal dominant disease, but it has been described in patients with no family history of ataxia.[4] Whereas a 34-CAG repeat allele never has been found in the normal population thus far examined, it has been described in affected members and asymptomatic at-risk members of SCA-2 families.[4,6,7] Thus, it is possible that the 34-CAG repeat allele caused the ataxic phenotype in our patients.

The 34-CAG repeat allele in our patients comprised the $(CAG)_{24}(CAA)(CAG)_9$ conformation. This contrasts with the previously described 34-CAG repeat allele, which consisted of a pure CAG stretch and was unstably transmitted within the SCA-2 families.[4] Interrupted CAG repeat alleles have been seen on normal chromosomes but never on disease chromosomes in SCA-2. From a viewpoint of DNA structure, the interrupted 34-CAG repeat allele in our patient may be considered as a normal allele, whereas the uninterrupted 34-CAG repeat allele may be considered as an at-risk allele. It has been shown that interrupted trinucleotide repeat alleles generally are more stable than uninterrupted alleles.[9] The interrupted 34-CAG repeat allele showed no detectable somatic instability in the blood, hair follicles, or buccal cells of Patient 1. Thus, although mitotic stability does not necessarily imply meiotic stability, there is a reasonable chance that the $(CAG)_{24}(CAA)(CAG)_9$ alleles in our patients were stably transmitted from generation to generation. Unfortunately, DNA samples of their family members were not available, and we could not directly examine the possibility that the $(CAG)_{24}(CAA)(CAG)_9$ alleles had arisen as a result of de novo mutations.

Assuming stable transmissions of the $(CAG)_{24}(CAA)(CAG)_9$ alleles, the lack of SCA-2 phenotype in our patients' parents suggests that this allele may not always be penetrant, unless it was going to cause symptoms at a later age. Because both $(CAG)_{24}(CAA)(CAG)_9$ and $(CAG)_{34}$ code for 34 tandem repeats of a glutamine residue, both alleles should behave similarly at the protein level. Our patients may represent the first cases of an interrupted CAG repeat allele with pathogenicity. We speculate that the combination of reduced penetrance and stable transmissions of the $(CAG)_{24}(CAA)(CAG)_9$ allele may be a potential basis for sporadic occurrences of SCA-2. Studies of similar cases are needed to further examine this hypothesis.

Acknowledgment

The authors thank Drs. Domenico Merigliano and Fabio Corsi for referring their patients, and Dr. Rodolfo Luna for evaluating the MR images.

References

1. Sanpei K, Takano H, Igarashi S, et al. Identification of the spinocerebellar ataxia type 2 gene using a direct identification of repeat expansion and cloning technique, DIRECT. Nat Genet 1996;14:277–284.
2. Pulst SM, Nechiporuk A, Nechiporuk T, et al. Moderate expansion of a normally biallelic trinucleotide repeat in spinocerebellar ataxia type 2. Nat Genet 1996;14:269–276.
3. Imbert G, Saudou F, Yvert G, et al. Cloning of the gene for spinocerebellar ataxia 2 reveals a locus with high sensitivity to expanded CAG/glutamine repeats. Nat Genet 1996;14:285–291.
4. Cancel G, Durr A, Didierjean O, et al. Molecular and clinical correlations in spinocerebellar ataxia 2: a study of 32 families. Hum Mol Genet 1997;6:709–715.
5. Schöls L, Gispert S, Vorgerd M, et al. Spinocerebellar ataxia type 2: genotype and phenotype in German kindreds. Arch Neurol 1997;54:1073–1080.
6. Giuffrida S, Lanza S, Restivo DA, et al. Clinical and molecular analysis of 11 Sicilian SCA2 families: influence of gender on age at onset. Eur J Neurol 1999;6:301–307.
7. Malandrini A, Galli L, Villanova M, et al. CAG repeat expansion in an Italian family with spinocerebellar ataxia type 2 (SCA2): a clinical and genetic study. Eur Neurol 1998;40:164–168.
8. Gambardella A, Annesi G, Bono F, et al. CAG repeat length and clinical features in three Italian families with spinocerebellar ataxia type 2 (SCA2): early impairment of Wisconsin Card Sorting Test and saccade velocity. J Neurol 1998;245:647–652.
9. Wells RD, Warren ST. Genetic instabilities and hereditary neurological diseases. San Diego: Academic Press, 1998.

Isolated musculocutaneous neuropathy caused by a proximal humeral exostosis

Article abstract—We report an isolated musculocutaneous neuropathy caused by a proximal humeral osteochondroma that became symptomatic after the patient played recreational basketball. Lesion resection resulted in complete deficit resolution. Mass lesions involving the musculocutaneous nerve should be considered in patients with atraumatic, isolated musculocutaneous neuropathies that are recurrent or fail to recover, even in the setting of strenuous exercise. **Key words:** Musculocutaneous neuropathy—Osteochondroma—Exostosis.

NEUROLOGY 2000;54:494–496

V.C. Juel, MD; J.M. Kiely, MD, PhD; K.V. Leone, MD; R.F. Morgan, MD, DMD, FACS; T. Smith, MD; and L.H. Phillips II, MD

Musculocutaneous neuropathy occurs most commonly in the context of trauma and is infrequently isolated.[1] Atraumatic cases of isolated musculocutaneous neuropathy are unusual, and cases have been related to strenuous exercise without apparent underlying disease.[2-5] We report an isolated musculocutaneous neuropathy after a recreational game of basketball in an otherwise healthy young man. Evaluation revealed a proximal humeral osteochondroma involving the musculocutaneous nerve.

Case report. A 22-year-old, left-handed man with no previous medical history developed painless right biceps brachii weakness and mild right anterolateral forearm tingling the morning after playing recreational basketball. Over the next 9 days, the symptoms evolved to complete inability to contract the right biceps brachii along with significantly reduced sensation and intensified tingling paresthesia on the right ventral forearm. There was no pain, antecedent trauma, or intercurrent illness.

Physical examination performed 9 days after symptom onset revealed normal brachial and radial pulses. No axillary masses were detected. The neurologic examination was remarkable for atrophy of the right biceps brachii, which the patient was unable to contract. Right forearm flexion was overcome with minimal resistance in full supination. With the forearm pronated, however, forearm flexion was overcome with maximal resistance. Supination was overcome with mild to moderate resistance with the right forearm flexed at 90 degrees. Anterior elevation of the right arm was full strength. Results of muscle strength testing were otherwise normal. Sensation was reduced to light touch and pinprick in a 3.5-cm–wide strip on the right anterolateral forearm from the elbow crease to the base of the thumb. The right biceps brachii tendon reflex was absent with otherwise normal deep tendon reflexes.

Electrodiagnostic studies were performed 14 days after symptom onset. Right median and ulnar motor and antidromic sensory nerve conduction studies were normal. Lateral antebrachial cutaneous sensory responses were normal bilaterally. Normal left and no right musculocutaneous motor responses were recorded with surface electrodes from the biceps brachii after stimulation at the axilla and at Erb's point. Concentric needle examination revealed normal insertional activity, no spontaneous activity, normal motor unit morphology, and markedly reduced motor unit recruitment in both heads of the right biceps brachii and in right brachialis. Findings were normal in right coracobrachialis, pronator teres, brachioradialis, triceps brachii, deltoid, and cervical paraspinal muscles. The findings suggested a right musculocutaneous neuropathy at or distal to its passage through the coracobrachialis muscle. Although the findings were compatible with neurapraxia, it was premature to exclude the possibility of axonal injury by the early absence of fibrillation potentials in paretic muscles.

Three weeks after symptom onset, the patient's symptoms and examination findings were unimproved, and a fullness in the medial aspect of the proximal humerus was appreciated. MRI of the right brachial plexus and proximal humerus was performed subsequently to evaluate for mass lesions associated with the proximal musculocutaneous nerve. A moderately pedunculated 2 × 2 cm bony protrusion arising medially and just distal to the proximal metaphysis was visualized (figure 1). The overlying cortex was contiguous with that of surrounding normal bone, and the signal within the lesion was equivalent to normal marrow. The cartilaginous cap of the lesion was less than 1 cm in maximal diameter, which suggested a benign process. The lesion impinged on the right musculocutaneous nerve after its origin from the lateral cord but did not apparently invade these neural elements. These findings suggested a benign metaphyseal osteochondroma of the humerus.

The lesion was resected using an anterior approach to the right humerus and proximal shoulder. A mass was identified between the pectoralis major medially and the deltoid muscle laterally (figure 2). The right musculocutaneous nerve was displaced by this bony lesion. External rotation of the arm caused the musculocutaneous nerve to stretch over the mass. At the site of displacement, the musculocutaneous nerve exhibited grossly visible vascular inflammation. No significant fibrosis or scarring was visualized on extensive dissection. The lesion was resected, and a 3 × 2 × 2 cm specimen was pathologically reviewed. Histopathologic features of a smooth cartilaginous surface and normal marrow confirmed the diagnosis of benign osteochondroma.

From the Departments of Neurology (Drs. Juel, Kiely, Leone, and Phillips) and Plastic Surgery (Drs. Morgan and Smith), University of Virginia School of Medicine, Charlottesville.

Received January 28, 1998. Accepted in final form August 6, 1999.

Address correspondence and reprint requests to Dr. Vern C. Juel, Department of Neurology, Box 394, University of Virginia School of Medicine, Charlottesville, VA 22908.

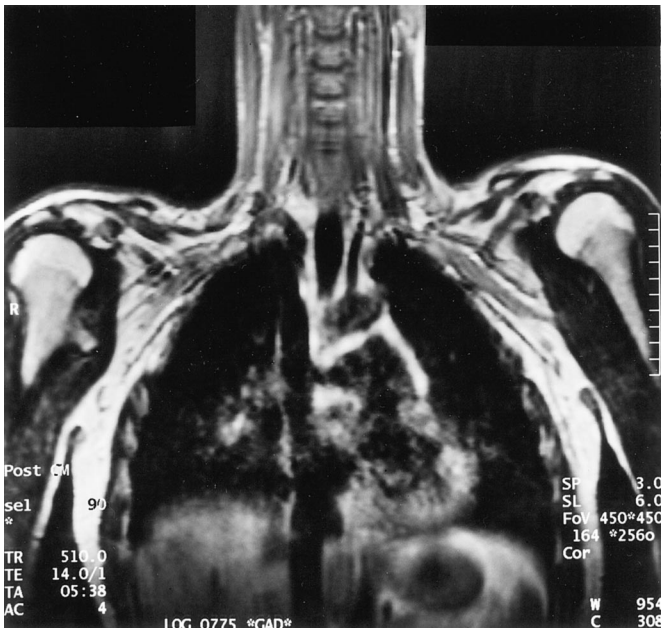

Figure 1. MRI of right brachial plexus and proximal humeral region with T1-weighted spin-echo sequence and gadolinium enhancement. A moderately pedunculated 2 × 2 cm bony protrusion arises medially and just distal to the proximal metaphysis. The lesion impinges on the musculocutaneous nerve distal to its origin from the lateral cord.

Figure 2. Operative exposure of a proximal humeral exostosis between the pectoralis major (medial) and the deltoid (lateral). A ligature is placed beneath the musculocutaneous nerve that is displaced by the lesion.

Within a few days postoperatively, the patient reported the return of normal sensation in the right lateral forearm. Voluntary contraction of the right biceps brachii returned after about 1 week. Three months postoperatively, the patient exhibited normal right biceps brachii muscle bulk and strength. Sensation was normal in the right lateral antebrachial cutaneous distribution. The right biceps brachii tendon reflex had returned and was normal.

Repeat electrodiagnostic studies performed 3 months postoperatively revealed a normal right musculocutaneous motor response in the biceps brachii with stimulation at Erb's point. A discrete right musculocutaneous motor response was not obtainable from stimulation in the axilla, which was attributed to the technical effect of postsurgical changes in this area. The evolution of electrophysiologic findings suggested a resolving neurapraxic lesion, given the initial findings of a normal right lateral antebrachial cutaneous sensory response and absence of fibrillation potentials in biceps brachii and brachialis followed by rapid postoperative recovery. Although conduction block of the musculocutaneous motor response was not demonstrated preoperatively, this might have been a technical effect of the axillary stimulation site being proximal to the lesion.

Discussion. Atraumatic, isolated musculocutaneous neuropathies are rare. Reported cases have been associated with positioning during general anesthesia[6] and peripheral nerve tumors.[7] Several cases have been attributed to strenuous upper extremity exercise without apparent underlying disease.[2-5] These activities included weight lifting,[2] football throwing,[3] rowing,[4] and carrying heavy textile rolls on the shoulder with the arm curled over the roll.[5] Mechanisms proposed for these exercise-related cases include entrapment within the coracobrachialis[2,4,5] as well as traction between a proximal fixation point at the coracobrachialis and a distal fixation point at the deep fascia at the elbow.[1] In one of these cases, a conduction block was demonstrated in the musculocutaneous nerve between the Erb's point and axillary stimulation sites to suggest coracobrachialis entrapment.[5] Because the musculocutaneous nerve does not penetrate the coracobrachialis muscle in some anatomic variants,[1] coracobrachialis entrapment may not account for all of the exercise-related cases.

Osteochondromas may arise from the metaphyses of endochondral and particularly from long bones as cartilage-capped exostoses. Humeral exostoses have resulted in axillary[8] and radial[9] mononeuropathies through direct impingement. A proximal humeral exostosis also resulted in a false aneurysm of the axillary artery with a secondary brachial plexopathy.[10] In all of these cases, the neuropathic symptoms were preceded by upper extremity exercise: a swimming contest in the axillary neuropathy case, overhead tennis serving in the radial neuropathy case, and weight training and football throwing in the patient with false aneurysm and brachial plexopathy.

In our patient with isolated musculocutaneous neuropathy and in the other reported patients

with humeral exostoses causing proximal upper extremity neuropathies, the neuropathic symptoms were initially elicited by some form of strenuous upper extremity exercise. Therefore, an etiology of coracobrachialis entrapment or traction should not be assumed when isolated musculocutaneous neuropathies develop in the context of upper extremity exercise.

Acknowledgment

The authors thank G.F. Wooten, MD, for referring the patient.

References

1. Sunderland S. The musculocutaneous nerve. In: Sunderland S, ed. Nerves and nerve injuries. Edinburgh: Churchill Livingstone, 1978:796–801.
2. Braddom RL, Wolfe C. Musculocutaneous nerve injury after heavy exercise. Arch Phys Med Rehabil 1978;59:290–293.
3. Kim SM, Goodrich JA. Isolated musculocutaneous nerve palsy: a case report. Arch Phys Med Rehabil 1984;65:735–736.
4. Mastaglia FL. Musculocutaneous neuropathy after strenuous physical activity. Med J Aust 1986;145:153–154.
5. Sander HW, Quinto CM, Elinzano H, Chokroverty S. Carpet carrier's palsy: musculocutaneous neuropathy. Neurology 1997;48:1731–1732.
6. Dundore DE, DeLisa JA. Musculocutaneous nerve palsy: an isolated complication of surgery. Arch Phys Med Rehabil 1979; 60:130–133.
7. Lusk MD, Kline DG, Garcia CA. Tumors of the brachial plexus. Neurosurgery 1987;21:439–453.
8. Witthaut J, Steffens KJ, Koob E. Intermittent axillary nerve palsy caused by a humeral exostosis. J Hand Surg 1994;19B: 422–423.
9. Coenen L. High radial nerve palsy caused by a humeral exostosis: a case report. J Hand Surg 1992;17A:668–669.
10. Gerrand CH. False aneurysm and brachial plexus palsy complicating a proximal humeral exostosis. J Hand Surg 1997; 22B:413–415.

Atypical Friedreich ataxia phenotype associated with a novel missense mutation in the *X25* gene

Article abstract—We describe two sisters with early onset gait ataxia, rapid disease progression, absent or very mild dysarthria and upper limb dysmetria, retained knee jerks in one, slight to moderate peripheral nerve involvement, and diabetes. Molecular analysis showed that they are compound heterozygotes for GAA expansion and a novel exon 5a missense mutation (R165P). This mutation appears to be associated with an atypical but not milder Friedreich ataxia phenotype. **Key words:** Friedreich ataxia—Phenotype—Missense mutation—*X25* gene.

NEUROLOGY 2000;54:496–499

G. De Michele, MD; A. Filla, MD; F. Cavalcanti, MD; A. Tammaro, PhD; A. Monticelli, MD; L. Pianese, PhD; F. Di Salle, MD; A. Perretti, MD; L. Santoro, MD; G. Caruso, MD; and S. Cocozza, MD

Friedreich ataxia (FRDA) is an autosomal recessive neurodegenerative disorder clinically characterized by progressive gait and limb ataxia, dysarthria, pyramidal weakness, loss of tendon reflexes and decreased vibration sense in the lower limbs, Babinski sign, and skeletal deformities. Cardiomyopathy is frequent and diabetes mellitus may occur in the late stages of the disease. Onset is usually around puberty and the disease shows a relentless progression leading to need for a wheelchair about 15 years after the onset.

The gene responsible for FRDA (*X25*) comprises six coding exons and encodes for a 210-amino acid protein, frataxin, located at the inner mitochondrial membrane.[1,2] Ninety-six percent of patients are homozygous for the expansion of a polymorphic GAA trinucleotide repeat in the first intron of *X25*. The remaining cases are compound heterozygotes for GAA expansion and a different mutation of *X25*.[3]

The trinucleotide repeat probably interferes with gene transcription and levels of frataxin are reduced in patients homozygous for the GAA expansion.[1,2] Both suppression of frataxin expression and severity of clinical presentation are proportional to the length of the trinucleotide repeat.[4,5]

We report a novel exon 5a missense mutation (R165P) in two affected sisters. The mutation appears to be associated with a variant FRDA phenotype.

Methods. *Neurophysiologic study.* The evoked potentials and nerve conduction recordings were performed using a Dantec (Copenhagen, Denmark) counterpoint electromyograph. Somatosensory evoked potentials for median nerve stimulation were recorded according to standard technique. Orthodromic sensory (SCV) and motor (MCV) conduction velocities were measured along the median and tibial nerves using needle electrodes.

From the Departments of Neurological Sciences (Drs. Caruso, De Michele, Filla, Perretti, and Santoro), Molecular and Cellular Biology and Pathology and CEOS (Drs. Tammaro, Monticelli, Pianese, and Cocozza), and Radiology (Dr. Di Salle), Federico II University, Naples; and the Institute of Experimental Medicine and Biotechnology, CNR (Dr. Cavalcanti), Cosenza, Italy.

Supported in part by a grant from MURST 40% to A.F. (Project: Encefaloneuromiopatie genetiche) and grant 969 from Italian Telethon to S.C.

Received July 8, 1999. Accepted in final form September 11, 1999.

Address correspondence and reprint requests to Prof. Alessandro Filla, Clinica Neurologica, Università Federico II, via Pansini 5, 80131 Napoli, Italy; e-mail: afilla@unima.it

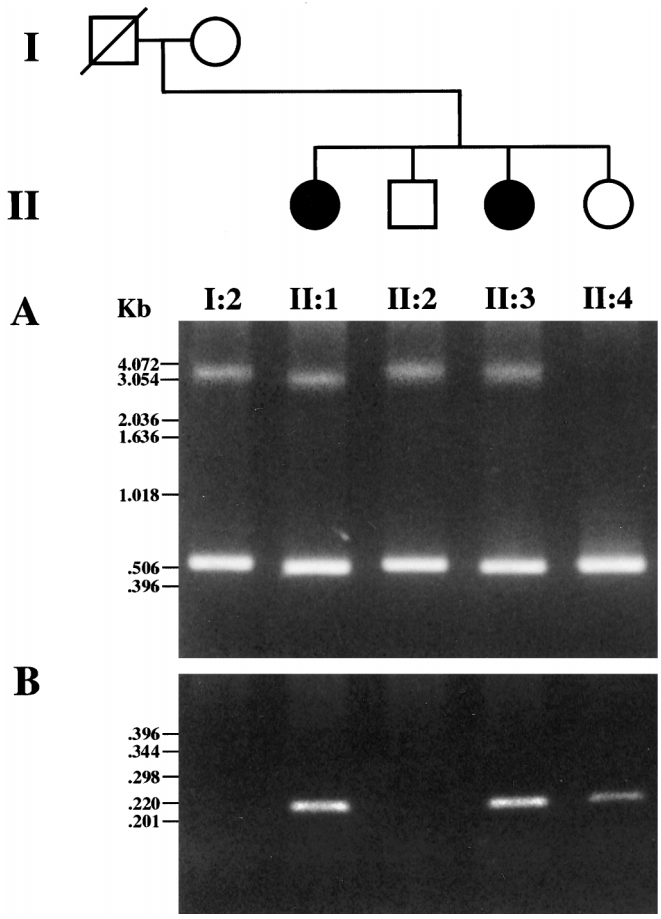

Figure 1. Segregation of the GAA expansion and of the R165P missense mutation in the family. (A) PCR amplification of the GAA triplet repeat: lanes I:2, II:1, II:2, and II:3 show both normal and expanded alleles; lane II:4 shows only normal alleles. (B) Allele-specific amplification–PCR of the R165P mutation: lanes II:1, II:3, and II:4 show specific amplification product.

Molecular analysis. Long-expand PCR amplification of the GAA triplet expansion and PCR of individual frataxin exons were performed as previously described.[6] We screened all six frataxin coding exons (exons 1–4, 5a, and 5b) for mutations by single-strand conformational polymorphism (SSCP).[1]

Exon 5a PCR product was subcloned in *Escherichia coli* (TA Cloning Kit; Invitrogen, Carlsbad, CA) and subclones containing the two different alleles were screened for SSCP. The gel-purified PCR products (Agarose Gel DNA Extraction Kit; Boehringer Mannheim, Indianapolis, IN) of the clones representing the two different alleles were sequenced (Silver Sequence DNA Sequencing System; Promega, Madison, WI) using the previously described oligoprimer ex5aR.[1]

Allele-specific amplification (ASA) was performed to confirm the presence of the novel mutation and to determine its frequency. Primer for ASA-PCR (ex5aF/mR165P) was 5′-TTCCAGTGGACCTAAGCC-3′. This primer was used with the reverse ex5a primer using reaction conditions previously described for exon 5a amplification,[1] except that the annealing temperature was 58 °C and that Perfect Match Polymerase Enhancer (Stratagene; La Jolla, CA) was added to ensure selective amplification of the mutation. AmpliTaq Gold (Perkin Elmer, Foster City, CA) was used.

Table. *Clinical and electrophysiologic findings*

Characteristics	Subject II-1	Subject II-3
Age at examination, y/sex	32/F	23/F
Age at onset/age to wheelchair, y	8/19	3/12
Abnormal gait and stance	+++	+++
Dysarthria	−	+
Optic atrophy	−	−
Abnormal eye movements*	−	+
Finger-to-nose dysmetria	−	+
Upper limb tendon jerks	Brisk	Brisk
Knee jerks	Absent	Brisk
Lower limb weakness	+++	+++
Lower limb increased tone	−	++
Lower limb decreased vibration/position sense	+/+	+++/++
Plantar response	Extensor	Extensor
Scoliosis/pes cavus	−/++	+/++
Abnormal ECG†/echocardiogram	+/−	+/−
Abnormal brain and cord MRI	−	−
Sensory conduction velocities (distal segments)		
Median nerve (lower limit 48 m/sec)	45	35
Tibial nerve (lower limit 36 m/sec)	30	28
SAP amplitude		
Wrist (lower limit 6.0 μV)	6.6	3.8
Medial malleolus (lower limit 0.2 μV)	0.6	0.2
Motor conduction velocities (distal latency)		
Median nerve (upper limit 3.8 msec)	4.1	4.9
Tibial nerve (upper limit 4.8 msec)	5.2	7.1

Upper and lower limits refer to normal controls from the laboratory.

* Jerky smooth pursuit.
† Repolarization abnormalities.

− = Absent; + = mild; ++ = moderate; +++ = severe; SAP = sensory action potential.

Case report. Among 149 patients who received a molecular diagnosis of FRDA, 139 were homozygous for the GAA expansion and 10 were compound heterozygotes. Six of them carried the I154F mutation, one carried the W173G mutation, and one 482 +3delA; these have been reported.[1,3] The last two patients are presented in this study.

The family pedigree is shown in figure 1. Parents are not consanguineous and originate from different villages of southern Italy. Two offspring (II-1 and II-3) are affected. The disease presented with gait disturbances and frequent falls in childhood and the patients were confined to a wheelchair in their teens. Insulin-dependent diabetes mellitus developed at age 27 in II-1. Diabetes appeared at age 22 in II-3, who is taking gliclazide. Both sisters have bipo-

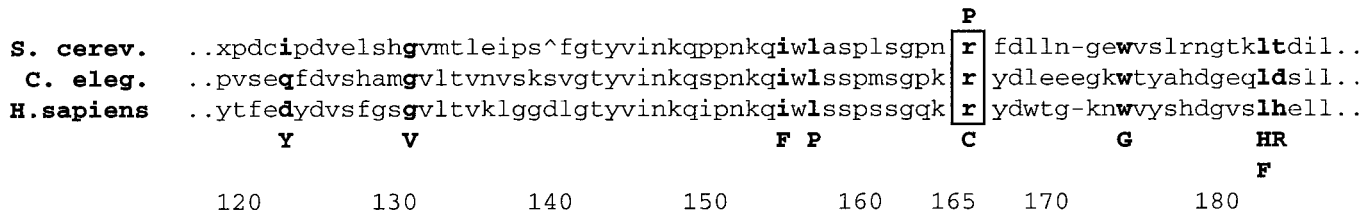

Figure 2. Multiple alignment of conserved frataxin region in S. cerevisiae, C. elegans, *and* Homo sapiens. *Amino acid residues where missense mutations were found are indicated in bold. The substituted amino acids are indicated. Arginine at position 165 is boxed.*

lar disorder and psychosis with delusions. Another sibling (II-4) also has bipolar affective disorder.

The two sisters were first seen in 1988 and received a diagnosis of familial spastic paraplegia. The current neurologic examination is shown in the table. Neurophysiologic investigation of the peripheral nerve showed slight distal slowing of SCV and MCV and very slight reduction of the amplitude of sensory potentials in Patient II-1. These abnormalities were more evident in Patient II-3, with absence of the sensory potential at popliteal fossa. The study of somatosensory evoked potentials showed a moderate prolongation of central conduction time in both and reduction of N20 wave amplitude in II-3. Brainstem evoked potentials were normal in both.

Results. Long-expand PCR analysis of the frataxin GAA triplet repeat expansion revealed one maternally derived expanded allele of 940 (II-1) and 1100 (II-3) GAA triplet repeats and a normal deduced paternally derived unexpanded allele (see figure 1).

SSCP analysis of the entire frataxin coding sequence revealed a different migration of the exon 5a PCR product from the two affected sisters with respect to a wild-type DNA. DNA sequencing of two different clones containing the SSCP variant of exon 5a revealed a G to C transversion at nucleotide 494. This novel mutation in exon 5a is predicted to result in a substitution of an arginine for a proline at amino acid position 165 (R165P).

To confirm the presence of R165P mutation, we designed an ASA-PCR using an oligoprimer with the last nucleotide at the 3′ end matching to the mutated nucleotide. The presence of the product in the two affected sisters and its absence in the mother unequivocally showed that the missense mutation has been paternally inherited (see figure 1). Their brother (II-2) is heterozygous for the expansion and their sister (II-4) for the point mutation. ASA-PCR was also used to screen 100 normal chromosomes from a southern Italian population, none of which was found to have this mutation. This finding suggests that the R165P mutation is not a polymorphism but a disease-causing mutation.

This nonconservative amino acid change leads to substitution of a basic hydrophilic with a neutral hydrophobic residue and affects an invariant position within the highly evolutionary conserved domain in the C-terminus of frataxin (figure 2).

Discussion. Point mutations represent the first genetic abnormality found in FRDA patients, which pointed out *X25* as the responsible gene. The expansion of a polymorphic GAA triplet repeat in the first intron of the gene was detected subsequently.[1] However, the majority of patients are homozygous for the expansion and few compound heterozygotes for GAA expansion and point mutations have been described.[1,3,7-10] A recent cooperative study[3] suggested that truncating mutations, independently from their location, and missense mutations in the C-terminus of mature frataxin result in a typical phenotype, whereas the missense mutations located in the N-terminus may cause an atypical and milder phenotype. Heterozygous patients carrying D122Y and G130V mutations—that is, missense mutations in the N-terminus—have slow disease progression, lower limb retained tendon reflexes, and absent dysarthria.

Here we describe a novel missense mutation located at the carboxy-terminal half of mature frataxin associated with an atypical but not milder FRDA phenotype. Onset age was earlier than in patients homozygous for GAA expansion and close to that reported by Cossèe et al.[3] in their study on 25 heterozygous patients (9.6 ± 6.9 years of age). Disease progression was fast in our patients and both were wheelchair-bound in their teens. Tendon reflexes were brisk at upper limbs in both and at knees in Patient II-3. Peculiar to our patients is absent or very mild dysarthria and upper limb dysmetria.

This report, in agreement with a recent study,[9] shows that patients with mutations in the C-terminus of the protein may show retained reflexes and minimal-absent dysarthria. Patient 3 in the article by Forrest et al.[9] is heterozygous for the R165C point mutation and a 381 repeat expansion. The resulting phenotype is atypical, but milder than in our patients, who have a different mutation in the same codon and a larger expansion. Different length of the GAA expansion or different amino acid substitution may account for the later onset (23 years) in the patient with the R165C mutation.

Another interesting characteristic of our patients is that some clinical manifestations of the disease, such as early onset and fast progression, are severe, whereas other features are not. Cerebellar impairment is mild, as shown by absent or minimal dysarthria and by normal cerebellum at MRI. Peripheral nerve involvement appears to be slight to moderate at neurophysiologic testing. Lower limb weakness and Babinski sign in both and increased tone and tendon jerks in one sister suggest marked corticospinal involvement and led to the diagnosis of familial

spastic paraplegia. The absence of spinal cord atrophy at MRI and the normal brainstem evoked potentials are unusual in patients in late disease stage. Also, patients with the G130V mutation show different severity of the disease features, with early onset, slow progression, mild cerebellar signs, and clear corticospinal involvement.[3,8]

A possible explanation for the variable severity of the clinical features is that frataxin has more than one function and that such functions are differently relevant for distinct neuronal populations. According to this hypothesis, homozygous GAA expansions and heterozygous truncating mutations determine reduced protein availability and uniform impairment of the central and peripheral nervous systems. Conversely, missense point mutations might lead to the synthesis of an abnormal frataxin and this might differently affect the protein functions or its interaction with partner proteins, causing specific impairment of some neuronal populations and, therefore, atypical clinical phenotypes.

References

1. Campuzano V, Montermini L, Moltò MD, et al. Friedreich's ataxia. Autosomal recessive disease caused by an intronic GAA triplet repeat expansion. Science 1996;271:1423–1427.
2. Campuzano V, Montermini L, Lutz Y, et al. Frataxin is reduced in Friedreich ataxia patients and is associated with mitochondrial membranes. Hum Mol Genet 1997;6:1771–1780.
3. Cossée M, Dürr A, Schmitt M, et al. Friedreich ataxia: point mutations and clinical presentation of compound heterozygotes. Ann Neurol 1999;45:200–206.
4. Filla A, De Michele G, Cavalcanti F, et al. The relationship between trinucleotide (GAA) repeat length and clinical features in Friedreich's ataxia. Am J Hum Genet 1996;59:554–560.
5. Dürr A, Cossée M, Agid Y, et al. Clinical and genetic abnormalities in patients with Friedreich's ataxia. N Engl J Med 1996;335:1169–1175.
6. De Michele G, Cavalcanti F, Criscuolo C, et al. Parental gender, age at birth and expansion length influence GAA repeat intergenerational instability in the X25 gene: pedigree study and analysis of sperm from patients with Friedreich's ataxia. Hum Mol Genet 1998;7:1901–1906.
7. Cossée M, Campuzano V, Koutnikova, et al. Frataxin fracas. Nat Genet 1997;15:337–338.
8. Bidichandani SI, Ashizawa T, Patel PI. Atypical Friedreich ataxia caused by compound heterozygosity for a novel missense mutation and the GAA triplet-repeat expansion. Am J Hum Genet 1997;60:1251–1256.
9. Forrest SM, Knight M, Delatycki MB, et al. The correlation of clinical phenotype in Friedreich ataxia with the site of point mutations in the FRDA gene. Neurogenetics 1998;1:253–257.
10. Bartolo C, Mendell JR, Prior TW. Identification of a missense mutation in a Friedreich's ataxia patient: implications for diagnosis and carrier studies. Am J Med Genet 1998;79: 396–399.

Micturitional disturbance in pure autonomic failure

Article abstract—We obtained micturitional histories and performed urodynamic studies in six patients with pure autonomic failure. All patients had urinary symptoms. Urodynamic studies showed postmicturition residuals in two, small bladder capacities in two, detrusor hyperreflexia in four, low bladder compliance in two, detrusor-external sphincter dyssynergia in one, neurogenic sphincter electromyography in three, and denervation supersensitivity of the bladder in two. Micturitional disturbance is a common feature in pure autonomic failure because of peripheral and central types of abnormalities. **Key words:** Pure autonomic failure—Neurogenic urinary incontinence—Urodynamic study—Detrusor hyperreflexia.

NEUROLOGY 2000;54:499–501

R. Sakakibara, MD; T. Hattori, MD; T. Uchiyama, MD; M. Asahina, MD; and T. Yamanishi, MD

Pure autonomic failure (PAF) is an idiopathic, sporadic disorder characterized by orthostatic hypotension usually with evidence of more widespread autonomic failure.[1,2] No other neurologic features are present, such as apparent parkinsonism or cerebellar or pyramidal signs, distinguishing this disorder from autonomic failure with multiple system atrophy (AF with MSA) or autonomic failure with PD (AF with PD).[1,2] Micturitional disturbance is described as one of the features in PAF. However, few reports are available of urodynamic studies in PAF that show detrusor hyperreflexia[3] and detrusor areflexia with denervation supersensitivity.[4] We describe the results of our detailed micturitional histories and urodynamic studies in PAF.

From the Departments of Neurology (Drs. Sakakibara, Hattori, Uchiyama, and Asahina) and Urology (Dr. Yamanishi), Chiba University, Chiba, Japan.

Received February 2, 1999. Accepted in final form September 11, 1999.

Address correspondence and reprint requests to Dr. Ryuji Sakakibara, Department of Neurology, Chiba University, 1-8-1 Inohana Chuo-ku, Chiba 260-8670 Japan.

Methods. We reviewed the records of six patients with PAF according to the published criteria.[1,2] They included five men and one woman, with mean age at onset of 59 years (range 46 to 66 years) and mean duration of 8 years

(range 4 to 18 years) (table). None of the patients had cerebellar or pyramidal signs. Four of six patients had increased rigidity of the wrist and ankle in response to contralateral muscle activation, which appeared 8.8 years (range 3 to 16 years) after the onset of autonomic symptoms. However, they lacked resting tremor, postural instability, or other evidence of PD. None of the patients were bedridden. All six patients had orthostatic hypotension, and mean systolic pressure decrease was 44 mm Hg (34 to 73 mm Hg) (normal <20 mm Hg) with minimal or no heart rate increase. Mean supine plasma noradrenaline level was 55.6 pg/mL (10 to 87 pg/mL) (normal >100 pg/mL). Mean coefficient of variation of the R-R interval was 0.7 (0.34 to 1.77) (normal >1.5). Mean increment of blood pressure was 76 mm Hg (range 53 to 118) (normal ≤30 mm Hg) in response to noradrenaline infusion at the rate of 0.1 mg/kg/min for 6 minutes, suggestive of denervation supersensitivity of the vessels. Brain CT scan and MRI showed no evidence of atrophy of the cerebellum or the brainstem, nor abnormal intensity in the putamen suggesting MSA. There was no abnormality in the EKG, chest roentgenogram, blood chemistry (including blood sugar), or urinalysis. None of the men had apparent prostate hypertrophy by ultrasound echography.

Detailed histories of urinary symptoms were obtained from all patients. Urodynamic studies consisted of measurement of postmicturition residuals, urethral pressure profilometry, and water cystometry with simultaneous external sphincter electromyography (EMG). A bethanechol test was performed as follows. After filling with 100 mL of water, 2.5 mg of bethanechol chloride was injected subcutaneously. Denervation supersensitivity of the detrusor is defined as detrusor pressure increase over 15 cm H_2O during a 30- minute observation.

Results. *Results of micturitional histories.* All of the patients had urinary symptoms (see table). The most common urinary symptom was nocturnal urinary frequency (more than twice a night) in six patients, followed by sensation of urgency in five and voiding difficulty (urinary hesitation, prolongation, straining, or sensation of residual urine) in five. Urinary incontinence was found in two patients, including urge type in one and stress type in one. The proportion of storage symptoms (e.g., urgency, frequency) over voiding symptoms (e.g., hesitation, prolongation) is six/five in the patients. One patient (Patient 4) was shown to have urinary symptoms at the onset of disease, whereas the other patients had urinary symptoms after the appearance of impotence or orthostatic faintness. Storage and voiding symptoms emerged almost at the same time in five patients.

Results of urodynamic studies. Two of six patients had residual urine of 126 mL (Patient 5; 10 years' duration) and 320 mL (18 years' duration). Urethral pressure profilometry was performed in three patients, and maximum urethral closure pressure was normal in all of them. Water cystometry showed decreased first sensation in one (Patient 4; 20 mL) and decreased bladder capacity in two (Patient 3, 150 mL; Patient 4, 80 mL). Four patients (Patients 2, 3, 4, and 5) had detrusor hyperreflexia, and two (Patients 1 and 6) had low bladder compliance. The bethanechol test was performed in three of the patients and showed denervation supersensitivity of the bladder in two (Patients 1 and 6 of Patients 1, 5, and 6). External sphincter EMG showed that one patient (Patient 6) had detrusor-

Table *Patients and micturitional symptoms*

	Patient no.					
Characteristic	1	2	3	4	5	6
Age at onset, y/sex	59/M	64/F	66/M	64/M	56/M	46/M
Initial symptoms	Impotence	Orthostatic syncope	Orthostatic faintness	Voiding difficulty, constipation	Impotence	Orthostatic faintness
Disease duration, y	4	4	6	9	10	18
Appearance of minimum rigidity, y after onset	–	3	6	–	10	16
Autonomic signs and symptoms						
Orthostatic syncope	+	+	+	+	+	+
Horner's syndrome	−	−	+	−	−	−
Laryngeal stridor	−	−	−	−	−	−
Perspiratory abnormality	+	+	+	+	−	+
Erectile dysfunction	+	N/A	?	?	+	+
Constipation	+	+	+	+	+	+
Micturitional symptoms						
Nocturnal frequency	+	+	+	+	+	+
Diurnal frequency	−	−	−	−	+	−
Urgency	−	+	+	+	+	+
Incontinence	Stress	−	Urge	−	−	−
Hesitancy/prolongation	+	+	+	+	−	+

N/A = not applicable.

sphincter dyssynergia, and none had uninhibited sphincter relaxation. EMG of the external urethral sphincter was performed in four patients, and neurogenic motor unit potentials were found in three of them (Patients 1, 2, and 5).

Discussion. PAF is clinically characterized by widespread autonomic failure without CNS involvement.[1,2] None of our patients had cerebellar or pyramidal signs. Four of the patients had minimum induced rigidity that appeared 8.8 years after the onset of autonomic symptoms. However, they lacked other evidence suggestive of AF with PD or AF with MSA. The current study showed that all six patients had urinary symptoms, indicating the frequent occurrence of micturitional disturbance in patients with PAF. The most common urinary symptom was nocturnal urinary frequency in six patients, followed by sensation of urgency in five and voiding difficulty in five, and urinary incontinence was found in two patients (33%). Residual urine was found in two (25%) (both over 100 mL and noted 10 years after onset of the disease), and none were in a state of urinary retention. Micturitional disturbance in PAF can be compared with that in MSA. In our previous study,[5] 98% of 86 patients with MSA had micturitional disturbance, including urinary incontinence in 56% and residual urine in 79%. Residual urine over 100 mL or retention was found in 51% of the patients. The results indicate that micturitional disturbance in PAF seems to be as common but less severe than that in MSA, probably reflecting slower progression of the disease[2] and less vulnerability of the urinary innervation in PAF.

Cystometry showed that two patients with PAF had low bladder compliance, indicating a preganglionic lesion of the pelvic nerves. The bethanechol test showed that two of three patients studied had denervation supersensitivity of the detrusor, indicating postganglionic lesion of the pelvic nerve.[4] These findings match the pathologic reports of neuronal cell loss in the intermediolateral (IML) columns of the spinal cord,[4,6,7] Lewy bodies in the IML cells[7] and in the bladder wall,[6] and the physiologic studies suggesting postganglionic abnormalities in PAF.[2] EMG of the external urethral sphincter showed neurogenic findings in three of four patients. This is evidence of pudendal nerve dysfunction.[8] This finding suggests the involvement of the sacral Onuf's nucleus or its fibers with the external sphincter in PAF. The urodynamic study also showed detrusor hyperreflexia in four of six (66%) patients, indicating the frequent occurrence of supranuclear parasympathetic lesions in this disorder.[3] External sphincter EMG showed that one patient had detrusor-sphincter dyssynergia, indicating a supranuclear pudendal lesion. The locus ceruleus, known as the pontine micturition center,[9,10] and nigrostriatal dopaminergic system, both having a role in regulating micturition in experimental animals and in humans,[9,10] are known to be involved in this disorder.[3,6] Lesions in these sites may contribute to the supranuclear type of micturitional disturbance in PAF. From these results, the responsible sites of micturitional disturbance in PAF seem to be both peripheral and central nervous system regulating the lower urinary tract. Our previous study in MSA[5] showed detrusor hyperreflexia in 62%, low bladder compliance in 28%, bethanechol supersensitivity in 75%, detrusor-sphincter dyssynergia in 32%, and neurogenic sphincter EMG in 65% of the patients, which resemble those in PAF. However, involvement of the evacuating function seems to be less severe in patients with PAF.

References

1. The Consensus Committee of the American Autonomic Society and the American Academy of Neurology. Consensus statement on the definition of orthostatic hypotension, pure autonomic failure, and multiple system atrophy. Neurology 1996; 46:1470.
2. Low PA, Bannister R. Multiple system atrophy and pure autonomic failure. In: Low PA, ed. Clinical autonomic disorders. 2nd ed. Philadelphia: Lippincott-Raven, 1997:555–575.
3. Terao Y, Takeda K, Sakuta M, Nemoto T, Takemura T, Kawai M. Pure progressive autonomic failure: a clinicopathological study. Eur Neurol 1993;33:409–415.
4. Santangelo L, Mandarino G, de Biase L, Pesce F, Giacomini P. Multisystem evaluation in one case of pure autonomic failure. Funct Neurol 1991;6:275–278.
5. Sakakibara R, Hattori T, Tojo M, Yamanishi T, Yasuda K, Hirayama K. Micturitional disturbance in multiple system atrophy. Jpn J Psychiatr Neurol 1993;47:591–598.
6. Hague K, Lento P, Morgello S, Caro S, Kaufmann H. The distribution of Lewy bodies in pure autonomic failure: autopsy findings and review of the literature. Acta Neuropathol 1997; 94:192–196.
7. Johnson RH, Lee de J, Oppenheimer DR, Spalding JMK. Autonomic failure with orthostatic hypotension due to intermediolateral column degeneration: a report of two cases with autopsies. Q J Med 1966;35:276–292.
8. Fowler CJ. Pelvic floor neurophysiology. In: Binnie C, ed. Clinical neurophysiology. Oxford: Butterworth-Heinemann, 1995:233–250.
9. Blok BFM, Holstege G. A PET study on brain control of micturition in humans. Brain 1997;120:111–121.
10. Sakakibara R, Fowler CJ, Hattori T. Voiding and MRI analysis of the brain. Int Urogynecol J 1999;10:192–199.

An FDOPA PET study in patients with periodic limb movement disorder and restless legs syndrome

Article abstract—The authors investigated nine drug-naïve patients with periodic limb movement disorder and restless legs syndrome (PLMD-RLS) and 27 healthy controls with PET using 6-[^{18}F]fluoro-L-dopa (FDOPA). In the patients, the FDOPA uptake (K_i^{occ}) in the caudate nucleus was 88% and in the putamen 89% of the control mean values. This equal affection of the caudate and the putamen differs, for example, from the dopaminergic dysfunction in Parkinson's disease, which affects the putamen earlier and more severely than the caudate. The current results indicate mild nigrostriatal presynaptic dopaminergic hypofunction in PLMD-RLS. **Key words:** Dopamine—FDOPA PET—Periodic limb movement disorder—Restless legs syndrome.

NEUROLOGY 2000;54:502–504

H.M. Ruottinen, MD, PhD; M. Partinen, MD, PhD; C. Hublin, MD, PhD; J. Bergman, MSc; M. Haaparanta, MSc; O. Solin, PhD; and J.O. Rinne, MD, PhD

Periodic limb movement disorder (PLMD) includes episodes of repetitive and stereotyped limb movements during sleep, and its diagnosis is confirmed with polysomnography.[1] PLMD occurs as an idiopathic form or associated with other sleep disorders including restless legs syndrome (RLS), obstructive sleep apnea syndrome, narcolepsy, or REM sleep behavior disorder.[1] Most patients with RLS have PLMD, but most patients with PLMD do not have RLS while awake.[1] RLS is divided into a primary type and a secondary type (e.g., secondary to neuropathy, uremia, or iron deficiency).

The etiology of PLMD and RLS is unknown. Positive effects of dopaminergic medication[2] support the role of the dopaminergic system in the pathogenesis of PLMD. In SPECT studies, decreased striatal dopamine D_2 receptor occupancy was found in patients with PLMD and RLS.[3] A mildly decreased dopamine D_2 receptor binding and 6-[^{18}F]fluoro-L-dopa (FDOPA) uptake has been reported in patients with RLS studied with PET.[4] No abnormality was found in FDOPA uptake in RLS patients.[5] The presynaptic dopaminergic system has been investigated in only a few PLMD-RLS patients.[4] Therefore, we investigated nigrostriatal presynaptic dopaminergic function in patients with PLMD-RLS with PET using FDOPA.

Methods. *Patients.* We investigated nine patients with PLMD-RLS (three women, six men). Mean (±SD) age of the patients was 52.2 ± 9.6 years (range 39 to 64 years). All patients were drug-naïve with respect to PLMD-RLS and were not taking dopaminergic medications. Extrapyramidal findings were assessed by the motor part (III) of the Unified Parkinson's Disease Rating Scale (UPDRS). All patients fulfilled the diagnostic criteria of the International Classification of Sleep Disorders[1] for PLMD and RLS[1,2] and underwent polysomnography. The disorders were both chronic (duration longer than 6 months) and moderate to severe (occurring several times weekly).[1] There was no significant medical history, and there were no clinical signs or abnormal blood test results indicating neuropathy, uremia, or iron deficiency.

Controls. Twenty-seven healthy volunteers (15 men, 12 women), mean age 53.0 ± 14.6 years (range 23 to 76 years) comprised the FDOPA control population in our PET center. They had no neurologic, psychiatric, or major physical illnesses. To rule out structural brain lesions, both patients and controls underwent brain MRI or CT.

PET. PET investigations were performed using the eight-ring ECAT 931/08-tomograph (Siemens/CTI Corp., Knoxville, TN). The study was approved by the Joint Ethical Committee of Turku University and Turku University Central Hospital. The individuals received 100 mg of carbidopa 60 minutes before the FDOPA injection to block the peripheral decarboxylation of FDOPA. For dynamic scanning, an average of 185 MBq of IV FDOPA was injected. The graphical analysis method with occipital reference region as an input function was used to calculate the decarboxylation rate of FDOPA to [^{18}F]fluorodopamine (K_i^{occ}).[6]

Statistics. The difference in FDOPA uptake values between patients and controls was compared using Student's unpaired two-sided *t*-test. The relationship between the FDOPA uptake (K_i^{occ} values) and the UPDRS motor score was evaluated by Pearson's correlation. Statistical significance was defined as $p < 0.05$.

Results. In the patients, the mean FDOPA uptake value (K_i^{occ}) was reduced to a similar degree in both the caudate nucleus to 88% of the control mean value ($p = 0.0008$) and in the putamen to 89% of the control mean value ($p = 0.0001$) (table).

The K_i^{occ} values overlapped between the patients and controls, both in the caudate and in the putamen (figure). The K_i^{occ} of two patients fell below −2 SDs of the control mean in the caudate, and in the putamen, five patients' K_i^{occ} values were below −2 SDs of the control mean value.

Six patients showed slightly increased muscle tone in arms during contralateral activation or mild bradykinesia in hand movements, which can be normal variants, especially in elderly individuals. The motor UPDRS scores ranged from 0 to 10 in the patients, and there was no significant association between the score and FDOPA up-

From the Department of Neurology (Drs. Ruottinen and Rinne), University of Turku; Haaga Neurological Research Centre (Drs. Partinen and Hublin), Helsinki; and Turku PET Centre (J. Bergman, M. Haaparanta, and Drs. Solin and Rinne), Turku, Finland.

Supported by the Turku University Foundation.

Received March 22, 1999. Accepted in final form August 31, 1999.

Address correspondence and reprint requests to Dr. Hanna M. Ruottinen, Department of Neurology, University of Turku, FIN-20520 Turku, Finland.

Table *The striatal 6-[^{18}F]fluoro-L-dopa uptake values (K_i^{occ}) in patients with PLMD-RLS and healthy controls*

	K_i^{occ} ($\times 10^{-3}$ min^{-1})	
Group	Caudate nucleus	Putamen
PLMD-RLS	10.36 ± 1.32*	10.35 ± 1.13*
Controls	11.82 ± 0.93	11.65 ± 0.63

Results are mean ± SD.

* $p < 0.001$ versus controls.

PLMD-RLS = periodic limb movement disorder–restless legs syndrome.

take ($r = 0.291$, $p = 0.484$, n = 8 for the caudate nucleus; and $r = -0.524$, $p = 0.182$, n = 8 for the putamen; r = Pearson's correlation coefficient [see the figure]).

Discussion. Our results show a slight but significant decrease in striatal FDOPA uptake to a similar degree both in the putamen and in the caudate nucleus in patients with PLMD-RLS compared with healthy controls. This equal affection of the caudate and putamen differs, for example, from the dopaminergic dysfunction in Parkinson's disease (PD), which affects the putamen earlier and more severely than the caudate. The caudate K_i^{occ} values in two patients and the putamen K_i^{occ} in five patients were more than 2 SDs below the control mean values. Also, in a previous PET study,[4] there was clear overlapping between controls and RLS patients: all the patients' individual caudate and putamen FDOPA uptake values were within the control range. Based on K_i^{occ} values alone, it is difficult to draw conclusions about whether an individual subject has PLMD-RLS because of the considerable overlapping. The individual patients with low FDOPA uptake values did not differ clinically from the rest of the PLMD-RLS patients.

PLMD occurs in 80% of patients with RLS.[2] Pure PLMD and pure RLS may represent two ends of a continuum, as many patients have both of these syndromes, with PLMD predominating in some and RLS in others. PLMD might be a forme fruste of autosomal dominant RLS.[7] Patients with PLMD have been shown to respond best to levodopa, whereas patients with severe RLS respond best to a dopamine agonist (pergolide).[8] Our findings are in accordance with the hypothesis that the brain dopaminergic system is involved in the pathogenesis of PLMD and RLS, based on the effectiveness of dopaminergic medication in PLMD[2] and the reversal of the therapeutic benefit by dopamine receptor blockers,[2] or the worsening of PLMD with a blocker of dopamine release.[2]

The dopaminergic hypothesis of both PLMD and RLS has been supported by decreased striatal dopamine D_2 receptor occupancy in ^{123}I-IBZM SPECT studies in patients with PLMD-RLS or PLMD alone.[3] In RLS patients, a mild but significant reduction in the putamen, both in the FDOPA uptake and in the dopamine D_2 receptor binding, has been reported.[4] In contrast, no difference in striatal FDOPA uptake was found between four RLS patients and controls in another current report.[5] However, it was not stated whether the patients also had PLMD.[5] The dopaminergic function may differ depending on whether the patients have pure RLS or PLMD-RLS. In addition, because of overlapping between control and patient values in this study and others,[4] significant differences are unlikely to be found between patients and controls in a small population.

Dopaminergic pathways in the CNS have been thought to be the primary transmitter system and the opioids the secondary one involved in PLMD and RLS. However, the pathophysiologic mechanism of PLMD-RLS probably is more complicated, including stimulating and inhibiting amino acids.[9] In addition, it has been found with functional MRI that in patients with PLMD-RLS, the cerebellar and thalamic activation may participate in the generation of sen-

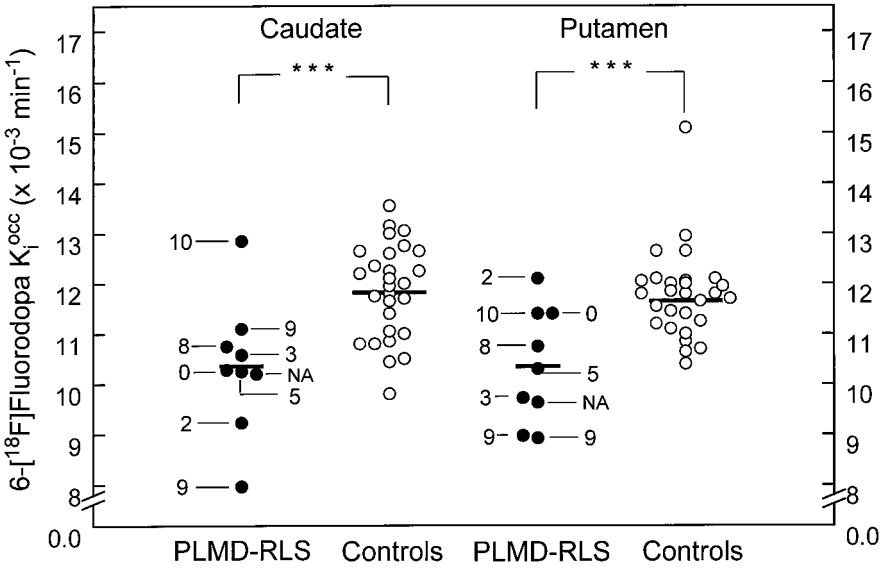

Figure. Comparison of individual 6-[^{18}F]fluoro-L-dopa K_i^{occ} values ($\times 10^{-3}$ min^{-1}) in patients with periodic limb movement disorder (PLMD) and restless legs syndrome (RLS), and in healthy controls. The numbers refer to the motor score of the Unified Parkinson's Disease Rating Scale (UPDRS). Bar = mean; NA = not available.

sory symptoms.[10] Functional MRI showed that PLMD in RLS mainly is associated with overactivity in the cerebellum, the red nuclei, and the brainstem. Reticular structures in the brainstem may be the primary generator of the RLS.[10]

The current study concerns only the nigrostriatal dopaminergic system. Detection of changes in other dopaminergic systems—possibly even more important in PLMD-RLS—remained outside of the resolution of our PET camera or the sensitivity of FDOPA. Our results of reduced FDOPA uptake in the caudate nucleus and putamen indicate mild striatal presynaptic dopaminergic dysfunction in PLMD-RLS.

Acknowledgment

The authors thank the staff of the Turku PET Centre.

References

1. American Sleep Disorders Association (ASDA). Periodic limb movement disorder and restless legs syndrome. In: International classification of sleep disorders: diagnostic and coding manual. Rochester, MN: Diagnostic Classification Steering Committee, 1990:65–71.
2. Walters AS. The International Restless Legs Syndrome Study Group. Toward a better definition of the restless legs syndrome. Mov Disord 1995;10:634–642.
3. Staedt J, Stoppe G, Kögler A, et al. Dopamine D_2 receptor alteration in patients with periodic movements in sleep (nocturnal myoclonus). J Neural Transm Gen Sect 1993;93:71–74.
4. Turjanski N, Lees AJ, Brooks DJ. Striatal dopaminergic function in restless legs syndrome: ^{18}F-dopa and ^{11}C-raclopride PET studies. Neurology 1999;52:932–937.
5. Trenkwalder C, Walters AS, Hening WA, et al. Positron emission tomographic studies in restless legs syndrome. Mov Disord 1999;14:141–145.
6. Ruottinen HM, Rinne JO, Haaparanta M, et al. [^{18}F]Fluorodopa PET shows striatal dopaminergic dysfunction in juvenile neuronal ceroid lipofuscinosis. J Neurol Neurosurg Psychiatry 1997;62:622–625.
7. Walters A, Picchietti D, Hening W, Lazzarini A. Variable expressivity in familial restless legs syndrome. Arch Neurol 1990;47:1219–1220.
8. Earley CJ, Allen RP. Pergolide and carbidopa/levodopa treatment of the restless legs syndrome and periodic leg movements in sleep in a consecutive series of patients. Sleep 1996; 19:801–810.
9. Williams DC. Periodic limb movements of sleep and the restless legs syndrome. Va Med Q 1996;123:260–265.
10. Bucher SF, Seelos KC, Oertel WH, Reiser M, Trenkwalder C. Cerebral generators involved in the pathogenesis of the restless legs syndrome. Ann Neurol 1997;41:639–645.

A kindred with Parkinson's disease not showing genetic linkage to established loci

Article abstract—We describe a kindred with PD with an onset age from the fifth to the eighth decade. Genetic analysis indicated that the genetic defect in this family was unlikely to be in the α-synuclein, parkin, or tau genes, or to reside on chromosomes 2p or 4p. **Key words:** Familial PD—Postural tremor—Linkage exclusion.

NEUROLOGY 2000;54:504–507

K.A. Gwinn-Hardy, MD; R. Crook, BSc; S. Lincoln, BSc; C.H. Adler, MD, PhD; J.N. Caviness, MD; J. Hardy, PhD; and M. Farrer, PhD

Idiopathic PD is common, with a prevalence of 3/1,000 and lifetime risk of 1/50. Increasing age and several genetic loci are the only known risk factors.[1,2] Six genetic loci, on chromosomes 2p13, 4p14-15 (two loci), 4q21-23, 6q25-27, and 17q21-23, have been linked/associated with familial parkinsonism.[3-8] The current study reports genetic analysis of a family (the Michigan kindred) in which affected individuals have parkinsonism consistent with a diagnosis of typical idiopathic PD.

Materials and methods. *The family and the phenotype.* The Michigan kindred is primarily of Dutch and English descent. Of 34 individuals examined, 5 have parkinsonism consistent with a diagnosis of typical PD. The proband is a 73-year-old woman (figure 1, 4024) who presented at age 66 after 4 years of progressive clumsiness and slowness. Examination indicated left arm and leg resting tremor, rigidity, shuffling gait, and mild postural instability. Initially carbidopa–levodopa treatment had excellent results; however, wearing off and dyskinesias developed 8 years later.

After informed consent, genealogic data were obtained through family interview. Clinical examination of participants included a complete mental status examination, neurologic examination, Unified Parkinson's Disease Rating Scale, and Hoehn and Yahr score. Neurophysiologic testing was performed in one subject (4006) and included surface electromyography of the bilateral upper extremity muscles.

Blood was obtained, and DNA was prepared by standard procedures. A total of 28 individuals were genotyped for this study. The pedigree used in power, linkage, and haplotype analysis is shown in figure 1.

Genetic analysis. The pedigree was conservatively evaluated for its power to detect linkage using the SIMLINK pro-

From the Mayo Clinic Jacksonville (Drs. Gwinn-Hardy, Hardy, and Farrer, and R. Crook and S. Lincoln), Jacksonville, FL; and the Mayo Clinic Scottsdale (Drs. Adler and Caviness), Scottsdale, AZ.

Supported by the Mayo Foundation, Center of Excellence for Genetics of Parkinson's Disease, NINDS grant AG17216.

Received January 18, 1999. Accepted in final form August 31, 1999.

Address correspondence and reprint requests to Dr. Gwinn-Hardy, Mayo Clinic Jacksonville, 4500 San Pablo Road, Jacksonville, FL 32224.

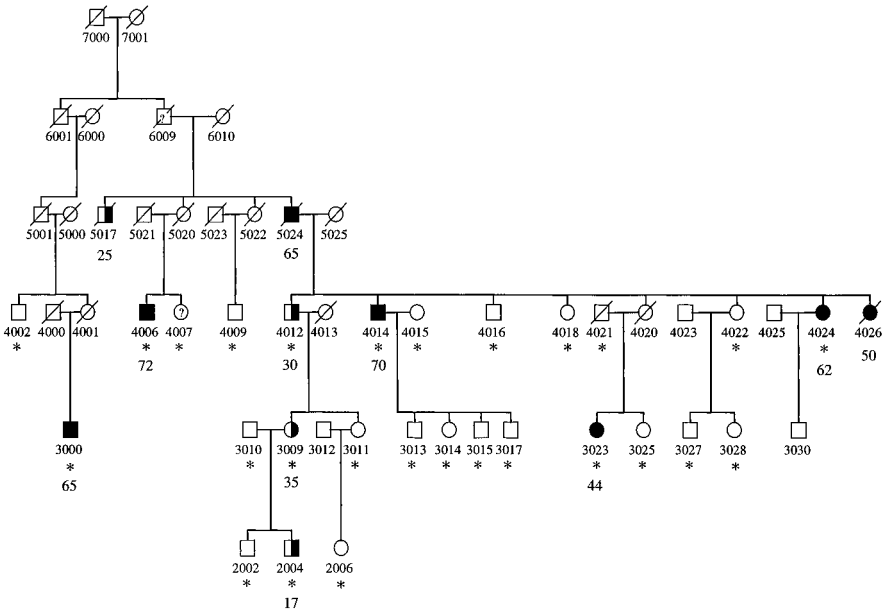

*Figure 1. The Michigan kindred. The family shown is abbreviated to protect family confidentiality; squares represent men, circles represent women. Filled symbols are individuals with PD, half-filled symbols are family members with essential tremor. Slashed symbols represent deceased individuals. Age at onset (where known), in years, is shown beneath affected individuals. *DNA was available.*

gram, version 4.12. Affecteds-only analysis was performed with the kindred as collected. Data are presented that assume least about the familial penetrance for disease (see figure 1). Alternative analyses using cumulative normal and linear penetrance functions or assuming essential tremor (ET) as evidence of variable expressivity were also performed (not shown). Parkinsonism was treated as a dichotomous, autosomal dominant trait with the disease allele frequency set at 0.0003 (the population prevalence of familial parkinsonism).[1] Individuals not related by blood were considered to be at risk from disease, as were individuals with ET (4012, 3009, and 2004). Subjects 4007 and 5024 were also considered as at risk rather than affected, as the former awaits clinical examination, while the latter was diagnosed historically. Marker frequencies were set at 0.40, 0.30, 0.20, and 0.10, and 500 replicates were performed.

Linkage/haplotype analysis of known loci for parkinsonism was performed. Markers shown in figure 2 were analyzed on an ABI 377 automated sequencer. Two-point linkage analysis was performed using affecteds-only analysis, with MLINK.[9] Marker allele frequencies were taken from Marshfield/CEPH. Two-point lod scores for chromosome 6 markers were calculated assuming an autosomal dominant model to illustrate that neither haplotypes nor consanguineous genotypes could be shared by individuals with disease. Subsequently, the VITESSE algorithm was used for rapid exact multilocus linkage analysis via genotype set-recoding and inheritance.[10] Affected-only analysis was performed taking intermarker distances from the Marshfield map. Haplotype configurations of legal genetic descent were examined using SIMWALK2. Data in LINKAGE format were converted using lsp from the LINKAGE package of programs and converted to MENDEL format using LINKMEND.[9]

Results. The mean age at onset of parkinsonism in this family is 61 ± 10 years, ranging from the fifth to eight decade. Seven family members in three generations were found to have parkinsonism by examination or by family history and review of medical records (two deceased) (see figure 1, 3000, 3023, 4006, 4014, 4024, 4026, and 5024). One individual, 72 years of age (4006), had resting tremor of the right upper extremity and mild rigidity on examination. The tremor characteristics were confirmed as parkinsonian on neurophysiologic testing. Briefly, while at rest, the right upper extremity had 5-Hz rhythmic grouping of motor units in the right wrist flexor group and right abductor pollicis brevis. This was present in an agonist-only pattern. After tonic activation of the upper extremities, this activity was suppressed. Such a pattern is consistent with the tremor of parkinsonism. Examination of other members of the family indicated four individuals (2004, 3009, 4012, and, by history, 5017) with activation tremor and no other neurologic findings, consistent with ET.

Discussion. *Power analysis and exclusion of loci for parkinsonism.* Aggregation of PD in current generations, along with historic evidence of PD in two deceased family members (5024 and 4026), suggests a genetic trait consistent with autosomal dominant inheritance of a major gene with reduced penetrance. Power analysis suggests that for a linked marker the pedigree may generate a maximum 2-point lod score of 1.82, with a mean of $z > 0.67$, $\Theta = 0$, and $z > 0.55$, $\Theta = 0.05$. As collected, the family would have a 20% probability of observing a lod score of >1.0, $\Theta = 0$, 16% for $z > 1.0$, $\Theta = 0.05$. The probability of obtaining a lod score >1.0, $\Theta = 0.01$ for an unlinked marker (false-positive, type I error) was 1/100. However, only at $\Theta = 0$ for unlinked markers are lod scores likely to reach −2.0, the accepted criteria for exclusion.

Affected-only two-point and multipoint linkage analysis were used to examine the contribution of loci for PD on chromosomes 2p13, 4p14-15 (both loci), and 4q21-23, and for atypical parkinsonism on 6q25.2-27 and 17q21-23 (see figure 2, A through D). Assuming an autosomal dominant model, all of these loci were excluded at $\Theta = 0$ by two-point analysis and between markers by multipoint scores ($z < -2.0$

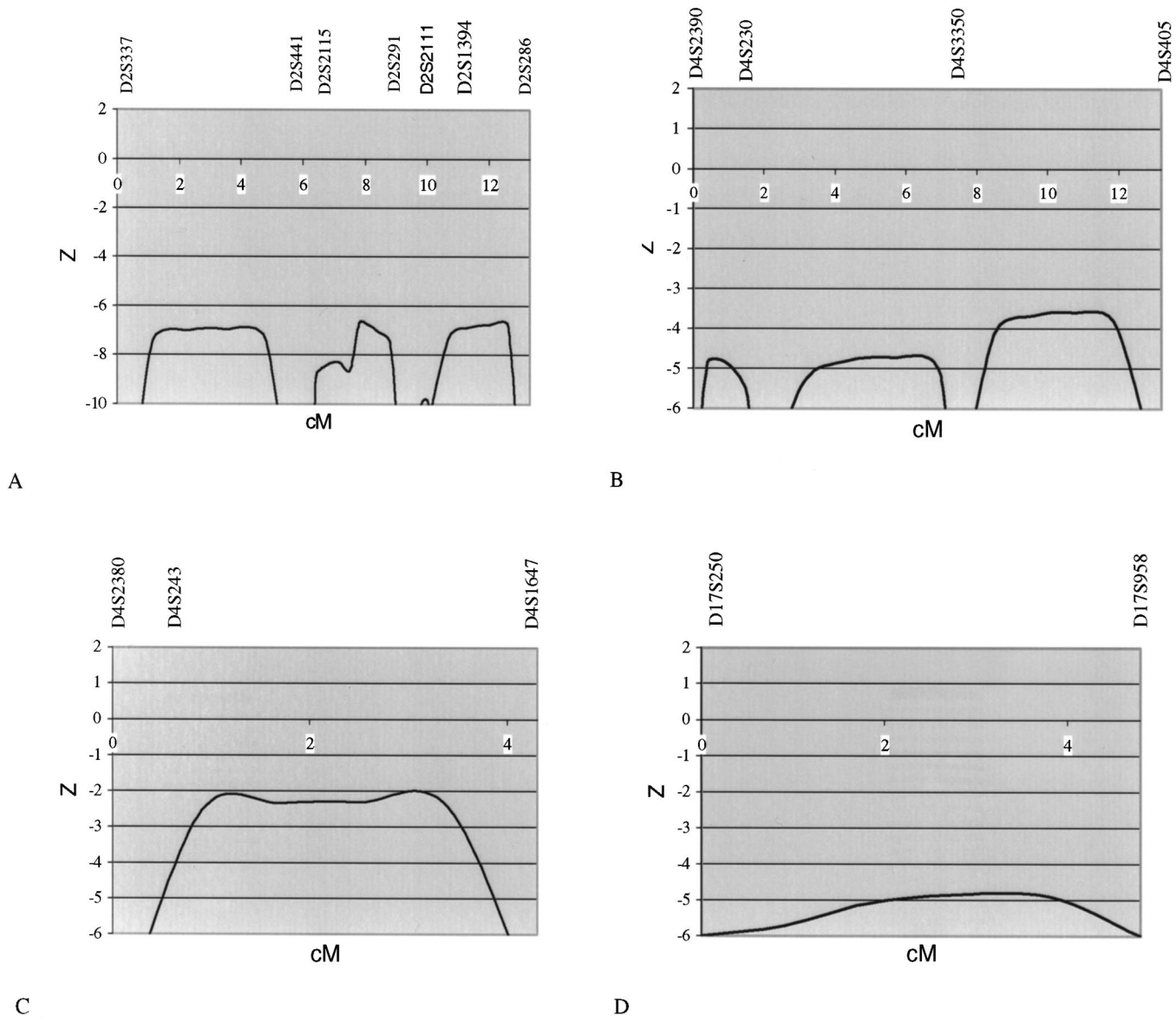

Figure 2. Multipoint analyses of candidate regions for parkinsonism calculated using MLINK as described in the text. Multipoint linkage analysis of 2p13 (A), 4p15-16.3 (B), 4q23-25 (C), and 17q21-23 (D).

for intermarker values of Θ). Model-free analyses based on Markov chain Monte Carlo simulation of data under the null hypothesis of no linkage supported this conclusion, demonstrating nonsignificant values of marker haplotype sharing; $p > 0.05$ for all markers examined (not shown).

Regarding age at onset and clinical characteristics, the phenotype is consistent with idiopathic PD. No atypical features, including either dementia or dysautonomia, have been noted in any of the individuals examined. No stigmata of PD were seen in individuals with ET. It remains possible that in some cases ET represents an alternate and variable phenotype of familial PD with a common genetic origin.[5]

Assuming an autosomal dominant model, affecteds-only analysis of parkinsonism is appropriate. Reduced penetrance, and possibly variable expressivity manifest as ET, would confound an analysis based on age-associated liability classes. Penetrance seems to be reduced; individuals 4020 and 5020 are not reported to have had any stigmata of PD (or ET). However, their deaths (at ages 33 and 60 years, respectively) prevent definitive statements on this issue. In addition, we have yet to discover any history of PD in the parents or grandparents of 3000. This individual may be a phenocopy given late-onset disease, his more distant genealogic relationship, and the age-associated prevalence of this disorder. We are searching for further evidence of trait segregation in branches descended from this person's great-uncles and aunts.

One pitfall of model-based approaches is the assumptions underlying disease transmission, which could invalidate a model-based method if misspecified. Multipoint analysis of a complex trait under an autosomal dominant model is inappropriate because

there is an increased propensity for false-negative results. Considering the pedigree, it is impossible to model disease segregation in this family with any certainty. However, all known loci for parkinsonism are excluded because both model-based and more conservative model-free methods provided results in good agreement (data not shown). Sequencing α-synuclein, tau, and parkin confirmed that these were unlikely to be the pathogenic loci. Thus, it is likely that there are other, as yet unmapped, loci for this disorder.

Acknowledgment

The authors thank the family presented in this study. Additionally, they thank E.V.H. and N.B. for their commitment, Kari MacElwee and Stephanie Cox Newman for collecting samples, and Valerie Thomas for preparing DNA.

References

1. Tanner CM, Goldman SM. Epidemiology of Parkinson's disease. Neurol Clin 1996;14:317–335.
2. Farrer M, Gwinn-Hardy K, Hutton M, Hardy J. The genetics of disorders with synuclein pathology and parkinsonism. Hum Mol Genet 1999;8:1901–1905.
3. Gasser T, Müller-Myhsok B, Wszolek ZK, et al. A susceptibility locus for Parkinson's disease maps to chromosome 2p13. Nat Genet 1998;18:262–265.
4. Leroy E, Boyer R, Auburger G, et al. The ubiquitin pathway in Parkinson's disease. Nature 1998;395:451–452.
5. Farrer M, Gwinn-Hardy K, Muenter M, et al. A chromosome 4phaplotype segregating with Parkinson's disease and postural tremor. Hum Mol Genet 1999;8:81–85.
6. Polymeropoulos MH, Lavedan C, Leroy E, et al. Mutation in the α-synuclein gene identified in families with Parkinson's disease. Science 1997;276:2045–2048.
7. Matsumine H, Saito M, Shimoda-Matsubayashi S, et al. Localization of a gene for an autosomal recessive form of juvenile Parkinsonism to chromosome 6q25.2-27. Am J Hum Genet 1997;60:588–596.
8. Foster NL, Wilhelmsen K, Sima AAF, et al. Frontotemporal dementia and parkinsonism linked to chromosome 17: a consensus. Ann Neurol 1997;42:85–94.
9. Ott J. Analysis of human genetic linkage. 3rd ed. Baltimore: John Hopkins University Press, 1999.
10. O'Connell JR, Weeks DE. The VITESSE algorithm for rapid exact multilocus linkage analysis via genotype set-recording and fuzzy inheritance. Nat Genet 1998;11:402–408.

A magnetization transfer imaging study of the brain in patients with migraine

Article abstract—The authors evaluated the magnetization transfer ratio (MTR) of T2 lesions, normal-appearing white matter (NAWM), and brain from 39 migraineurs, 17 healthy volunteers, and 22 patients with MS. Migraineurs had NAWM and brain MTR values similar to those of normal subjects but significantly higher than those of MS patients. Average lesion MTR values also were significantly lower in MS patients than in migraineurs. In patients with migraine, other etiologies should be considered in the presence of tissue damage beyond that seen on T2-weighted scans. **Key words:** Migraine—MRI—Magnetization transfer imaging.

NEUROLOGY 2000;54:507–509

M.A. Rocca, MD; B. Colombo, MD; A. Pratesi; G. Comi, MD; and M. Filippi, MD

White matter (WM) abnormalities can be seen on T2-weighted MRIs of the brain from patients with migraine.[1] However, T2-weighted abnormalities lack pathologic specificity and are found in a variety of neurologic conditions.[2] Thus, patients with migraine and multiple T2-weighted abnormalities might represent a diagnostic challenge. The nature of such abnormalities also is uncertain because it is difficult to obtain definitive histopathologic correlations in such patients.

Magnetization transfer imaging (MTI) provides a quantitative index, the magnetization transfer ratio (MTR), which may reflect the underlying composition of tissue with increased specificity over conventional imaging.[3] MTI also may be able to detect WM abnormalities that would go undetected with conventional imaging.[3] In this study, we used MTI to improve our understanding of WM changes in migraineurs and to increase diagnostic confidence in these patients.

Patients and methods. We studied 39 patients with migraine[4] (34 women and 5 men; 27 without and 12 with aura; mean age 35.0 years, range 18 to 58 years; mean duration of disease 16.8 years, range 4 to 40 years; mean numbers of attacks per year 54.7, range 12 to 120). Two control groups were identified. The first consisted of 17 healthy volunteers (14 women and 3 men; mean age 36.3 years, range 24 to 62 years). The second group consisted of 22 patients (13 women and 9 men; mean age 35.1 years, range 16 to 53 years; median disease duration 4.0 years, range 1 to 19 years) with mildly disabling relapsing–remitting MS.

The following pulse sequences were acquired using a 1.5-T system: 1) dual-echo turbo spin-echo (repetition time [TR] = 3300, echo time [TE] = 16/98); 2) two-dimensional

From the Neuroimaging Research Unit, Departments of Neuroscience (Drs. Rocca and Filippi, and A. Pratesi) and Neurology (Drs. Colombo and Comi), Scientific Institute Ospedale San Raffaele, University of Milan, Italy.

Received July 26, 1999. Accepted in final form August 31, 1999.

Address correspondence and reprint requests to Dr. Massimo Filippi, Neuroimaging Research Unit, Department of Neuroscience, Scientific Institute Ospedale San Raffaele, Via Olgettina, 60, 20132 Milan, Italy.

Table 1 *Mean (SD) magnetization transfer ratio values (%) of different brain regions from healthy volunteers, patients with migraine, and patients with MS*

Region	Healthy volunteers	Migraine patients	MS patients	*p* Value*
Internal capsule	44.1 (0.9)	44.3 (1.0)	43.3 (1.3)	0.002
Periventricular white matter	43.6 (1.1)	43.7 (1.4)	42.7 (1.1)	0.008
Juxtacortical white matter	42.4 (1.4)	42.7 (1.5)	40.9 (1.5)	0.0001

* Statistical analysis: one-way ANOVA. Post hoc analysis (two-tailed Student's *t*-test for nonpaired data): 1) *internal capsule*: healthy volunteers vs MS patients $p = 0.03$; migraine vs MS patients $p = 0.001$; 2) *periventricular white matter*: healthy volunteers vs MS patients $p = 0.01$; migraine vs MS patients $p = 0.004$; 3) *Juxtacortical white matter*: healthy volunteers vs MS patients $p = 0.004$; migraine vs MS patients $p < 0.0001$.

gradient echo (TR = 640, TE = 12, $\alpha = 20°$) with and without an off-resonance radiofrequency pulse centered 1.5 kHz below the water frequency, with a Gaussian envelope of duration of 7.68 milliseconds and $\alpha = 500°$; and 3) T1-weighted spin-echo (TR = 768, TE = 14). For all scans, 24 contiguous axial slices were acquired with 5-mm slice thickness, 192 × 256 matrix, and 188 × 250 mm field of view.

Hyperintense T2 lesions and hypointense T1 lesions were identified and marked on the hard copies by agreement of two observers (M.A.R., M.F.) who did not know to whom the scans belonged. Lesion volume measurements were performed by a single observer (A.P.) using a semiautomated segmentation technique.[5] From the two gradient echo images, MTR maps were derived following the method described previously.[5] After image coregistration, the lesion outlines on the dual-echo images were superimposed onto the MTR maps, and average lesion MTR was calculated, as reported elsewhere.[5] For each MTR map and whenever possible, square regions of interest (area = 3 × 3 pixels) were placed bilaterally in the normal-appearing white matter (NAWM) of the internal capsules, the WM close to the anterior and posterior parts of the lateral ventricles, and the WM close to the cortical gray matter of the central fissures. We also derived MTR histograms for the overall brain from patients and control subjects, as described previously.[5]

One-way analysis of variance was used to compare MTR-derived measures among the three groups. Post hoc analyses were performed using Student's *t*-test. Univariate correlations were performed using the Spearman rank correlation coefficient.

Results. Fifteen (38%) migraineurs had 118 lesions on the dual-echo scans. No lesions were detected on the scans from healthy volunteers, whereas 781 were seen on the dual-echo scans of all the MS patients. Median T2 lesion loads were 0.2 ml (range 0.05 to 4.3 ml) in migraineurs and 5.8 ml (range 0.3 to 30.9 ml) in MS patients ($p < 0.0001$). Three (2.5%) of the dual-echo hyperintense lesions from migraineurs were T1 hypointense, whereas this was the case for 208 (26.6%) of those from MS patients ($p < 0.0001$).

The MTR of all the regions of NAWM studied were similar in healthy volunteers and migraineurs, whereas MS patients had significantly lower MTR values than those from the two other groups for all regions studied (table 1). Mean average lesion MTR values were 40.8% (SD 1.8%) in migraineurs and 37.6% in MS patients (SD 1.9%) ($p < 0.0001$).

In table 2, the MTR histogram-derived measures from the entire brain tissue of healthy volunteers and patients with migraine and MS are reported. The three groups had significantly different average MTR and peak height. At post hoc analysis, no difference was found for any of the MTR histogram-derived metrics between migraineurs and healthy volunteers, whereas MS patients had lower peak height ($p = 0.0005$) than healthy volunteers. Compared with migraineurs, MS patients had lower average MTR ($p = 0.005$) and peak height ($p < 0.0001$). The same analysis was conducted considering only the patients with migraine and brain MRI abnormalities. These patients had MTR histogram-derived metrics similar to those from healthy controls and had higher average MTR ($p = 0.01$) and peak height ($p = 0.0009$) than MS patients. None of the migraineurs had any of the MTR histogram-derived metrics 2 SD below the mean values from healthy volunteers. No significant correlation was found between duration of migraine and frequency of the attacks and any of the MR-derived measures.

Discussion. Several studies report the presence of hyperintense T2-weighted abnormalities in WM from migraineurs.[1] This is confirmed by this study, where such abnormalities were found in 38% of pa-

Table 2 *Mean (SD) brain MTR histogram metrics in healthy volunteers, patients with migraine, and patients with MS*

MTR metrics	Healthy volunteers	Migraine patients	MS patients	*p* Values*
Average brain MTR, %	40.9 (7.0)	41.1 (5.3)	40.6 (7.0)	0.02
Peak height	91.3 (6.4)	92.7 (5.2)	83.9 (7.8)	<0.0001
Peak position, %	35.5 (1.0)	35.5 (0.7)	35.0 (0.9)	NS

* Statistical analysis: one-way ANOVA. Post hoc analysis: two-tailed Student's *t*-test for nonpaired data (the results of between-group comparisons are reported in the text).

MTR = magnetization transfer ratio; NS = not significant.

tients with migraine. We also obtained brain MTI scans from migraineurs to assess the severity of tissue damage within T2-visible lesions and to investigate whether additional microscopic changes occur in the NAWM.

Reduced MTR values were found in the NAWM from patients with progressive multifocal encephalopathy,[6] HIV encephalitis,[6] subcortical ischemic vascular dementia,[7] and MS.[8] This was not the case for the NAWM from elderly patients with periventricular WM hyperintensities (WMH).[9] We found that NAWM-MTR values of migraineurs are similar to those of controls and significantly higher than those of MS patients. This suggests that in migraineurs, even in the presence of nonspecific T2-weighted abnormalities, there are no microscopic changes in the NAWM. Also suggested is that other etiologies should be considered in these patients in the presence of tissue damage beyond that seen using conventional MR.

We also showed that the amount of tissue damage in T2-visible lesions is relatively mild. This is supported by two pieces of evidence. First, the prevalence of T1-hypointense lesions was lower and the lesion MTR higher in patients with migraine than in those with MS. In MS, T1-hypointense lesions correspond to areas with severe tissue destruction, and lesion MTR is strongly correlated with the amount of axonal loss and demyelination.[3] As we observed in our migraineurs, WMH from elderly patients have moderately reduced MTR values,[9] and gliosis might be one of the prominent features of these lesions.[10] Although the pathologic substrate of WMH in migraine remains unknown, the most tempting speculation to explain these abnormalities is to hypothesize ischemia without infarction and subsequent reactive gliosis.

MTR histogram analysis allows evaluation of data from all of the MR pixels of the brain tissue, thus providing a complete assessment of disease burden. In this study, MTR histograms from migraineurs were similar to those from healthy volunteers. We also did not find any difference in MTR histogram metrics between migraineurs with and without T2 abnormalities. This was not the case for patients with MS who, as shown previously,[3] had dramatic histogram changes resulting from damage in lesions and NAWM. Interestingly, none of our migraineurs had histogram peak height 2 SD below the mean value from healthy volunteers. MTR histogram peak height is considered a measure of the amount of tissue with truly normal MTR.[3] This further supports the integrity of brain tissue outside of T2 lesions in migraineurs.

References

1. Cooney BS, Grossman RI, Farber RE, Goin JE, Galetta SL. Frequency of magnetic resonance imaging abnormalities in patients with migraine. Headache 1996;36:616–621.
2. Fazekas F, Barkhof F, Filippi M. Unenhanced and enhanced magnetic resonance imaging in the diagnosis of multiple sclerosis. J Neurol Neurosurg Psychiatry 1998;64:S2–S5.
3. Filippi M, Grossman RI, Comi G. Magnetization transfer imaging in multiple sclerosis. Neurology 1999;53(suppl 3):S1–S52.
4. Headache Classification Committee of the International Headache Society. Proposed classification and diagnostic criteria for headache disorders, cranial neuralgias and facial pain. Cephalalgia 1988;8(suppl 7):1–96.
5. Filippi M, Iannucci G, Tortorella C, et al. Comparison of MS clinical phenotypes using conventional and magnetization transfer MRI. Neurology 1999;52:588–594.
6. Dousset V, Armand JP, Lacost D, et al. Magnetization transfer study of HIV encephalitis and progressive multifocal leukoencephalopathy. Am J Neuroradiol 1997;18:895–901.
7. Tanabe JL, Ezekiel F, Jagust WJ, et al. Magnetization transfer ratio of white matter hyperintensities in subcortical ischemic vascular dementia. Am J Neuroradiol 1999;20:839–844.
8. Filippi M, Campi A, Dousset V, et al. A magnetization transfer imaging study of normal-appearing white matter in multiple sclerosis. Neurology 1995;45:478–482.
9. Wong KT, Grossman RI, Boorstein JM, Lexa JF, McGowan JC. Magnetization transfer imaging of perivascular hyperintense white matter in the elderly. Am J Neuroradiol 1995;16:253–258.
10. Brun A, Englund E. A white matter disorder in dementia of the Alzheimer type: a pathoanatomical study. Ann Neurol 1986;19:253–262.

Decreased hemispheric water mobility in hemiplegic migraine related to mutation of *CACNA1A* gene

Article abstract—We report a reversible reduction of water diffusion in the brain during a prolonged attack of hemiplegic migraine. The patient had a sporadic mutation of the *CACNA1A* gene. The diffusion changes were observed in the contralateral hemisphere 3 and 5 weeks after the onset of hemiplegia. These results suggest the occurrence of hemispheric cytotoxic edema during severe attacks of hemiplegic aura. The mechanisms underlying such ultrastructural modifications are unknown but an abnormal release of excitatory amino acids can be hypothesized. **Key words:** MRI—Diffusion—Hemiplegic—Migraine—*CACNA1A* gene.

NEUROLOGY 2000;54:510–512

H. Chabriat, MD; K. Vahedi, MD; C.A. Clark, PhD; C. Poupon, PhD; A. Ducros, MD, PhD; C. Denier, MD; D. Le Bihan, MD, PhD; and M.G. Bousser, MD

The exact origin of the aura frequently inaugurating migraine attacks remains unknown. Familial hemiplegic migraine (FHM) is an autosomal dominant form of migraine associated with hemiparetic aura. The severity and duration of the aura in FHM can vary from a brief mild motor deficit to a severe long-lasting hemiplegia, sometimes associated with coma, seizures, and fever.[1] The recent identification of mutations in the *CACNA1A* gene, encoding the main subunit of a neuronal calcium channel, as the cause of the disease might be a crucial key to the understanding of the mechanisms underlying the aura.[2,3] Missense mutations in the *CACNA1A* gene account for approximately 50% of all FHM cases and for all those with associated permanent cerebellar symptoms. They are located in important functional domains of the channel; however, the precise mechanisms leading from these genetic defects to the hemiplegic aura are unknown.[2,3] A young woman with *CACNA1A* gene–related hemiplegic migraine was studied repeatedly with the diffusion tensor MRI technique during a long-lasting attack of hemiplegic migraine.

Case report. A 33-year-old woman had had six severe attacks of hemiplegic migraine since age 7 years in the absence of identified precipitating factors (heat was reported as a possible trigger of one attack). Each time, the symptoms included throbbing headaches, nausea or vomiting, coma or confusion, fever (38 to 39 °C), and meningism lasting 2 to 3 days, associated with a severe hemiplegia that always outlasted the other signs. Focal seizures were occasionally observed during the course of the most severe episodes. Hemiplegia was either on the left or on the right side and in the latter case, was always associated with aphasia. Each time, the clinical recovery was complete after 3 to 6 weeks. Results of laboratory investigations performed between attacks were normal. During one attack, the CSF was found to contain 100 neutrophils per mL in the absence of identified infectious agents. T2- and T1-weighted MRI studies performed during attacks showed a hemispheric edema in the absence of any focal lesion and a discrete unilateral meningeal enhancement after gadolinium injection. These signs always subsided after the attacks and there was no evidence of infarction. The patient also had a cerebellar atrophy, as observed in 20% of FHM families with the mutated gene, and a right hemispheric atrophy, exceptionally reported after prolonged attacks of hemiplegic migraine.[4] No familial history of hemiplegic migraine was found. *CACNA1A* genotyping revealed a de novo missense mutation of the *CACNA1A* gene (Y1384C).[5]

Methods. We performed repeated MRI studies using the diffusion tensor imaging (DTI) technique[6] during the last attack of our patient. The onset was as usual with throbbing headache, vomiting, fever (39 °C), confusion associated with a right hemiplegia, and mutism appearing within the first 24 hours. The first diffusion MRI examination was performed at day 21 when the patient started to recover. At this time, she still had a dense hemiplegia and was mutic. The second examination was done 5 weeks after the onset, when the patient had only a mild motor deficit and dysphasia. The third examination was done 2 months later after a complete clinical recovery. No ionic or hematocrit abnormality was observed with usual biologic assessment. The patient was treated with sodium valproate and aspirin.

DTI was performed on a 1.5-T Signa Horizon Echospeed MRI system (Signa General Electric Medical Systems, Milwaukee, WI) equipped with magnetic field gradients of up to 22 mT/m. A standard quadrature head coil was used for radiofrequency transmission and reception of the nuclear magnetic resonance signal. Diffusion-weighted images were acquired in the axial plane at 16 slice locations, 5 mm thick. For each slice location a T2-weighted image with no diffusion sensitization followed by five b values (incrementing linearly to a maximum value of 1,000 seconds/mm^2) in each of six noncolinear directions were acquired. To improve the signal-to-noise ratio, this was repeated four times, providing 124 images per slice location. The image resolution was 128 × 128, field of view 24 cm x 24 cm, TE = 82.4 msec, TR = 2.5 seconds. The total acquisition time was 10 minutes 24 seconds. The mean diffusivity (a directionally averaged measure of diffusion) and volume

From the Service de Neurologie (Drs. Chabriat, Vahedi, and Bousser), Hôpital Lariboisière, Paris; DRM-SHFJ-CEA (Drs. Chabriat, Clark, Poupon, and Le Bihan), Orsay; and INSERM U25 (Drs. Ducros and Denier), Faculté de Médecine Necker, Paris, France.

Received July 15, 1999. Accepted in final form September 11, 1999.

Address correspondence and reprint requests to Pr. Bousser, Service de Neurologie, Hôpital Lariboisière, 2 rue Ambroise Paré, 75010 Paris, France.

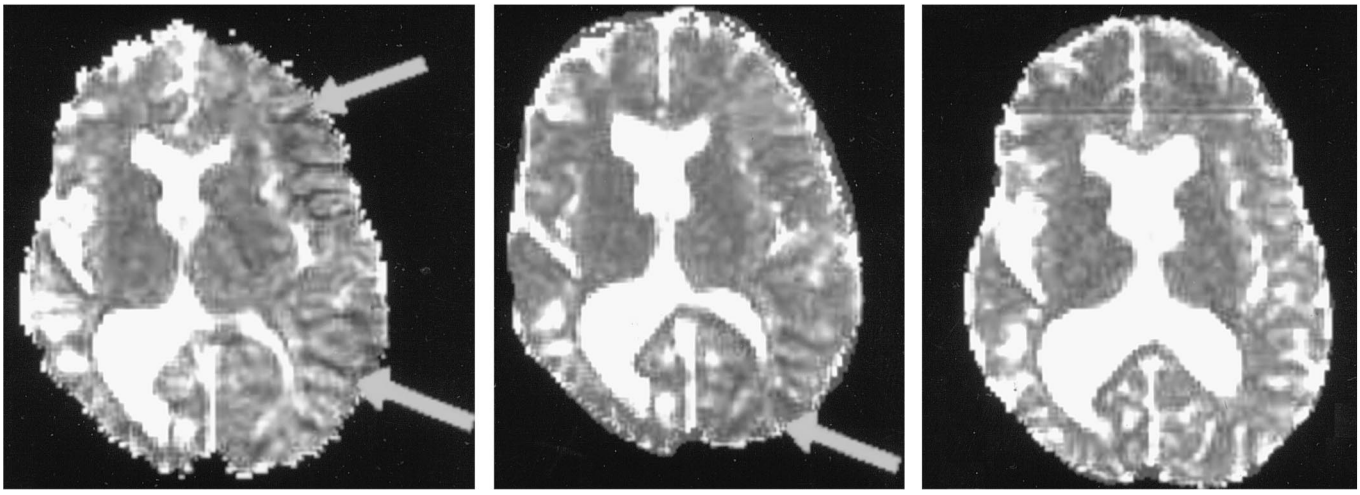

Figure. Quantitative maps of the mean diffusivity. The areas of decreased diffusion in the left hemisphere correspond to the darkest voxels and are shown by arrows. Note the atrophy of the right hemisphere and the transient increase of the left hemispheric volume. A, 3 weeks; B, 5 weeks; C, 3 months.

ratio (VR) (a measure of diffusion anisotropy) were calculated on a pixel-by-pixel basis as previously described.[6] The region corresponding to abnormal diffusion was manually outlined on four planes based on a visual assessment and the mean diffusivity was determined in the region of interest. A large region of normal appearing tissue was selected for a quantitative comparison with the abnormal region at the same levels.

Results. No increased signal on T2-weighted imaging and no decreased signal on T1-weighted imaging were observed. At day 21, the images of mean diffusivity (figure) revealed confluent subcortical zones with reduced diffusion at all levels of the left hemisphere (darker pixels on the first and second images); at day 36, the size of this zone decreased; 3 months after onset, the mean diffusivity was found to normalize in the whole of the left hemisphere. The mean diffusivity values of the abnormal region were 0.55×10^{-3} mm^2/second at day 21 and 0.64×10^{-3} mm^2/second at day 36; the mean diffusivity value in the normal region was $0.73 \pm 0.03\ 10^{-3}$ mm^2/second. The region of reduced mean diffusivity was found predominantly localized to the white matter as evidenced by the value of anisotropy (0.71) (mean VR in normal white matter = 0.68, mean VR in cortex = 0.96).

Discussion. This is the first report of a decrease of cerebral water mobility during the aura of a migraine attack. Cutrer et al. previously failed to find modifications of water diffusion in four patients having attacks of migraine with visual aura.[7] However, their quantification of water diffusion was not always performed during the visual symptoms. Moreover, the symptoms of their patients were much less severe and long-standing than in our case.

The reduction of water mobility measured in the abnormal region strongly suggests the shrinkage of the extracellular space and the accumulation of intracellular water.[8] In our patient, we found that the reduction of water mobility was mostly observed within areas of high anisotropy, which indicates that the reduction of the mean diffusivity was prominent within the white matter.[6] The hydropic swelling of astrocytes, oligodendroglial cells or myelinated fibers or both, might cause such ultrastructural modifications, as observed during ischemia. Interestingly, these diffusion modifications were parallel to the global increase of the hemispheric volume on the affected side. This hemispheric swelling has been previously reported in severe attacks of hemiplegic migraine.[1]

In our patient the decrease in diffusion was about 25% at day 21 and 10% at day 36. This reduction is much less than the 40 to 50% decrease within the core of acute cerebral ischemia in humans related to variations of ionic gradients after the abrupt decrease of energy requiring Na^+,K^+ ATPase activity.[8,9] Furthermore, whereas the diffusion reduction in ischemic stroke lasts no more than 5 to 10 days,[9] the reduction of water mobility was observed more than 5 weeks after onset in our case. Moreover, this reduction was not followed by increased diffusion as found within ischemic lesions after the membrane disruption of lytic cells.[9] Such moderate and reversible reduction of water diffusion in the absence of a residual lesion has been reported previously in experimental reversible ischemic injury, within the ischemic penumbra or during spreading depression.

Our patient has a missense mutation of the *CACNA1A* gene. The mutations observed in FHM are thought to affect the ion selectivity and permeability of the calcium channel pore at the neuronal level.[3] How does this alteration of the calcium channel lead to the modifications of water diffusion observed in our case? Hess previously emphasized that calcium channel activation and inactivation occur in vivo on the order of milliseconds to at most seconds in contrast with the prolonged phenotypic events observed in humans and animals having the mutated gene.[2] Therefore, the acute calcium channel dysfunction might precipitate biochemical events promoting

both a very long depolarization of hemispheric cells as supported by the sustained slowdown of the electrical activity during hemiplegic aura and also a possible shift of water from the extra to the intracellular compartment, compatible with our observation. During experimental ischemia, there is a close relationship between the ATP level and the decrease in apparent diffusion coefficient within the core of the lesion. However, in hemiplegic aura, a normal cerebral oxygen consumption has been reported.[10] These data suggest that the cerebral metabolic activity is relatively preserved during attacks of hemiplegic migraine and that a failure of energy supply is not a necessary cause of the reduction of water diffusion. It is noteworthy that the calcium channel does not modulate only the neuronal electrical activity but also its exocytotic release.[2] Several authors have recently demonstrated that the neurotransmitter release of neuronal cells is mediated by calcium channels. Within the ischemic penumbra, the release of excitatory amino acids has been shown to promote membrane depolarization through the activation of NMDA receptors and the prolonged swelling of astrocytes up to several days after the ischemic insult.[8] In addition, the administration of NMDA receptor antagonists can reverse the reduction of diffusion during ischemia or spreading depression.[8] Therefore, whether the modifications of diffusion during severe hemiplegic aura are also precipitated or maintained by an abnormal release of neuroexcitatory amino acids caused by specific mutations of *CACNA1A* gene should be investigated.

Acknowledgment

The authors are indebted to Professor Hagueneau for his helpful and kind collaboration to this work.

References

1. Fitzimons R, Woldefen W. Migraine coma. Meningitic migraine with cerebral edema associated with a new form of autosomal dominant cerebellar ataxia. Brain 1985;108:555–577.
2. Hess E. Migraines in mice? Cell 1996;87:1149–1151.
3. Ophoff R, Terwindt G, Vergouwe M, et al. Familial hemiplegic migraine and episodic ataxia type 2 are caused by mutations in the Ca2+ channel gene *CACNL1A4.* Cell 1996;87:543–552.
4. Hayashi R, Tachikawa H, Watanabe R, Honda M, Katsumata Y. Familial hemiplegic migraine with irreversible brain damage. Intern Med 1998;37:166–168.
5. Vahedi K, Denier C, Ducros A, et al. Sporadic hemiplegic migraine with de novo *CACNA1A* missense mutation. Neurology 1999;52:A274. Abstract.
6. Pierpaoli C, Jezzard P, Basser P, Barnett A, Di Chiro G. Diffusion tensor MR imaging of the human brain. Radiology 1996;201:637–648.
7. Cutrer F, Sorensen A, Weiskoff R, et al. Perfusion-weighted imaging defects during spontaneous migrainous aura. Ann Neurol 1998;43:25–31.
8. Hossmann K, Hoehn-Berlage M. Diffusion and perfusion MR imaging of cerebral ischemia. Cerebrovasc Brain Metab Rev 1995;7:185–217.
9. Warach S, Gaa J, Siewert B, Wielopolski P, Edelman R. Acute human stroke studied by whole brain echoplanar diffusion-weighted magnetic resonance imaging. Ann Neurol 1995;37:231–241.
10. Herold S, Gibbs J, Jones A, et al. Oxygen metabolism in migraine. J Cereb Blood Flow Metab 1985;5:S444–S446.

Ischemic strokes are more severe in Poland than in the United States

Article abstract—Case fatality rates for stroke were ascertained prospectively in two regional catchment hospitals in Poland and 36 teaching hospitals in the US University Hospital Consortium. Case fatality rates in Poland (23.9%) were higher than in the United States (7.5%). Angina, atrial fibrillation, and congestive heart failure were more frequent in Polish stroke patients (40%, 26%, and 25%, respectively) than in US patients (17%, 12%, and 10%). Stroke severity as indicated by higher frequencies of hemiplegia, disordered consciousness, dysphagia, and aphasia was greater in Poland (19%, 39%, 28%, and 42%, respectively) than the United States (11%, 13%, 14%, and 26%). **Key words:** Ischemic stroke—Stroke mortality—Poland—United States.

NEUROLOGY 2000;54:513–515

D. Ryglewicz, MD, PhD; D.B. Hier, MD; M. Wiszniewska, MD; S. Cichy, MD; W. Lechowicz, MD; and A. Czlonkowska, MD, PhD

Although stroke mortality has declined in many industrialized countries in recent decades, not all countries have benefited.[1] Poland has one of the highest stroke mortality rates in Europe and it has not declined since at least 1984.[2] High levels of stroke mortality could be due to high stroke incidence rates, high case fatality rates, or both. Analysis of the Warsaw Stroke Registry (1991–1992) showed that ischemic stroke incidence rates in Poland were comparable to those of other industrialized countries.[3] However, early case fatality rates (28%) were two times higher than in Western Europe and the United States.[2-3] The purpose of this study was to determine whether greater stroke severity was a contributing factor to higher case fatality rates in Poland.

Methods. We compared patients in the US University Hospital Consortium (UHC) Ischemic Stroke Clinical Benchmarking Project[4] with those in two Polish stroke epidemiologic studies. In Warsaw, the Neurologic Department of the Institute of Psychiatry and Neurology has collected data on all stroke patients from its catchment area (population 182,000) since January 1, 1991. Data are stored in the Warsaw Stroke Registry, which was designed to parallel the Stroke Data Bank.[5] The same registry has been used to collect data on stroke patients from the Pila catchment (population 210,000) in western Poland.

Data were collected from January 1, 1995 to December 31, 1997 in Warsaw, and from January 1, 1996 to December 31, 1996 in Pila. In the United States, UHC data were collected from January 1, 1996 to March 31, 1996. In Poland, all consecutive patients fulfilling inclusion criteria who were admitted to the Neurologic Department of the Institute of Psychiatry and Neurology in Warsaw (n = 252) or the Neurologic Department in Pila (n = 57) were entered. The UHC Ischemic Stroke Clinical Benchmarking Project was initiated in April 1995 at 36 US teaching hospitals. Each hospital contributed up to 30 consecutive cases of ischemic stroke during a 3-month registration period (n = 961). Inclusion criteria in all studies was age greater than 17 years and primary discharge diagnosis of ischemic stroke (ICD-9 codes 433, 434, and 436). Neurologic state on admission was defined as severe if the patient was unresponsive, had a decreased level of consciousness, had two or more body areas that were completely paralyzed, or had one paralyzed area and two areas with weakness. Discharge status was classified as mild (functionally independent, corresponding to grade 0–1 on the Rankin scale), moderate (requires some assistance, grade 2–3 on the Rankin scale), or severe (disabled/dependent, grade 4–5 on the Rankin scale). The relationship among risk factors, severe neurologic status at the onset of stroke, medical complications, and neurologic status at discharge was assessed by the χ^2 test. Confidence intervals (CI) for analyzed variables were calculated using standard procedures.

Results. In the United States, 961 patients were registered (51.5% men); in Poland, 309 patients (44.4% men) were registered. The US patients were younger than the Polish patients (31% versus 19% of patients were in the group younger than 61 years, $p < 0.05$). In Poland, 100% of the patients were white. In the United States, race was 65.9% white, 29.5% African American, 3.4% Hispanic, 0.7% Asian, 0.2% Native American, and 0.3% other.

Cardiac diseases (coronary disease, myocardial infarction, atrial fibrillation, and congestive heart failure) were more frequent in Poland than in the United States (40% versus 17%, 24% versus 12%, 26% versus 12%, and 25% versus 10%, respectively). The prevalence of hypertension (64% versus 65%), smoking (23% versus 23%), prior stroke (19% versus 26%), and diabetes mellitus (22% versus 27%) was similar in Poland and the United States. The proportion of treated hypertension was similar in Poland (50%) and the United States (50%). Admission to the hospital was within 24 hours in 48% of the US patients and 42% of the Polish patients. By 48 hours, 68% were admitted in the United States and 65% in Poland.

The neurologic state of patients at the time of admission differed between countries. Severe neurologic state was

From the Department of Neurology (Drs. Ryglewicz, Cichy, Lechowicz, and Czlonkowska), Institute of Psychiatry and Neurology, Warsaw, Poland; the Department of Neurology (Dr. Hier), University of Illinois at Chicago; and the Department of Neurology (Dr. Wiszniewska), Municipal Hospital, Pila, Poland.

Supported by a grant from the Marie Sklodowska-Curie Joint Fund II.

Received February 12, 1999. Accepted in final form September 16, 1999.

Address correspondence and reprint requests to Dr. Daniel B. Hier, 912 S. Wood Street (MC 796), Department of Neurology, University of Illinois at Chicago, Chicago, IL 60612-7330.

Table 1 *Ischemic stroke rated as severe by age group in Poland and the United States*

Age group, y	Poland	US
18–45	11; 36.4 (11–69)	98; 24.5 (16–34)
46–60*	48; 33.3 (20–48)	203; 13.8 (9–18)
61–75*	129; 40.3 (32–49)	354; 16.9 (13–21)
>75*	121; 51.2 (42–60)	306; 26.1 (21–31)

Values are n; % (95% CI).

* Polish patient group differs from US group, $df = 1$, $p < 0.05$.

more common in Poland than in the United States at all age levels (table 1). This greater stroke severity of the Polish patients was related to a higher frequency of hemiplegia, disordered consciousness, dysphagia, and aphasia (table 2).

Drugs prescribed during hospitalization in the United States and in Poland included antiplatelet drugs (66.4% and 63%), oral anticoagulants (28.3% and 15.8%), antihypertensives (56% and 63%), and diuretics (24.1% and 19.2%). Heparin use was more common in the United States (57.9%) than in Poland (3.1%). Pneumonia was more frequent in Poland (21.3%) than in the United States (5.1%), as were decubitus ulcer (7.1% versus 1.2%) and pulmonary embolism (3.1% versus 0.3%). Neurologic complications such as seizures (1.3% and 1.2%) and stroke progression (6.9% and 6.2%) were similar in the United States and Poland. Length of stay was longer in Poland (mean 17 days) than in the United States (mean 7.5 days). Discharge status differed between countries. More US patients were independent at discharge than were Polish patients (table 3). Polish case fatality rates during hospitalization (23.9%) were three times higher than in the United States (7.5%). Discharge destination differed between countries, with 30.7% of the US patients going to rehabilitation centers compared to 2.6% in Poland.

Discussion. Hospitalized stroke patients in Poland differed from stroke patients admitted to 36 US teaching hospitals. Polish stroke patients were more likely to have atrial fibrillation, congestive heart failure, coronary artery disease, or remote myocardial infarction when compared with their US counterparts. Polish patients had more severe strokes as reflected by greater weakness and lower levels of consciousness. Polish stroke patients were more likely to have serious medical complications including pneumonia, decubitus ulcer, and pulmonary embolism. Length of stay was longer for the Polish patients. Polish patients were less likely to be discharged to rehabilitation centers, and their functional level at discharge was lower than that of US patients. These differences may contribute to case fatality rates that were three times higher in Poland (23.9%) than in the United States (7.5%).

Severity of the neurologic deficit is likely to contribute to the high stroke case fatality rate in Poland. Decreased level of consciousness at stroke onset and severity of motor disability are two important predictors of fatality.[6-9] Greater stroke severity in Polish patients may be related to the high frequency of cardiac etiology for the stroke.[10] Atrial fibrillation was three times more frequent in Poland than in the United States. Congestive heart failure was also more common in Poland.

The Polish stroke patients showed higher levels of stroke severity at the time of admission, and this likely contributes to their poorer outcomes and higher case fatality rates. We cannot exclude a possibility that systematic differences in stroke care also contributed to differences in outcome. Length of stay was longer in Poland than in the United States, possibly reflecting differences in stroke severity, stroke care, or both. Although drug use was similar between the two countries, actual drug use protocols were not compared. Heparin use was significantly more common in the United States, although it is uncertain whether that contributed to the better outcomes of US stroke patients. The stroke patients in the United States were younger, possibly contributing to their better outcomes. Nonetheless, high stroke severity appears to contribute to high stroke fatality rates in Poland.

Table 2 *Occurrence of neurologic signs at admission*

Neurologic signs	Poland, n = 309	US, n = 961
New paralysis*	59; 19 (15–24)	104; 11 (9–13)
New paresis	235; 76 (71–81)	702; 73 (70–76)
Decreased level of consciousness*	121; 39 (33–46)	125; 13 (11–15)
Dysphagia*	87; 28 (23–33)	135; 14 (12–16)
Aphasia*	130; 42 (37–46)	253; 26 (23–29)
Visual changes	58; 19 (14–23)	211; 22 (19–25)

Values are n; % (95% CI).

* Difference statistically significant, chi-square, $p < 0.05$.

Table 3 *Discharge status after ischemic stroke in Poland and US*

Discharge status	Poland	US
Mild deficit*	24.9 (20–30)	39.3 (36–42)
Moderate deficit	29.1 (24–34)	32.0 (29–35)
Severe deficit	22.0 (17–27)	21.3 (19–24)
Death*	23.9 (14–35)	7.2 (6–9)

Values are % (95% CI).

* United States differs from Poland, $df = 1$, $p < 0.05$.

References

1. Asplund K. Stroke in Europe: widening gap between east and west. Cerebrovasc Dis 1996;6:3–6.
2. Ryglewicz D, Polakowska M, Lechowicz W, et al. Stroke mortality rates in Poland did not change between 1984 and 1992. Stroke 1997;28:752–757.
3. Czlonkowska A, Ryglewicz D, Weissbein T, Barañska-Gieruszczak M, Hier DB. A prospective community-based study of stroke in Warsaw, Poland. Stroke 1994;25:547–551.

4. University Health System Consortium. Ischemic stroke clinical benchmarking database, report 1, 9/30/1996. Clinical process improvement. Oak Brook, IL: University Health System Consortium.
5. Foulkes MA, Wolf PA, Price TR, Mohr JP, Hier DB. The Stroke Data Bank: design, methods and baseline characteristics. Stroke 1988;19:547–554.
6. Oxbury JM, Greenhall RCD, Grainger KMR. Predicting theoutcome of stroke: acute stage after cerebral infarction. BMJ 1975;3:125–129.
7. Chambers BR, Norris JW, Shurvell BL, Hachinski VC. Prognosis of acute stroke. Neurology 1987;37:221–225.
8. Ryglewicz D, Hier DB, Weissbein T, Baranska-Gieruszczak M, Czlonkowska A. Factors predicting 30-day mortality in the Warsaw Stroke Registry. J Stroke Cerebrovasc Dis 1995;5:73–77.
9. Weissbein, Czlonkowska A, Popow J, Ryglewicz D, Hier DB. Analysis of 30-day mortality in a community-based registry in Warsaw, Poland. J Cerebrovasc Dis 1994;4:63–67.
10. Sen S, Oppenheimer M. Cardiac disorders and stroke. Curr Opin Neurol 1998;11:51–56.

Exploratory saccades show no direction-specific deficit in neglect

Article abstract—In patients with spatial neglect, contralesional reflexive saccades toward suddenly appearing targets show direction-specific deficits. We examined whether these deficits also occur during free exploration of space. Neglect patients' voluntary eye movements showed reduced amplitudes for saccades in all directions but no direction-specific deficit. The results argue against an interpretation of spatial neglect as a general deficit to disengage attention or to program saccades in contralesional direction. **Key words:** Spatial neglect—Eye movements—Attention—Parietal lobe—Brain damage—Human.

NEUROLOGY 2000;54:515–518

Matthias Niemeier; and Hans-Otto Karnath, MD, PhD

Patients with spatial neglect performing reflexive eye movements toward targets suddenly appearing in the left or right periphery exhibit a direction-specific deficit of saccadic orienting. Saccades in contralesional direction show increased reaction times, are hypometric, and are increased in number (e.g., reference 1).

This deficit might be associated with an impairment in disengaging attention before shifting it in the contralesional direction,[2,3] which has been discussed as the basic mechanism leading to spatial neglect. The pathologic pattern has also been attributed to a "fractionation of eye movement programming" due to an underactivity of the ipsilesional superior colliculus.[4] According to both explanations, contralesional saccades should be affected not only in tasks provoking reflexive saccades to peripheral targets[1] but also in situations requiring voluntary saccadic orienting.

In a search task performed in complete darkness,[5] neglect patients' voluntary saccades carried out in contralesional direction did not differ from those in ipsilesional direction. However, it might be easier to disengage fixation in darkness than while scanning a visual scene. Therefore, we investigated whether neglect patients would show direction-specific deficits when searching in a large array of visual stimuli that almost entirely surrounded the subjects.

Methods. *Participants.* Four patients with right parietal lesions and neglect took part in the study (3 men, 1 woman, median age 57 years). Spatial neglect was assessed with a battery of standard neglect tests.[6] Subjects with visual field defects, as examined by confrontation testing with and without cueing, were excluded from the study. For further clinical data, see reference 6. Six neurologic patients without brain lesions served as controls (3 men, 3 women, median age 65 years).

Apparatus. Subjects sat in a cabin with the head in the center of the upper spherical part of the cabin (see reference 6). The trunk was immobilized. Eye and head movements were recorded independently using two different search coils.

Procedure. In a first task, the subject had to search for a (nonexistent) laser spot in complete darkness. Three trials were performed, each lasting 20 seconds. For the second task, the cabin was illuminated. A random array of 340 letters was presented on the inner surface of the sphere within a range of ±140° left and right of the body's midsagittal plane almost entirely surrounding the subject. In three trials, each lasting 20 seconds, the subject had to search for a single (nonexistent) target letter.

Data analysis. Exploratory eye movements were sorted according to the relative direction of the saccades (leftward/rightward/upward/downward). A first analysis included all movements. Saccades were assigned to the respective category of direction within a range of ±45° (figure 1A). A second analysis of the same data focussed

From the Department of Cognitive Neurology, University of Tübingen, Germany.

Supported by grants from the Deutsche Forschungsgemeinschaft and the Bundesministerium für Bildung, Wissenschaft, Forschung und Technologie awarded to H.-O.K.

Received June 1, 1999. Accepted in final form September 16, 1999.

Address correspondence and reprint requests to Dr. H.-O. Karnath, Department of Cognitive Neurology, University of Tübingen, Hoppe-Seyler-Str. 3, D-72076 Tübingen, Germany; e-mail: Karnath@uni-tuebingen.de

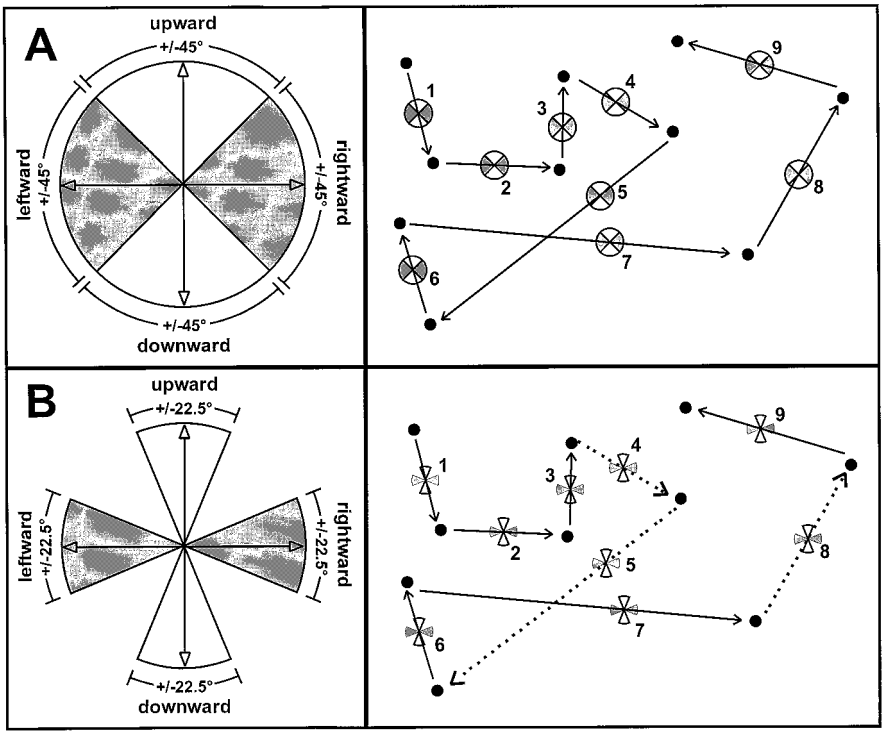

Figure 1. Sorting procedure for exploratory saccades. The small black dots indicate the fixations in a sequence of saccades. Saccades are depicted as arrows. (A) In a first analysis of the data, all saccades were assigned to the respective category of saccade direction they fell in within a range of ±45°. Saccade 1 falling into the range of ±45° of downward direction was classified as "downward saccade." Accordingly, saccades 2, 4, and 7 were "rightward saccades"; saccades 3, 6, and 8 were "upward saccades"; and saccades 5 and 9 were "leftward saccades." (B) In a second analysis of the data, only saccades within ±22.5° of one of the four principal directions were included. Saccades 4, 5, and 8 exceeded ±22.5° and thus were excluded from this analysis.

only on saccades performed within ±22.5° of one of the four principal directions, excluding the more oblique saccades (figure 1B).

Results. The controls explored space almost symmetrically. In contrast, the neglect patients showed a bias, searching most of the time in the right hemispace (darkness: 78%, letter array: 89%). This prominent asymmetry did not allow a direct comparison between saccades performed in the left versus right hemispace.

Saccades within ±45° of the principal directions (see figure 1A). In darkness but not in the letter array, the "number of saccades" differed with respect to direction ($F = 13.05$, $p < 0.001$), due to more horizontal saccades compared to vertical saccades in both subject groups (see table). Neglect patients showed a reduced "saccade amplitude" in *all* directions (darkness: $F = 6.69$, $p = 0.032$; letter array: $F = 11.02$, $p = 0.011$; figure 2). Subtracting the component of head movements from "saccade amplitude" revealed the same result for the pure eye-in-head movement component. Thus, the head movements were not employed to compensate for possibly impaired eye movements. The "duration of fixation" differed with respect to the direction of the subsequent saccade in both

Table *Average number of saccades and average duration of fixation (msec) preceding a saccade in leftward, rightward, upward, and downward direction during the search task in darkness and during the letter-search task*

No. of saccades/duration of fixation	Leftward	Rightward	Upward	Downward
Number of saccades				
Darkness				
Neglect	59.3 (22.8)	49.0 (3.7)	20.5 (7.9)	19.0 (12.0)
Controls	48.0 (15.6)	42.3 (12.2)	28.5 (8.7)	29.3 (12.7)
Letter-search				
Neglect	37.8 (2.6)	50.0 (18.5)	49.5 (10.8)	37.3 (19.5)
Controls	52.0 (15.4)	46.3 (10.1)	50.8 (12.0)	52.7 (15.3)
Duration of fixation				
Darkness				
Neglect	289 (58)	293 (125)	273 (112)	348 (115)
Controls	288 (69)	283 (58)	311 (63)	323 (38)
Letter-search				
Neglect	285 (59)	279 (37)	238 (45)	296 (13)
Controls	239 (24)	235 (18)	228 (24)	258 (57)

Standard deviations are in parentheses.

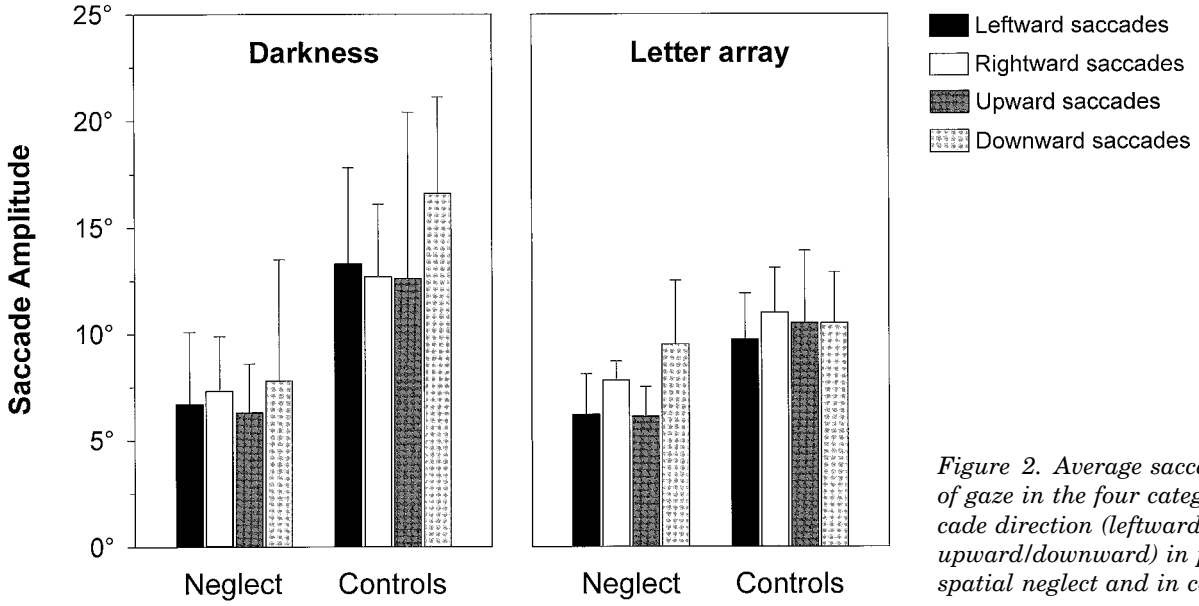

Figure 2. Average saccade amplitude of gaze in the four categories of saccade direction (leftward/rightward/upward/downward) in patients with spatial neglect and in controls.

subject groups (darkness: $F = 3.13$, $p = 0.044$; letter array: $F = 5.89$, $p = 0.004$; see the table), reflecting differences in latencies before vertical (compared to horizontal) saccades. The analyses revealed no direction-specific deficit in the neglect patients' saccades.

Saccades within ±22.5° of the principal directions (see figure 1B). A second analysis of the data excluded saccades with oblique orientations (neglect patients 40%, controls 42%; see figure 1B). Even with this stricter criterion, we found no direction-specific deficit for contralesional saccades of neglect patients.

Saccades performed in the right hemispace. The neglect patients' bias searching predominantly in the right hemispace let to an increased percentage of centripetal movements in their leftward saccades. Because there might be a difference in the performance of centrifugal versus centripetal saccades,[7] we equalized the likelihood of centripetal leftward saccades in both subject groups analyzing exclusively the saccades performed in the right hemispace. (We thus excluded all centrifugal leftward saccades in both groups.) Again, the ANOVAs revealed no direction-specific deficit in the neglect patients' exploratory eye movements.

Discussion. In the current study, subjects were required to search for a visual target in the surroundings. In darkness and in normal light, neglect patients' voluntary saccades differed from those of control subjects in significantly reduced amplitudes in *all* directions, but did not show any direction-specific deficit.

Posner et al.[2,3] assumed that parietal lesions result in a disruption of attentional disengaging and thus in increased latencies before contralesional shifts of attention, which has been discussed as the basic mechanism leading to spatial neglect. There is growing evidence for common central mechanisms of saccades and attentional orienting.[8,9] Therefore, such lesions should also result in increased durations of fixations before saccades are carried out in contralesional direction. The current study showed that patients with parietal lesions and neglect do not have increased latencies of fixations before contralesional saccades. Our findings also oppose the view of a general disturbance of programming contralesionally directed saccades in neglect patients with parietal lesions.[4] Not only for the duration of fixation but also for the amplitude and the number of saccades, we found no direction-specific deficit in the neglect patients.

One might speculate that a direction-specific deficit of voluntary saccades only occurs on the patients' left side. If so, this argument would contrast Posner et al.'s view of an impaired disengagement of attention as well. These authors assumed an impaired disengagement in these patients regardless of the spatial location of the current focus of attention.[3] Likewise, the hypothesis of Walker and Findlay[4] would predict a direction-specific deficit of saccadic programming in the left *and* the right hemispace, as the ipsilesional superior colliculus is involved in any contralesional saccades.[10]

Another objection might concern the subjects being free to move the head in the current study. Even though we found no head movements that would have compensated for defective eye-in-head movements, it is possible that saccadic orienting and underlying attentional shifts were selectively spared under free head conditions. If so, no spatial neglect should have occurred in the current search tasks. However, in both tasks the neglect patients almost completely ignored the left hemispace.

Finally, direction-specific deficits could occur in contralesional saccades that are reflexively elicited by stimuli suddenly appearing in the periphery,[1] but

not in saccades performed voluntarily during visual search, as was shown in the current study. If so, the reflexive deficit cannot explain the basic feature in spatial neglect; namely, that these patients show a strong ipsilesional bias in voluntary exploration of space.

The current findings show that there is no direction-specific deficit in neglect patients' voluntary exploratory saccades. This argues against the assumption of a generally defective disengaging of attention or of a generally disturbed saccade generation as the mechanisms underlying spatial neglect.

Acknowledgment

The authors are grateful to Douglas Tweed for helpful discussion, Susanne Ferber for technical assistance, and Beth E. Snitz for her help with the language.

References

1. Girotti F, Casazza M, Musicco M, Avanzini G. Oculomotor disorders in cortical lesions in man: the role of unilateral neglect. Neuropsychologia 1983;21:543–553.
2. Posner MI, Walker JA, Friedrich FJ, Rafal RD. Effects of parietal injury on covert orienting of attention. J Neurosci 1984;4:1863–1874.
3. Posner MI, Walker JA, Friedrich FA, Rafal RD. How do the parietal lobes direct covert attention? Neuropsychologia 1987; 25:135–145.
4. Walker R, Findlay JM. Saccadic eye movement programming in unilateral neglect. Neuropsychologia 1996;34: 493–508.
5. Karnath H-O, Fetter M, Dichgans J. Ocular exploration of space as a function of neck proprioceptive and vestibular input—observations in normal subjects and patients with spatial neglect after parietal lesions. Exp Brain Res 1996;109: 333–342.
6. Karnath H-O, Niemeier M, Dichgans J. Space exploration in neglect. Brain 1998;121:2357–2367.
7. Evdokimidis I, Liakopoulos D, Papageorgiou C. Cortical potentials preceding centrifugal and centripetal self-paced horizontal saccades. Electroencephalogr Clin Neurophysiol 1991; 79:503–505.
8. Kustov AA, Robinson DL. Shared neural control of attentional shifts and eye movements. Nature 1996;384:74–77. Letter.
9. Kowler E, Anderson E, Dosher B, Blaser E. The role of attention in the programming of saccades. Vision Res 1995;35: 1897–1916.
10. Schiller PH, Stryker M. Single-unit recording and stimulation in superior colliculus of the alert rhesus monkey. J Neurophysiol 1972;35:915–924.

Spinal cord astrocytoma: Response to PCV chemotherapy

Article abstract—Information regarding the value of chemotherapy for spinal cord astrocytomas that progress after irradiation is limited. We describe a patient whose conus medullaris astrocytoma responded to PCV (procarbazine, lomustine, and vincristine) chemotherapy after failing radiation and cisplatin-based chemotherapy. PCV should be considered in patients with progressive spinal cord astrocytomas. **Key words:** Spinal neoplasm—Astrocytoma—Chemotherapy.

NEUROLOGY 2000;54:518–520

John W. Henson, MD; Allan F. Thornton, MD; and David N. Louis, MD

Astrocytomas of the spinal cord are rare neoplasms, occurring with an incidence of 0.8 to 2.5 per 100,000 population per year.[1] Surgery and radiation therapy are standard treatments for patients with these tumors. Because of their rarity, information regarding the value of chemotherapy for spinal cord astrocytomas that progress after irradiation is limited. We present a patient whose astrocytoma responded to PCV (procarbazine, lomustine [CCNU], and vincristine) chemotherapy, and review the literature on the subject.

From the Brain Tumor Center and Spine Tumor Center (Drs. Henson and Thornton), Department of Radiation Oncology (Dr. Thornton), Department of Pathology and Neurosurgical Service (Dr. Louis), Massachusetts General Hospital, Boston; and Harvard Medical School (Drs. Henson, Thornton, and Louis), Boston, MA.

Supported by the Brian D. Silber Memorial Fund for spine tumor research at the Massachusetts General Hospital.

Received July 22, 1999. Accepted in final form September 11, 1999.

Address correspondence and reprint requests to Dr. John W. Henson, Brain Tumor Center and Spine Tumor Center, Cox 315, 100 Blossom Street, Boston, MA 02114; e-mail: henson@helix.mgh.harvard.edu

Patient. An enhancing mass lesion in the conus medullaris was discovered by MRI in a 41-year-old man with progressive bilateral lower extremity weakness. Biopsy revealed low-grade astrocytoma (figure 1). He received a total of 5040 cGy in 180-cGy fractions, with a return of normal muscle strength. Two years later, he developed progressive lower extremity symptoms and MRI revealed new areas of contrast enhancement (figure 2A). Cisplatin and etoposide produced clinical stabilization, but after the fourth cycle the strength in both legs began to deteriorate and MRI suggested progression of disease (see figure 2B). PCV chemotherapy was administered, although without vincristine after the first cycle owing to neurotoxicity. By the beginning of the third cycle improvement in lower extremity strength and function was apparent. An MRI scan after seven cycles revealed a decrease in size and degree of enhancement of the tumor (see figure 2C). Glucocorticoids were not administered during either of the two chemotherapy regimens. After a total of 11 cycles, he again experienced progressive disease, having a time to progression of 23 months from the start of PCV treatment. The patient died after failing to respond to additional therapy with topotecan or temozolomide. Overall survival was 6 years.

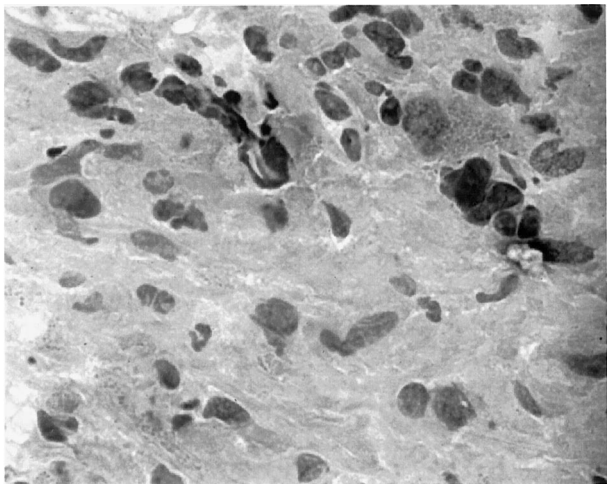

Figure 1. Biopsy of the conus medullaris mass reveals moderate hypercellularity and nuclear pleomorphism of astrocytic cells. Mitotic activity, vascular proliferation, and necrosis were not noted, although the biopsy was small. The tumor focally involved a sample of spinal nerve root. (Hematoxylin and eosin, ×400.)

Discussion. Spinal cord astrocytomas are devastating tumors that pose serious risks to function and life. Histopathologic grading, using the same criteria as for cerebral astrocytomas, correlates well with clinical behavior and, together with location along the spinal cord, is helpful in determining prognosis.[2] Thus, patients with high-grade tumors in the cervical cord have the worst prognosis, with survivals measured in several months.[3,4] Spinal cord astrocytomas usually progress locally, although dissemination throughout the spinal cord and leptomeninges is not uncommon with high-grade tumors.

Surgery and radiation therapy are the first-line treatments for these tumors. The extent of resection is usually limited by the infiltrative nature of spinal cord astrocytomas. With the use of operating microscopes, however, partial surgical resection can lead to improvement in the neurologic deficits in patients with low-grade tumors. The value of aggressive resection in high-grade spinal cord astrocytomas is unclear.

Radiation therapy is usually administered to spinal cord astrocytomas following biopsy or surgery. Although it has been difficult to quantitate the value of radiation, there may be a lower rate of progression among patients who receive radiation therapy.[2,5]

There is scant literature regarding the use of chemotherapy for spinal cord astrocytomas. Of 10 children treated with the "8-in-1" drug regimen before radiation for high-grade spinal cord astrocytoma, five showed a response after two cycles of chemotherapy.[6] Bouffet et al. reported a complete clinical and radiographic response of a low-grade astrocytoma of the spinal cord to boplatin and vincristine without irradiation.[7] Linstadt et al.[8] reported a 6-plus–year response of a progressive spinal cord astrocytoma to reirradiation plus carmustine. The current case showed a significant clinical and radiographic response to PCV.

Thus, spinal cord astrocytomas can respond to chemotherapy. Although astrocytomas of the cere-

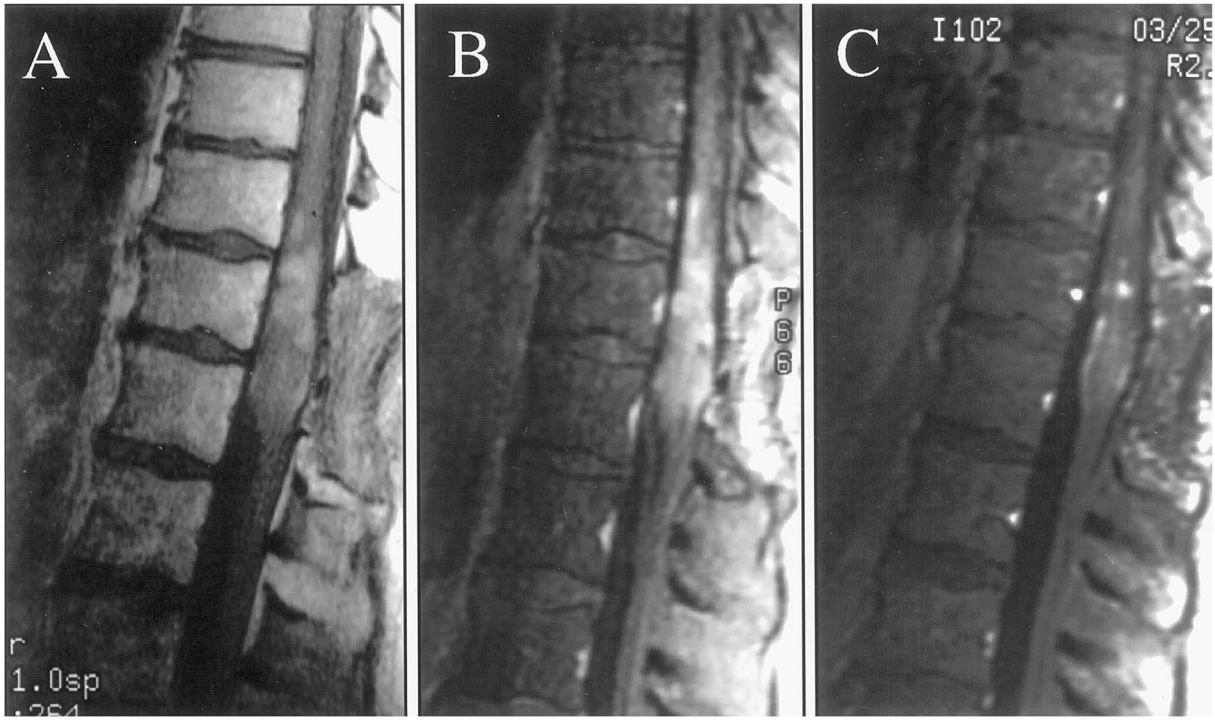

Figure 2. Contrast-enhanced MRI scans of astrocytoma of the conus medullaris. (A) Tumor at the time of progression after irradiation. (B) Clinical progression after four cycles of cisplatin and etoposide. (C) Radiographic and clinical response after seven cycles of PCV.

bral hemispheres are not highly responsive to chemotherapy, recent evidence has suggested that astrocytomas with 1p loss may be sensitive to chemotherapy (submitted for publication, 1999). Allelic loss of chromosome 1p is a powerful predictor of chemosensitivity in patients with anaplastic oligodendroglioma.[9] There was insufficient tumor tissue available in the current case to determine the status of 1p. Salvage therapy with PCV should be considered in patients with progression of spinal cord astrocytoma after radiation therapy.

References

1. Alter M. Statistical aspects of spinal cord tumors. In: Klawans HL, ed. Tumors of the spine and spinal cord: part I. Handbook of clinical neurology. New York: American Elsevier, 1975:1–22.
2. Kopelson G, Linggood RM, Kleinman GM, Doucette J, Wang CC. Management of intramedullary spinal cord tumors. Radiology 1980;135:473–479.
3. Garcia DM. Primary spinal cord tumors treated with surgery and postoperative irradiation. Int J Radiat Oncol Biol Phys 1985;11:1933–1939.
4. Guidetti B, Mercuri S, Vagnozzi R. Long-term results of surgical treatment of 129 intramedullary spinal gliomas. J Neurosurg 1981;54:323–330.
5. Shirato H, Kamada T, Hida K, et al. The role of radiotherapy in the management of spinal cord glioma. Int J Radiat Oncol Biol Phys 1995;33:323–328.
6. Allen JC, Aviner S, Yates AJ, et al. Treatment of high-grade spinal cord astrocytoma with "8-in-1" chemotherapy and radiotherapy: a pilot study of CCG-945. J Neurosurg 1998;88:215–220.
7. Bouffet E, Amat D, Devaux Y, Desuzinges C. Chemotherapy for spinal cord astrocytoma. Med Pediatr Oncol 1997;29:560–562.
8. Linstadt DE, Wara WM, Leibel SA, Gutin PH, Wilson CB, Sheline GE. Postoperative radiotherapy of primary spinal cord tumors. Int J Radiat Oncol Biol Phys 1989;16:1397–1403.
9. Cairncross JG, Ueki K, Zlatescu MC, et al. Specific genetic predictors of chemotherapeutic response and survival in patients with anaplastic oligodendrogliomas. J Nat Cancer Inst 1998;90:1473–1479.

Loss of ability to sneeze in lateral medullary syndrome

Article abstract—Four consecutive patients with lateral medullary syndrome reported reversible inability to complete a reflex sneeze, despite retaining the urge to do so and the ability to mimic the motor act. This previously undescribed feature of a relatively common syndrome is in keeping with the known location of a "sneeze center" in the lateral medulla of cat. In man, unilateral brainstem lesion is sufficient to abolish the sneeze reflex temporarily. **Key words:** Sneeze—Lateral medullary syndrome—Stroke.

NEUROLOGY 2000;54:520–521

Mark Hersch, MD, PhD

The lateral medullary syndrome (LMS) of Wallenberg is a constellation of signs attributable to unilateral infarction of the brainstem and cerebellum in the territory of the ipsilateral posterior inferior cerebellar artery. Signs include dysphagia, contralateral loss of spinothalamic sensation and ipsilateral palatal palsy, Horner's syndrome, ataxia, and impairment of trigeminal nociception. Hiccups may occur at onset. We have observed inability to sneeze in four consecutive patients with typical LMS. The clinical history of our "index case" follows.

Case reports. *Index case.* A previously healthy 49-year-old man awoke with vomiting, ataxia, and severe dysphagia. He had left-beating nystagmus, and fell to the left when he attempted to stand. Horner's syndrome was present on the left, and pinprick and temperature sensation were absent on the right side of the trunk and limbs, but spared on the face. His voice was hoarse, and he was unable to swallow safely. He did not have hiccups. An MRI scan confirmed infarction of the left lateral medulla and inferior cerebellum; no predisposing factors were identified. Modified barium swallow showed impaired pharyngeal clearance and delayed upper esophageal sphincter relaxation. The left vocal cord was seen to be paralyzed on laryngoscopy. He was anticoagulated with warfarin for 6 months, during which time he improved progressively and returned to work. He could eat normally, and balance was satisfactory. Horner's syndrome and sensory impairment persisted.

At his 6-month follow-up, he expressed considerable frustration at the fact that he "*still* could not sneeze," and, although he had not thought to report this symptom previously, he was confident that this had been the case since the stroke. When, from time to time, he felt the urge to sneeze in response to a typical tickling irritation in the nose, he would automatically inhale deeply, but the subsequent explosive exhalation would simply fail to occur. The sneeze would "peter out," leaving him dissatisfied. He was able to mimic a sneeze on demand, including the elusive phase of rapid exhalation complete with typical "sound effects," but he could never "enjoy" a spontaneous sneeze. Approximately 1 year after the stroke, he reported with obvious satisfaction that his ability to sneeze had returned.

From the Department of Neurology, New South Wales University, St. George Hospital, Sydney, Australia.

Received August 23, 1999. Accepted in final form September 6, 1999.

Address correspondence and reprint requests to Dr. Hersch, Staff Specialist in Neurology, New South Wales University, St. George Hospital, Sydney, Australia 2217.

Other cases. The second and third patients were men who presented with right LMS and had consistent MRI findings. The fourth was a woman who had residual signs and MRI features of right lateral medullary infarct 6 weeks after the ictus. In response to nonleading questions about the effect of the stroke on their breathing, coughing, or sneezing, all three gave almost identical descriptions of an annoying inability to complete a sneeze despite the occasional urge to do so and the normal inspiratory buildup. None had reported this to his or her physician, but the fourth patient had mentioned it to her husband. The three patients recovered their ability to sneeze within 6 months, 5 days, and 6 weeks of the ictus, respectively. The rate of recovery of the sneeze reflex appeared to parallel that of improvement of dysphagia other than in the case of the fourth patient, who was able to eat within days of the ictus.

Spinothalamic facial sensation was spared in our first patient, and was abnormal on the side of the medullary infarct in the second and fourth patients and on the contralateral side of the face in the third.

Discussion. Sneezing, or "sternutation," is a complex protective respiratory reflex, stimulated by an initial sensory or nasal phase, mediated by trigeminal afferents. These afferents feed back to a putative "sneeze center," where input appears to be integrated until threshold is reached, at which stage violent exhalation though the mouth and nose, accompanied by involuntary eye closure, occurs; the irritant is expelled from the airway. Most individuals sneeze only once, whereas others have a flurry of rapidly repeated, usually less violent, sneezes.

In the current series, four patients with classic features of LMS experienced the frustrating inability to complete the expiratory phase of a spontaneous sneeze. In each case, the sneeze reflex recovered as other brainstem signs improved. Abnormality of reflex sneezing in patients presenting with LMS has not been reported previously, although inability to sneeze has been reported in a patient with a medullary neoplasm.[1] That patient, like our own, retained the ability to mimic a sneeze even when he had lost the ability to sneeze reflexively, and his sneeze reflex recovered after surgery.[1]

The fact that each patient was able to blow the nose and to mimic the expiratory phase of sneezing even when it did not occur reflexively indicates that the motor pathways were intact. They felt the urge to sneeze—for example, when their noses felt ticklish or irritated—suggesting that the sensory arc of the reflex was at least partially intact. It is possible that the sensory stimulus failed to reach the threshold required to trigger the all-or-none expulsive motor response. Alternatively, integration of reflex sneezing in a brainstem "sneeze center" (see below) may have been abnormal.

Abnormality of the sneezing reflex in patients with LMS is in keeping with the location of a pontomedullary sneeze center adjacent to the descending trigeminal nucleus and tract in cat, electrical stimulation of which causes sneezing indistinguishable from that resulting from nasal irritation.[2] In cat, unilateral stimulation of the appropriate medullary site[2] or anterior ethmoidal nerve[3] gives rise to a sneeze. The effect of ablating the sneeze center has not been studied in cat, but in our patients, complete loss of the ability to sneeze was lost even though only one side of the medulla underwent infarction. This observation suggests that, in man, both the left and right "sneeze centers" must be intact for reflex sneezing to occur.

Subsequent to our becoming aware of difficulties in sneezing in our "index case," three consecutive patients with acute or recent LMS admitted to identical problems. It seems probable that many patients with LMS have transient dysfunction of reflex sneezing, but do not complain of it spontaneously.

To study further the effect of LMS on the sneeze reflex, patients could be challenged with sneeze-inducing stimuli. Ground pepper proved an unreliable stimulus in the author and other controls. Dilute capsaicin may be more useful.[4] In our small group of patients, dysphagia and the sneeze reflex seemed to improve at similar rates, suggesting that the "sneeze center" in humans may lie close to the swallowing center. Rostrally placed lateral medullary lesions are more likely to give rise to severe dysphagia,[5,6] which may correlate with the relatively rostral site of the sneezing center in cat. Careful correlation of the effect of LMS on sneezing with the exact anatomic extent of the medullary lesion on MRI may permit more precise localization of the sneezing center in man.

Acknowledgment

The author acknowledges the support of Assistant Professor A.S. Zagami and Professor J.G. McLeod, who encouraged publication of these observations. Assistant Professor Zagami kindly read the manuscript.

References

1. Martin RA, Handel SF, Aldama AE. Inability to sneeze as a manifestation of medullary neoplasm. Neurology 1991;41:1675–1676.
2. Nonaka S, Unno T, Ohta Y, Mori S. Sneeze-evoking region within the brainstem. Brain Res 1990;511:265–270.
3. Wallois F, Bodineau L, Macron JM, Duron B. Role of respiratory and non-respiratory neurones in the region of the NTS in the elaboration of the sneeze reflex in cat. Brain Res 1997;768: 71–85.
4. Geppetti P, Fusco BM, Marabini S, Maggi CA, Fanciullacci M, Sicuteri F. Secretion, pain and sneezing induced by the application of capsaicin to the nasal mucosa in man. Br J Pharmacol 1988;93:509–514.
5. Kim JS, Lee JH, Suh DC, Lee MC. Spectrum of lateral medullary syndrome. Correlation between clinical findings and magnetic resonance imaging in 33 subjects. Stroke 1994;25:1405–1410.
6. Cook IJ, Wallace KL, Ali GN, Zagami AS, Enis JM. Mechanisms of pharyngeal dysphagia in lateral medullary syndrome (LMS). Gastroenterology 1996;110:A650. Abstract.

Right frontal areas 6 and 8 are associated with simultanapraxia, a subset of motor impersistence

Article abstract—The authors examined brain lesions that cause simultanapraxia, a subset of motor impersistence. Simultanapraxia was defined as the inability to perform two motor acts simultaneously: closing the eyes and protruding the tongue. Simultanapraxia was found in 9 (5.6%) of 160 hospitalized patients with cerebrovascular diseases. The lesions were located in areas 6 and 8 in the right middle cerebral artery territory. This site was spared in five patients who did not show simultanapraxia, even with a large infarction in the right middle cerebral artery area. **Key words:** Simultanapraxia—Right frontal areas 6 and 8—Motor impersistence.

NEUROLOGY 2000;54:522–524

Y. Sakai, MD; T. Nakamura, MD; A. Sakurai, MD; H. Yamaguchi, MD; and S. Hirai, MD

In 1956, Fisher introduced the term motor impersistence to describe the inability to sustain simple acts such as closing the eyes, protruding the tongue, or keeping the mouth open.[1] Motor impersistence is a clinically important symptom and a factor that predicts the functional prognosis of patients with cerebrovascular diseases (CVD). The presence of motor impersistence is associated with rehabilitation difficulties.[2] Fisher considered motor impersistence to be a nondominant hemisphere–specific symptom, and emphasized both voluntary closure of the eyelids and protruding of the tongue as the most prominently affected tasks. Joynt et al. investigated the phenomenon using nine motor impersistence tasks: closing the eyes, protruding the tongue (patient blindfolded), protruding the tongue (eyes open), fixating gaze in lateral visual fields, keeping the mouth open, fixating on the examiner's nose, turning the head, squeezing a dynamometer, and saying "Ah."[3] However, they found no hemispheric dominance with respect to the motor impersistence lesions. They believed that motor impersistence must not represent localizable damage of the brain, but that it is associated with advancing age, mental impairment, and disorientation. Hirai et al.[4] defined motor impersistence as the inability to perform two simultaneous motor acts—namely, closing the eyes and protruding the tongue. They considered motor impersistence to be a symptom of a nondominant hemispheric lesion, and suggested that lesions in areas 6 and 8 in the right middle cerebral artery (MCA) territory cause motor impersistence, based on pathologic findings of three patients. The lesion responsible for motor impersistence remains controversial.

We considered that different findings concerning the lesion causing motor impersistence were due to an obscure definition. We herein name the inability to perform two simultaneous motor acts simultanapraxia, because our previous study[5] showed simultanapraxia as a subset of motor impersistence.[3] We clearly revealed simultanapraxia to be a nondominant hemispheric symptom.

Patients and methods. We examined 252 patients with brain lesions admitted to the Maebashi Red Cross Hospital between July 1, 1992 and March 31, 1997. When they were alert, we asked them to perform two single acts, closing their eyes or protruding their tongue (opening the mouth in cases of severe bulbar palsy), independently. We excluded 32 patients who could not close their eyes or protrude their tongue due to dementia, sensory aphasia, or apraxia of closing eyes. No patient had buccofacial apraxia. We then asked them to perform these two acts simultaneously. They were given two opportunities to produce the correct response. If they failed the first time, they were given strong encouragement and asked to try again. Only when they failed both attempts did we consider them to have simultanapraxia. We did not classify patients as having simultanapraxia if they were able to produce the two movements simultaneously even for a brief period and even when there was significant delay between the onsets of the two movements. Of 252 inpatients, 220 obeyed our verbal orders: 140 patients with cerebral infarction, 20 with cerebral hemorrhage, 31 with encephalitis, 15 with multiple sclerosis, and 14 with other neurologic diseases. Among those 220 inpatients, 9 exhibited simultanapraxia according to our definition. We also included one outpatient with simultanapraxia resulting from cerebral hemorrhage. All patients also had motor impersistence as defined by Joynt et al.[3] In these 10 cases, we investigated common MRI (T2-weighted) lesions corresponding to simultanapraxia by overlaying 10 images of identical slices, using image processing software on a personal computer.

Results. All nine inpatients with simultanapraxia exhibited cerebral infarction in the right hemisphere. These patients constituted 5.6% (9/160) of CVD patients, 10.7% (9/84) of CVD patients with right hemispheric lesions, 15.5% (9/58) of patients with right MCA lesions, and 64.2% (9/14) of patients with large infarctions in the right MCA territory involving the cortex. No patients with left hemispheric lesions exhibited simultanapraxia.

Five cases were followed up until the simultanapraxia phenomenon disappeared. The duration of simultanapraxia after the onset of stroke ranged from 20 to 72 (mean 35) weeks in four infarct cases. However, it continued for 332 weeks in a case of putaminal hemorrhage.

From Gunma University School of Health Sciences, Gunma, Japan.
Received February 16, 1999. Accepted in final form September 6, 1999.
Address correspondence and reprint requests to Dr. Yasujiro Sakai, Gunma University School of Health Sciences, 3-39-15 Showa-machi, Maebashi, Gunma 371-8514, Japan; e-mail: ysakai@akagi.sb.gunma-u.ac.jp

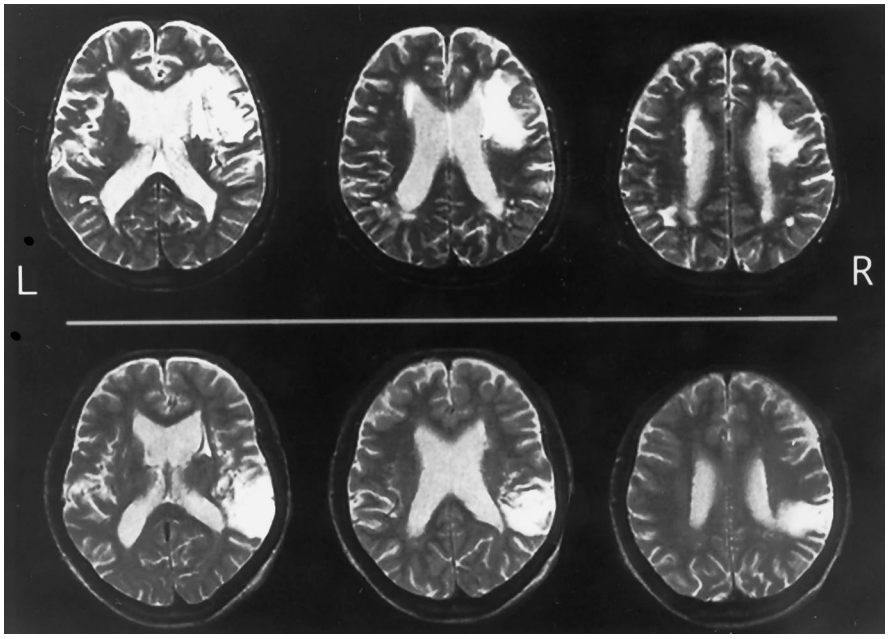

Figure 1. Axial T2-weighted MRI of two cases. Upper panel shows a representative case with simultanapraxia. Lower panel shows one without simultanapraxia.

After simultanapraxia disappeared, motor impersistence persisted in all of these five cases.

MRIs of two representative cases with and without simultanapraxia are seen in figure 1. Common MRI lesions in 10 simultanapraxia cases, shown on a template by overlaying, included the cortex and subcortical white matter of areas 6 and 8 in the territory of the right MCA (figure 2). This site was spared in five patients who did not show simultanapraxia even with a large infarction in the right MCA (see figure 1, lower three images). Simultanapraxia was negative in all 15 patients with left area 6 and 8 lesion.

Discussion. Impairments of higher cortical functions, such as hemispatial neglect and constructional apraxia, remit and disappear in the natural course of strokes. Simultanapraxia also disappears in the temporal course. Therefore, we observed each patient from the acute stage. In previous studies, motor impersistence disappeared within 54 weeks,[6] or occasionally continued for years.[1] Our results showed that simultanapraxia can persist for as long as 83 months, and its duration varies among cases. In our study, patients with simultanapraxia always had motor impersistence, and motor impersistence persisted longer than simultanapraxia. Therefore, we consider simultanapraxia to be a subset of motor impersistence.

The prevalence of simultanapraxia was about 5.6% in our inpatients with CVD, although it was 3.4% in a previous study of CVD patients in the chronic stage.[4]

We showed that simultanapraxia often appears in patients with cerebral infarction in the right MCA territory. Based on our clinical experience, simultanapraxia is rare in patients with cerebral hemorrhage, although we found one such case. Simultanapraxia was found in one case of brain metastasis and one case of brain abscess.[4] Simultanapraxia is essentially a symptom of cerebral infarction in the right MCA territory.

Some investigators have considered motor impersistence to be a nondominant hemisphere–specific symptom,[1,4,6,7] but others have denied this descrip-

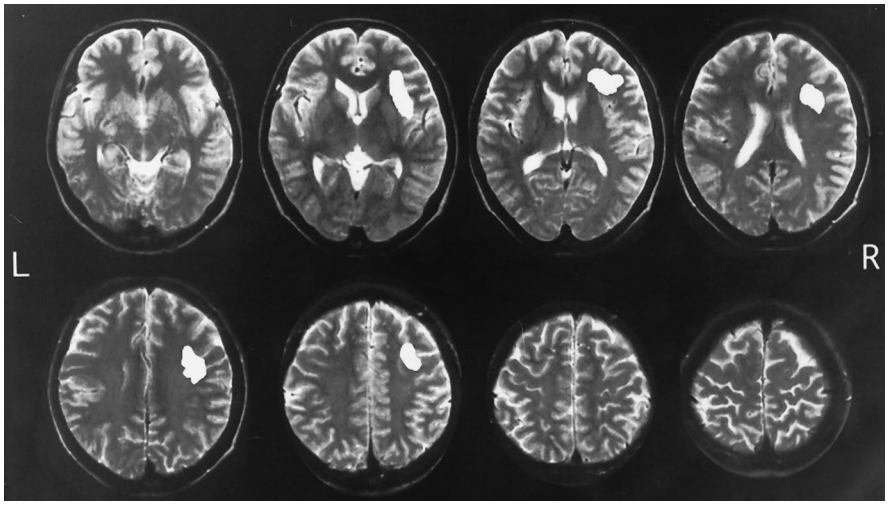

Figure 2. Common MRI lesions of 10 patients with simultanapraxia shown by the overlaying method. The lesions are located in right frontal areas 6 and 8.

tion.[2,3] This controversy may be due to different definitions of motor impersistence used by each investigator. The latter groups defined motor impersistence as the inability to sustain more than two of eight to nine motor acts for a certain time. In the former groups, the definition varied.

Voluntary closure of the eyelids and protrusion of the tongue are the most prominently affected acts in motor impersistence tasks.[1] If patients are asked to simultaneously close their eyes, open their mouth, and protrude their tongue, one of these motor acts is interrupted more readily.[7] What is the essence of this motor impersistence phenomenon? We considered this phenomenon to have the following two features: the inability to maintain a simple act as long as normal persons do and the inability to perform two acts simultaneously. Furthermore, we considered the latter to be more important than the former. In this study, we used the latter feature, named the inability to perform two simultaneous acts simultanapraxia, and found that this phenomenon was clearly related to right frontal areas 6 and 8.

We eliminated 14 aphasic patients who could not close their eyes or protrude their tongue. After recovery of aphasia, we re-evaluated them and found no simultanapraxia. Furthermore, no patients with left area 6 and 8 lesion showed simultanapraxia. The simultanapraxia patients, as identified by our definition, showed highly localized lesions in right frontal areas 6 and 8. Therefore, simultanapraxia, a subset of motor impersistence, becomes a clinically important sign in the neurologic examination of patients with CVD.

References

1. Fisher M. Left hemiplegia and motor impersistence. J Nerv Ment Dis 1956;123:201–218.
2. Ben-Yishay Y, Diller L, Gerstmann L, Haas A. The relationship between impersistence, intellectual function and outcome of rehabilitation in patients with left hemiplegia. Neurology 1968; 18:852–861.
3. Joynt RJ, Benton AL, Fogel ML. Behavioral and pathological correlates of motor impersistence. Neurology 1962;12:876–881.
4. Hirai S, Morimatsu M, Muramatsu A, Yoshikawa M. A study of motor impersistence (in Japanese with English abstract). Clin Neurol 1975;15:870–877.
5. Hirai S, Sakai Y, Hatta M. Motor impersistence (in Japanese with English abstract). Jpn J Neuropsychol 1987;3:11–17.
6. Hier DB, Mondlock J, Caplan LR. Recovery of behavioral abnormalities after right hemisphere stroke. Neurology 1983;33: 345–350.
7. Berlin L. Compulsive eye opening and associated phenomena. Arch Neurol Psychiatr 1955;73:597–601.

Hemodynamic changes in simple partial epilepsy: A functional MRI study

Article abstract—We performed functional MRI (fMRI) on a patient with a mass lesion while she happened to experience a simple partial seizure. We used regional T2* signal changes to localize seizure-related hemodynamic changes. Seizure activity was associated with changes in MR signal in different regions that showed sequential activation and deactivation. Our study has shown that epileptic activity leads to changes in cerebral hemodynamics. In selected patients, therefore, it might be possible to use fMRI as a noninvasive tool to detect and investigate cortical patterns of activation associated with seizure activity. **Key words:** MRI—Functional MRI—MR signal time course—Epilepsy—Cerebral hemodynamics.

NEUROLOGY 2000;54:524–527

T. Krings, MD; R. Töpper, MD; M.H.T. Reinges, MD; H. Foltys, MD; U. Spetzger, MD; K.H. Chiappa, MD; J.M. Gilsbach, MD; and A. Thron, MD

Epileptic activity causes changes in cerebral blood flow (CBF), cerebral blood volume (CBV), and blood oxygenation. During focal seizures and focal status epilepticus, there are large increases in cerebral blood flow, volume, and metabolism, and increased perfusion may exceed the increase in oxygen consumption.[1] Functional MRI (fMRI) using the blood oxygenation level dependent (BOLD) technique can detect these cerebral hemodynamic changes.[2] The excellent spatial resolution of fMRI offers the possibility to study cortical activation during epileptic activity and to relate the pattern of activation to the anatomy.[3-6] In the current investigation, fMRI was performed on a patient with a focal seizure.

Case history. A 62-year-old right-handed woman presented to our department with an increasing frequency of

From the Department of Neuroradiology (Drs. Krings and Thron), the Department of Neurology (Drs. Töpper and Foltys), the Interdisciplinary Center for Clinical Research—Central Nervous System (Drs. Krings, Foltys, Spetzger, Gilsbach, and Thron), and the Department of Neurosurgery (Drs. Krings, Reinges, Spetzger, and Gilsbach), University Hospital of the Technical University, Aachen, Germany; and the Clinical Neurophysiology Laboratory, Department of Neurology (Dr. Chiappa), Massachusetts General Hospital, Harvard Medical School, Boston.

Received April 1, 1999. Accepted in final form September 11, 1999.

Address correspondence and reprint requests to Dr. Timo Krings, Department of Neuroradiology, University Hospital of the Technical University Aachen, Pauwelsstrasse 30, 52057 Aachen, Germany.

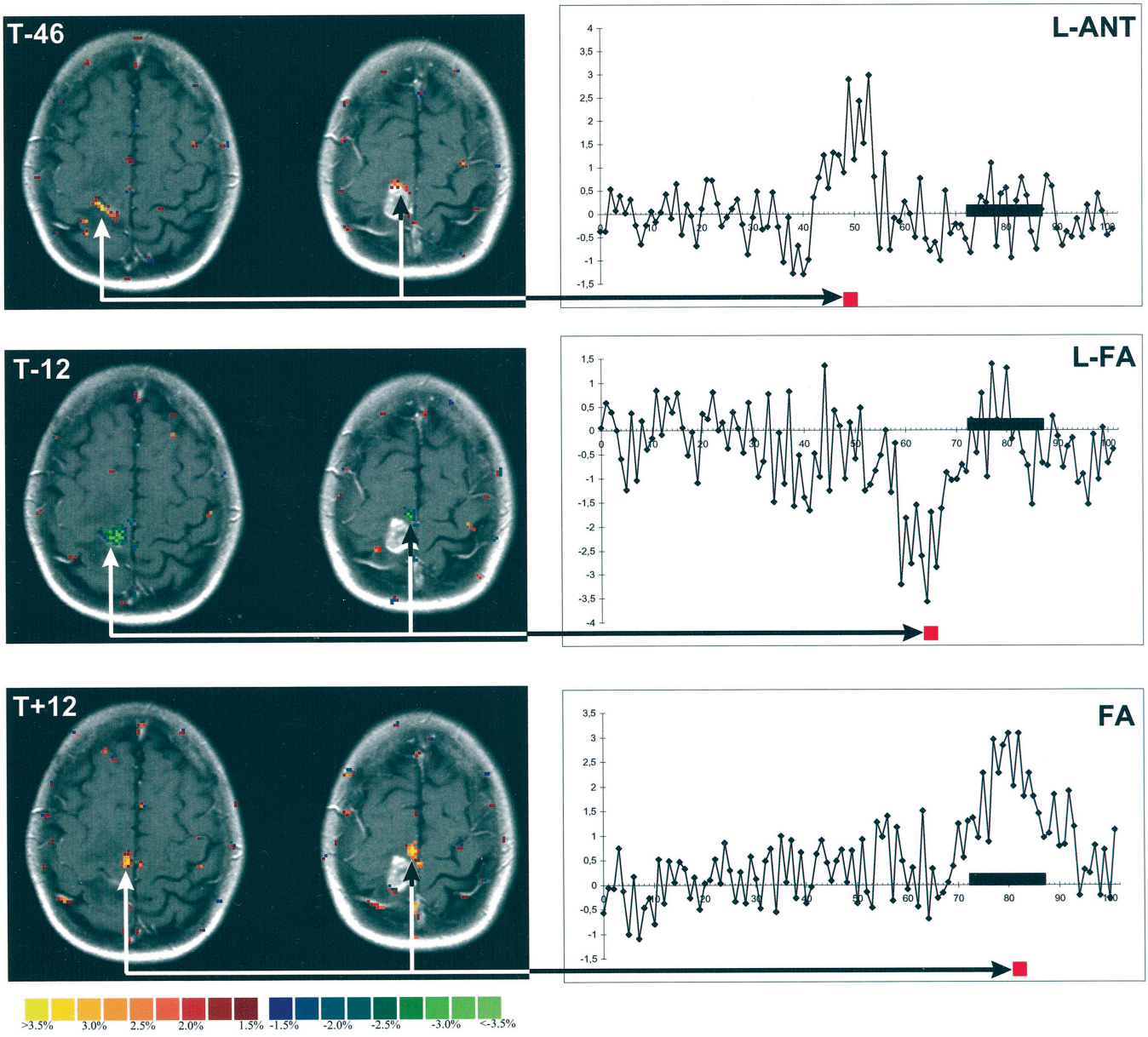

Figure. Spatial extent of significant signal intensity changes overlaid on the high-resolution T1-weighted scan in a temporal sequence and MR time courses in three different regions. Sixty-five seconds before foot movements indicating seizure start were visible, there was a significant hemodynamic change in the perilesional cortical area (L-Ant) without any change in the foot area or other cortical regions (upper row, the MR signal time course is averaged over the 30 voxels, showing significant hemodynamic changes at that timepoint). Thirty-five seconds later, a significant decrease in MR signal is seen in a cortical area between the lesion and the foot area (L-FA) (middle row, the time course is averaged over the 56 activated voxels). During the clinical seizure (black horizontal bar), a significant MR signal increase can be found in the foot area (FA) (lower row, the MR time course is averaged over 34 activated voxels). The y axis and the thermal scale indicate the percent MR signal change. Functional MRI allows for demonstrating seizure evolution and spread.

simple partial seizures consisting of a Jacksonian march of convulsions starting in the left foot and involving the whole left leg. The seizures never generalized and were refractory to several anticonvulsant drug regimens. The seizure frequency at the time of the fMRI examination was up to five events per hour, during which the patient never lost consciousness. The patient was taking 625 mg primidone/day. MRI revealed irregular contrast enhancement within a space-occupying intraparenchymal lesion of the right central region with perifocal edema consistent with a malignant glioma. Interictal and ictal EEG were normal. Neuropathologic examination after surgery revealed a glioblastoma multiforme.

Methods. Functional imaging was performed on a 1.5-T Philips ACS NT Gyroscan using a multishot multislice T2*-weighted gradient-echo echoplanar imaging sequence (repetition time/echo time/flip angle [FA] 278/35/35, voxel size 3 × 3 × 5 mm, temporal resolution 2.2 sec/image). The patient was monitored by a neurologist and the video

equipment of the scanner and experienced one of her typical seizures that started with toe curling, proceeding to foot twitching and, finally, calf shaking. The seizure lasted 33 seconds, during which the patient remained responsive. Start and stop times of the seizure were noted and correlated to the sequence numbers of the functional images.

The image data set was checked for motion by running an animated loop through the 102 consecutive images. Although no motion was seen during the animation, we employed an automated image realignment algorithm to minimize the effects of subvoxel interimage motion-related artifacts in the brain.[2] For each voxel, we identified signal intensity fluctuations of the T2* signal by calculating the percent signal change from the voxel baseline for each timepoint. Once a baseline value was computed (mean of MR signal of first 20 images of the given voxel), the MR signal value on each timepoint could be expressed as a percent signal increase or decrease for every voxel. This percent signal change was color-coded on a thermal scale and then overlaid on the T1-weighted scan for anatomic reference. We were able to visualize and quantify the sequential MR signal changes by scrolling through the functional images in an animated loop. Only voxels exhibiting percent signal changes larger than 1.5% from baseline were visualized to exclude random MR signal noise.

Results. Analysis of the MR signal raw data revealed three areas of signal intensity changes related to the seizure activity. The first active focus was located anterior to the space-occupying lesion at the border between the lesion and normal tissue and occupied 30 voxels (L-Ant). The second area was between the lesion border and the foot area where 56 voxels were involved (L-FA). The third area colocalized with an area in the precentral gyrus that was identified in a previous functional scan as the foot area (size: 34 voxels, FA). The temporal sequence of these areas and the MR time courses for each of these regions are shown in the figure. Three events are evident, the first starting approximately 65 seconds before the seizure movement started (indicated by the black horizontal bar) in L-Ant; the second one immediately thereafter but still 30 seconds before the seizure in L-FA; and the third following the clinical symptoms of the seizure. During the first event, an average increase for the entire region L-Ant (30 voxels) in MR signal of up to 2.2% is noted lasting for 30 seconds. The second event was characterized by an average MR signal intensity decrease of up to 3.5% lasting for approximately 25 seconds in the entire region L-FA. In FA, clinical seizure activity was closely associated with an increase in MR signal that commenced 4 seconds after movements were apparent, then increased to a plateau that lasted for the duration of the seizure and was subsequently followed by a delayed return to baseline. Percent signal change from baseline was up to 3.1%. Similar signal intensity changes were not seen elsewhere in the brain, as demonstrated by the figure. This figure shows the spatial extent of signal intensity changes overlaid on the high-resolution contrast-enhanced T1-weighted scan in a temporal sequence.

Discussion. This report has shown that it is possible to use fMRI as a noninvasive tool to detect and investigate cortical patterns of activation associated with seizure activity. Increased MR signal values presumably indicate increased perfusion and blood volume with a concomitant increase in venous oxyhemoglobin content secondary to increased neuronal firing rates. Because the tissue surrounding a cerebral lesion often is epileptogenic, the initial increase in MR signal in L-Ant might indicate the onset of neuronal activity related to the overt clinical seizure.[7] This would demonstrate the potential of fMRI to delineate and detect the epileptogenic zone noninvasively. The increase during the overt seizure in FA, on the other hand, provides evidence for the theoretical concept of the symtomatogenic zone, i.e., the portion of the brain that produces the clinical symptomatology. The decrease in MR signal, conversely, might reflect a mismatch between oxygen consumption and oxygen delivery, either due to decreased perfusion or to increased oxygen extraction secondary to excessive neuronal activity. Using functional MRI signal time course characteristics, the temporal and spatial spread of a seizure might therefore be investigated noninvasively and correlated to the underlying anatomy. Thereby, the theoretical concepts of epileptogenic and symtomatogenic zone can be validated.[8] Seizure spread will be difficult to elucidate as a 2.2-second interval between consecutive scans is probably not sufficient to detect the fast spread between epileptogenic regions and areas of propagated activity, because electric activity can propagate at high velocities using intrinsic neuronal circuits.[9] However, the identification of cortical areas with different types of hemodynamic seizure-related changes may help in delineating seizure generators from areas with propagated activity, even if the propagation time is too fast to be detectable with fMRI. Without further knowledge of the EEG data, however, only assumptions can be made about the propagation and the role of L-Ant in triggering the foot area. Our results and those of other groups have demonstrated that fMRI can detect possible subclinical seizure activity.[3-6] We have found that the first significant increase from baseline values preceded the onset of clinical symptoms by 65 seconds, which was also noted previously.[3] The implication of these findings is that, in some patients, hemodynamic changes might be detectable earlier than the clinical events associated with the seizure. Furthermore, they demonstrate that subclinical activity can be identified and localized using fMRI. This could broaden the scope of epileptic patients applicable for fMRI investigations, especially as it is now possible to record EEG during MRI studies.[5,6,10] By recording the EEG while the patient is in the scanner, subclinical epileptic activity could be identified and the timing correlated to the fMRI signal time course. Coregistration of fMRI with EEG will therefore help to localize subclinical activity and provide a new window into brain and epilepsy research.

References

1. Franck G, Sadzot B, Salmon E, et al. Regional cerebral blood flow and metabolic rates in human focal epilepsy and status epilepticus. Adv Neurol 1986;44:935–948.
2. Kwong KK. Functional MRI with echo planar imaging. Magn Reson Q 1995;11:1–20.
3. Jackson GD, Connelly A, Cross JH, Gordon I, Gadian DG. Functional magnetic resonance imaging of focal seizures. Neurology 1995;44:850–856.
4. Detre JA, Sirven JI, Alsop DC, O'Connor MJ, French JA. Localization of subclinical activity by functional magnetic resonance imaging: correlation with invasive monitoring. Ann Neurol 1995;38:618–624.
5. Warach S, Ives JR, Schlaug G, et al. EEG-triggered echo-planar functional MRI in epilepsy. Neurology 1996;47:89–93.
6. Seeck M, Lazeyras F, Michel CM, et al. Non-invasive epileptic focus localization using EEG-triggered functional MRI and electromagnetic tomography. Electroencephalogr Clin Neurophysiol 1998;106:508–512.
7. Krings T, Chiappa KH, Cuffin BN, Buchbinder BR, Cosgrove GR. Accuracy of EEG dipole localization of epileptiform activities in the presence of focal brain lesions. Ann Neurol 1998; 44:76–86.
8. Luders HO, Engel J Jr., Munari C. General principles. In: Engel J Jr., ed. Surgical treatment of the epilepsies. 2nd ed. New York: Raven Press, 1993:137–154.
9. Emerson RG, Turner CA, Pedley TA, Walczak TS, Forgione M. Propagation patterns of temporal spikes. Electroencephalogr Clin Neurophysiol 1995;94:338–348.
10. Ives JR, Warach S, Schmitt F, Edelman RR, Schomer DL. Monitoring the patient's EEG during echo planar MRI. Electroencephalogr Clin Neurophysiol 1993;87:417–420.

Neuro*Images*

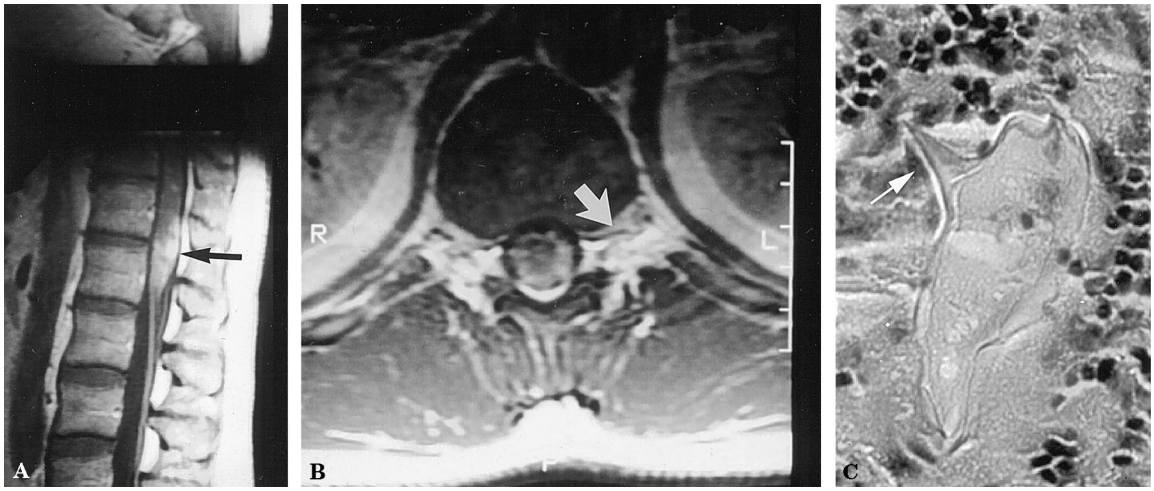

Figure. (A) Sagittal postcontrast T1-weighted MR scan showed enhanced enlargement of the region of the conus medullaris, which is multinodular in nature (arrow). (B) Uniform nerve root enhancement at the cauda equina level, axial view (arrow). (C) Schistosoma mansoni *egg with arrow pointing to lateral spine (H-E, ×1,000 before 43.1% reduction).*

Spinal schistosomiasis

Charles L. Gellido, MD, Stephen Onesti, MD,
Josefina Llena, MD, Miguel Suarez, MD,
Bronx, NY

A 40-year-old man had numbness of the buttocks associated with progressive difficulty in urination and bowel movements as well as impotence during a 6-week period. Neurologic examination revealed flaccid rectal tone, reduced sensation in the T11–T12 level, and absent ankle jerks. There was no weakness of the lower extremities. He had a history of travel in Puerto Rico 10 years ago and remembered swimming in freshwater streams.

MRI of the lower spine showed mild enlargement of the conus medullaris with heterogeneous signal intensity (T1-weighted) within it. The contrast-enhanced images demonstrated evidence of abnormal enhancement involving the conus medullaris at T10–L1 that is multinodular in nature. The examination also demonstrated evidence of abnormal smooth uniform enhancement of several roots of the cauda equina at L1–L5. No other lesions were found on MRI of the brain and the rest of the spinal cord. These findings are most commonly noted in patients with ependymoma; hence, an open tissue biopsy was performed. Biopsy revealed granulomatous inflammatory lesions containing parasitic ova consistent with *Schistosoma mansoni*. The patient was treated with praziquantel and dexamethasone and has undergone rehabilitation with improvement of symptoms.

Three species of the trematode Schistosoma cause CNS disease. *S. japonicum* and *S. hematobium* cause cerebral schistosomiasis, whereas *S. mansoni* is the primary cause of spinal cord disease. *S. hematobium* also may cause spinal cord disease. The prominent lateral spine of *S. mansoni* differentiates it from other species and probably also impedes *S. mansoni* from reaching the brain. Freshwater snails serve as an intermediate host and infect man by skin penetration. Schistosoma then reside in the blood vessels and may remain alive for 20 to 30 years. Schistosomiasis continues to be a major health problem and ranks second only to malaria, infecting 10% of the world population.[1]

1. McCully RM, Barron CN, Cheever AW. Diseases caused by trematodes. In: Binford CH, Connor DH, eds. Pathology of tropical and extraordinary diseases. Washington, DC: Armed Forces Institute of Pathology, 1976: 482–508.

